Solvatochromic Effects and Photophysical Properties of Levofloxacin and Norfloxacin Drugs and their Fluorescence Quenching Mechanism with Caffeine using Spectroscopic and Computational Methods

Kinfe Woldegiorges Bachare

A Dissertation Submitted to the Department of Applied Physics

School of Applied Natural Sciences

Presented in Fulfilment of the Requirement for the Degree of Doctor of Philosophy in Physics (Laser Spectroscopy)

Office of Graduate Studies

Adama Science and Technology University

Adama, Ethiopia

December, 2022

Solvatochromic Effects and Photophysical Properties of Levofloxacin and Norfloxacin Drugs and their Fluorescence Quenching Mechanism with Caffeine using Spectroscopic and Computational Methods

Kinfe Woldegiorges Bachare

Supervisor: Abebe Belay Gemta (Professor)

Co-Supervisor: Alemu Kebede (PhD)

A Dissertation Submitted to the Department of Applied Physics

School of Applied Natural Sciences

Presented in Fulfilment of the Requirement for the Degree of Doctor of Philosophy in Physics (Laser Spectroscopy)

Office of Graduate Studies

Adama Science and Technology University

Adama, Ethiopia

December, 2022

APPROVAL OF BOARD OF EXAMINERS

I/we hereby certify that the recommendations and suggestions made by the board of examiners are appropriately incorporated into the final version of the dissertation entitled entitled "**Solvatochromic Effects and Photophysical Properties of Levofloxacin and Norfloxacin Drugs and their Fluorescence Quenching Mechanism with Caffeine using Spectroscopic and Computational Methods**" by Kinfe Woldegiorges Bachare.

Major Supervisor	Signature	Date
Co-supervisor	Signature	Date

We the undersigned, members of the board of examiners of the final open defence by Kinfe Woldegiorges Bachare have read and evaluated his thesis entitled "**Solvatochromic Effects and Photophysical Properties of Levofloxacin and Norfloxacin Drugs and their Fluorescence Quenching Mechanism with Caffeine using Spectroscopic and Computational Methods**" and examined the candidate. This is therefore, to certify that the dissertation has been accepted in partial fulfilment of the requirement of the Degree of Doctor of Philosophy in Physics (Laser Spectroscopy).

Chairperson	Signature	Date
Internal Examiner 1	Signature	Date
External Examiner 1	Signature	Date
External Examiner 2	Signature	Date

Finally, approval and acceptance of the dissertation is contingent upon submission of its final copy of the Office of Postgraduate Studies (OPGS) through the candidate's Department Graduate Council (DGC) and School Graduate Committee (SGC).

Department Head	Signature	Date
School Dean	Signature	Date
Postgraduate Dean	Signature	Date

DECLARATION

I hereby declare that, this Dissertation entitled "**Solvatochromic Effects and Photophysical Properties of Levofloxacin and Norfloxacin Drugs and their Fluorescence Quenching Mechanism with Caffeine using Spectroscopic and Computational Methods**" is my original work. That is, it has not been submitted for the award of any academic degree, diploma or certificate in any other university. All sources of materials used for this thesis have been duly acknowledged through appropriate citations.

_____ _____ _____

Name of student Signature Date

APPROVAL OF SUPERVISORS

I/we, the advisor(s) of this dissertation, hereby certify that I/we have read the revised version of the dissertation entitled "**Solvatochromic Effects and Photophysical Properties of Levofloxacin and Norfloxacin Drugs and their Fluorescence Quenching Mechanism with Caffeine using Spectroscopic and Computational Methods**" submitted in partial fulfilment of the requirements for the degree of Doctor of Philosophy in Laser Spectroscopy, the Graduate program of the Department of Applied Physics, and has been carried out by Kinfe Woldegiorges Bachare, ID. No PGR/18130/11, under our supervision. Therefore, I/we recommend the submission of revised version of the dissertation to the department following the applicable procedures.

1. Abebe Belay (Professor) _____ _____

   (Major Supervisor) Signature Date

2. Alemu Kebede (Assi. Prof., Ph.D.) _____ _____

   (Co-Supervisor) Signature Date

ACKNOWLEDGEMENTS

A lot of time and effort have been committed to put this dissertation to its final form. My appreciations goes to all those who have extended their assistance to me in preparing it. To begin with, above all, I would like to express my sincere thanks to the Lord God for his inexpressible support. My sincere appreciation goes to my Advisor, Professor Abebe Belay Gemta who has given me limitless help, close guidance, and has been very accessible in dedicating part of his valuable time to respond to all my repeated inquiries and successful supervision. I also wish to express my sincere appreciation to my co-Advisor, Alemu kebede (PhD), for his continuous follow up, very thoughtful contributions, kindness and advice from the initial proposal writing up to the final dissertation writing.

I express my deepest and sincere gratitude to the entire Adama Science and Technology University, Department of applied Physics staff for their encouragement in boosting my intellectual potential and support. I respectfully acknowledge the financial support of Adama Science and Technology University, Bule Hora University and Ministry of Innovation and Technology.

I owe my deepest thanks to all my family and friends, specially my wife Wosene Tesfaye, my daughter Asanti Kinfe, and my son Moti Kinfe who did their most in keeping up the moral and material needs for the successfulness of my work. I am very much indebted to them for the amount of effort they put into this task, which made the study to be completed successfully.

TABLE OF CONTENTS

CHAPTER **PAGE**

LIST OF TABLES

TABLE **PAGE**

LIST OF FIGURES AND ILLUSTRATIONS

FIGURE **PAGE**

LIST OF ACRONYMS AND ABBREVIATIONS

BBB	Blood Brain Barrier
CF	Caffeine
DFT	Density Functional Theory
DNA	Deoxyribonucleic Acid
EMR	Electromagnetic Radiation
FTIR	Fourier Transform Infrared Spectroscopy
FQ	Fluoroquinolone
GI	Gastrointestinal
HIV	Human Immunodeficiency Virus
HK	Hohenberg Kohn
HOMO	Highest Occupied Molecular Orbital
ICT	Internal Charge Transfer
LVF	Levofloxacin
LUMO	Lowest Unoccupied Molecular Orbital
KCV	Kawski-Chamma-Viallet
NRF	Norfloxacin
TAS2Rs	Taste Type 2 Bitter Receptors
TDDFT	Time Dependent Density Functional Theory
TDM-ESP	Total Density Matrix with Electrostatic Potential
TD-SCF-DFT	Time-Dependent Hartree-Fock Density-Functional Theory.
TICT	Twisted Internal Charge Transfer
UV/Vis	Ultraviolet-Visible

ABSTRACT

Levofloxacin (LVF) and Norfloxacin (NRF) are among groups of fluoroquinolone antibiotics, broad-spectrum used to treat various infections caused by many bacterial species. The drugs contain functional groups which control the type and degree of interaction with different solvents. In this research, the effects of solvent polarity on LVF and NRF drugs were determined using spectroscopic and computational work to realise change in electronic properties and geometrical structure of the drugs. The results indicated that, the emission spectra are more strongly affected by solvent polarity than the absorption spectra. The calculated excited state dipole moment is larger than that of the ground state dipole moment which indicate the probe compounds are significantly more polarized in the excited state than in the ground state. From computational work, the HOMO-LUMO energy bandgap, the dipole moments, electron charge density distribution, and oscillator strength were determined using the semi-empirical MP6 method, DFT-B3LYP-3-21G, and DFT-B3LYP-6-31G employing Gaussian 09 software. Large dipole moments were obtained by computational method than experimental results due to the absence of solvent effects in computational methods. In addition, the effects of solvents and concentrations on the photophysical properties of LVF and NRF were investigated using UV/Vis absorption and fluorescence spectroscopic techniques. The results indicate that, the quantum yields, fluorescence life time, rate of radiative, and non-radiative decay of the drugs were affected by solvent polarity and concentration of the sample. Also, the binding interaction mechanism of LVF-Caffeine and NRF-Caffeine were determined using fluorescence quenching method. From fluorescence quenching spectral analysis, the quenching rate constant (k_q)*, binding constant* (k_a)*, and thermodynamic parameters were determined in different temperatures. The result obtained indicates that the binding between the drugs and Caffeine occurs spontaneously in which electrostatic force in LVF-CF, hydrogen and Van der Waals force in NRF-CF, play major role in the reaction.*

Keywords: *Levofloxacin, Norfloxacin, Solvatochromic, Photophysical properties, quenching, Dipole moments, and DFT*

1. INTRODUCTION

1.1. Background

Levofloxacin (LVF) and Norfloxacin (NRF) are antibiotics active against *Gram-negative* and *Gram-positive bacteria*. The drugs contain several proton binding sites such as carboxyl, carbonyl and amino groups (Sharma et al., 2009). Different studies indicated that the polarity parameters of a drug originated from its chemical structure and functional groups attached to the compound (Kian et al., 2019). Due to these properties, the physical and chemical behaviour of the drugs are altered in solvents (Sárközy, 2001; Viola et al., 2007). The functional groups that exist in drugs are control the type and degree of interaction with solvents (Kian et al., 2020; Kian, et al., 2017b). It was also observed that due to these functional groups the antibacterial activity of the drugs are pH dependent (Prabodh Chander Sharma et al., 2009; Viola et al., 2004). Hence, studying the interaction of solvents with drugs is important for biological applications and to get information about change in electronic distribution upon excitation (Siddlingeshwar et al., 2011).

Investigating the photophysical properties of biologically active compounds are receiving great interest from researchers. The photophysical properties are important to understand the electronic properties and geometrical structures of the drug molecules (García et al., 2005). The biological activities of the molecules basically depend on their molecular structures. Investigation of the photophysical properties also assists in observing different biochemical interaction through which a drug substance produces its pharmacological effect in different micro environments (Gonçalves, 2021; Sharma et al., 2021a). Previously, the photophysical properties of various drugs were reported for quinine (Mallick et al., 2016), Ciprofloxacin (Boraste et al., 2018), Folic acid (Khadem Sadigh et al., 2016), Naproxen (Miotke & Józefowicz, 2017), Deoxyribonucleic acid (Meena & Kishore, 2021) and many more.

Further, the effects of solvent media on the photophysical properties of different drug such as Vitamin A (Kian et al., 2015), Vitamin B (Zakerhamidi et al., 2017), Triarlymethane (Kian, et al., 2017), and Folate derivatives (Khadem Sadigh et al., 2017), were investigated using different spectroscopic techniques. The results of the study indicated that the general solvent effect due to relative permittivity and refractive index and specific due to hydrogen bonding and intermolecular charge transfer were observed between the drugs and solvents. As the

solvents polarity changes, shifts of the absorption and emission peaks are observed and result in change in the dipole moments due to the effect of the solvent's polarity (Gülseven Sidir, 2015; Thiaré et al., 2015). Estimating the ground and excited state dipole moments of drugs from solvatochromic effects and computational work has also great importance to reveal information concerning the electronic and geometrical structures of these drug molecules (Desai et al., 2016; Kian et al., 2019). It also reflects the charge distribution in the molecule and is useful in parameterization in quantum chemical procedures (Raikar et al., 2006). The biological activities of the molecules are mainly depending on their molecular structures. This can be obtained from ground and excited-state dipole moments. A small change of the dipole moments and molecular structure may cause different biological activities related to the drug, making the dipole moments important measurable properties of drugs (Sıdır, 2011).

Caffeine is one of the most pharmacologically active compound found in coffee beans, and tea leaves (Willson, 2018). It acts as a central nervous system stimulant. It is a common ingredient in medications to treat or manage drowsiness, headaches, and migraines. Recent study indicated it's safe for most healthy adults to consume up to 400 milligrams of caffeine per day (Nawrot et al., 2003).

Studying the interactions between drugs and caffeine from the level of molecules enable us to understand effects of caffeine on drugs and to provide valuable information of drugs design and development. Caffeine can enhance the effectiveness of the drug as it can reduce the adverse effects of antidepressants (Camarasa et al., 2006). In contrast, interaction of caffeine and drug causes some idiosyncratic reaction in the body. Previous study on the interaction of caffeine and ecstasy drugs on rat results in increased heart rate, hyperthermia, and mortality (Camarasa et al., 2006; Downey et al., 2014). It may also cause binding with other endogenous and/or exogenous ligands as a result of overlap of binding sites and/or conformational changes (Chirasani et al., 2021). Therefore, studying the interaction of drugs with caffeine is highly important since caffeine interaction make a complex with different drugs and influence the drug pharmacodynamics and pharmacokinetic properties (Kokiashvili et al., 2012; Mrkalić et al., 2021). Previously, the interaction of LVF and NRF with divalent toxic metal ion (Mohd et al., 2010), Humic acid (Ferrie et al., 2017), P-acetyl aminophenol, Aspirin, and Ibuprofen (Wang et al., 2020) were studied.

Several analytical methods have been used to qualitatively and quantitatively study the binding of organic ligands including drugs-drug binding, and fatty acids to proteins such as serum

albumin. Traditional methods including equilibrium dialysis and surface tension (MacManus-Spencer et al., 2010) were used. But, more recent studies have used calorimeter (Tardioli et al., 2010) mass spectrometry (Han et al., 2003) absorbance and fluorescence spectroscopy (Tardioli et al., 2010) ion-selective electrodes, (Messina et al., 2005) potential measurements, (Malik, 2015) and NMR spectroscopy (Khazaee et al., 2021; MacManus-Spencer et al., 2010; Sauter et al., 1989). Among these, absorption and fluorescence spectroscopy are powerful techniques for the study of the reactivity of chemical and biological systems (Li et al., 2005). These spectroscopic techniques are very useful for the calculation of binding parameters of drug with other molecules interactions (MacManus-Spencer et al., 2010). The spectral changes observed on the binding of drugs with another molecules are an important tool for the investigations of the topology of binding sites, conformational changes, and characterization of substrate to ligand binding (Lakowicz, 2006).

Overall dissertation work was structurally organized as follows. Following the introduction, under Chapter 2, fluoroquinolone concepts, mechanism of drug action and resistance, photophysical properties and solvent polarity effects and the effects of caffeine on pharmacokinetic properties of some of the previously studied drugs were discussed. In addition, concepts and theories necessary for a good understanding of the light matter interaction were also presented. The phenomena of fluorescence such as photophysical properties, general and specific solute solvents interactions, theory of fluorescence quenching and the theoretical background of quantum chemical calculation used in density functional theory were also discussed under this chapter.

Chapter 3, is dedicated to the description of the materials and methods. In the first section, chemicals and solvents to carry out the research are discussed. In addition, how instruments such as UV-vis absorption, fluorescence, and FTIR spectroscopy used to characterize the samples are presented. The second section includes procedures utilized in this work, as well as the methods of data treatment and analysis. Finally, in section three the quantum chemical calculation methods are briefly presented.

In Chapter 4, results and discussions of the dissertation were presented. First section deals with effects of solvent polarity on absorption and emission spectra of Levofloxacin and Norfloxacin drugs, evaluation of dipole moments, and quantum chemical calculations of the drugs in different environments were discussed. Under the second section, the photophysical properties, the effects of solvents polarity and sample concentration were discussed. In

addition, in this section the optical transition probability of LVF and NRF were presented. Fluorescence quenching of LVF and NRF by caffeine, nature of binding force between drugs and caffeine, UV/vis absorption spectroscopy study and Fourier transform infrared spectroscopy of the LVF and NRF drugs interaction with caffeine were presented in last section of this chapter.

Finally, the conclusion, recommendations and future work of the overall work was discussed under chapter 5.

1.2. Statement of the Problem

Levofloxacin and Norfloxacin are a broad medicinal spectrum and flourescent antibiotic drugs usually prescribed for many deases. Currently, investigating the solvent polarity effects and photophysical properties of flourescent drugs through spectrscopic method is exciting research field. Solvatochromic study gives information such as drug structural change, rearrangement of drug molecules around solvents molecules, changes that occur in dipole moments at the ground and excited states, and appropriate electronic transition energies between the ground and the excited states. Photophysical properties also provide extensive information about electronic properties and phototoxicity of drugs. In addition, probing the interaction between caffeine and drug is useful in understanding of pharmacology of the drugs, effectiveness, distribution, and their metabolism activities.

So far, the photophysical properties of drugs in different pH condition, bio-mimicking environments formed by bile salts, in solvents with different polarities were studied. But, to the best of our knowledge, Norfloxacin and Levofloxacin antimicrobial drugs solvatochromic effect study for determination of dipole moment of a molecule on the ground and exited states were not investigated experimentally and computationally. Drugs' photophysical properties (quantum yield, life time, oscillator strength, transition dipole moments, and Einstein coefficients) in different solvents and concentration were also not investigated yet. In addition, the interaction mechanism of Levofloxacin and Norfloxacin antibiotic drugs with caffeine through fluorescence quenching to determine the binding constants and binding sites, and thermodynamic parameters were not studied.

Therefore, this research investigated the solvatochromic effect of LVF and NRF in polar and nonpolar solvents and determined the ground and excited states dipole moments of the drugs experimentally and theoretically. The study also provides the effects of solvent polarity and

concentration on photophysical properties of LVF and NRF drugs. In addition, the investigation provides information about the interaction of LVF and NRF drugs binding mechanism with Caffeine using fluorescence quenching and UV/Vis absorption methods. From fluorescence quenching spectra, the quenching rate constant (k_q), binding constant (k_a) and thermodynamic parameters are determined in different temperatures.

1.3. Objectives

1.3.1. General Objective

The general objective of this research is to study solvatochromic effects and photophysical properties of Levofloxacin and Norfloxacin drugs and their fluorescence quenching mechanism with Caffeine using spectroscopic and computational methods.

1.3.2. Specific Objectives

The specific objectives of this research are to:

- Identify the effects of solvent polarity on the absorption and emission spectra of Levofloxacin and Norfloxacin drugs.
- Estimate the ground and excited-state dipole moments of Levofloxacin and Norfloxacin drugs using solvatochromic effects and computational work.
- Determine the HOMO-LUMO energy band gap of Levofloxacin and Norfloxacin compounds using computational techniques.
- Determine the photophysical properties and optical transition strength of Levofloxacin and Norfloxacin drugs in different solvent polarity and concentration.
- Identify interaction mechanism of Levofloxacin and Norfloxacin antibiotic drugs with Caffeine using fluorescence quenching and UV/Vis absorption spectra.

1.4. Significance of the Study

Inside human body, solvents such as water, and dimethylsulfoxide and chemicals like, hydrochloric acids, and bilesalts naturally exist. When we take drugs, different micro enviroment such as solvent polarity, pH condition, and temperature affects the structure and electronic properties of drugs which can affects the efiicicency of the drugs and raise drug toxicity. In addition in our life practice, it is very common that drugs are administered simultaneously with caffeine sources such as tea and coffee. More of antibiotics are more frequently used than other drugs and the risk of interactions at the level of binding to caffeine is much higher. Therefore, there is great clinical interest in understanding the binding of

different drugs to caffeine and the effects of fluoroquinolones and other competitors on this binding. Therefore, from this study, the following unique advantages have been summarized.

- The finding of the study of solvatochromic and photophysical properties of LVF and NRF antibiotic drugs provides detail understanding of what happened to the electronic properties, and the geomtrical structure of these drugs in different solvent polarity and drug concentration. These have incredible advantages since biological actions of the molecules are fundamentally depend on their molecular structures. Investigation of these properties also supports in noting diverse biochemical interaction through which a drug substance produces its pharmacological outcome in different micro environments.
- The computational investigation of HOMO-LUMO energy band gap, dipole moments and electrostatic potential map of the LVF and NRF are also highly valuable to identify the stability or the reactivity of the drugs and determine the site of attack due to photochemical reactions.
- Investigation of LVF-Caffeine and NRF-Caffeine interaction mechanism through fluorescence quenching also highly importants to understand the presence of reaction or complex formation between the caffene and drugs. Complex formation between the drug and caffeine affects the pharmacokinetic properties of the drugs.

Hence, based on the significance of the investigation of solvatochromic and photophysical properties of LVF and NRF and their interaction mechanism with caffeine, this research will expected

- To put a platform for researchers and post graduate students to apply on other drugs.
- The study would be helpful for pharmaceutical drugs industries to consider the findings during drug designing.
- Enables to identify the electrophilic and nucleophilic regions attacked during photochemical reactions.

1.5. Scope of the Study

The study covered the effect of solvent polarity on LVF and NRF antibiotic drugs and their photophysical properties in different solvents and sample concentration. The main focus of this investigation was to observe the effects of solvent polarity on absorption and emission spectra of the drugs, evaluate the ground and excited state dipole moments, optical transition

probability of LVF and NRF in different solvents. The photophysical properties study was done in different solvent polarity and sample concentrations. To support the experimental investigation, theoretical study was focused to obtain the optimized structure, the transition dipole moments, oscillator strength, and HOMO-LUMO energy band gaps. This research also includes investigation of interaction mechanism between LVF-CF and NRF-CF to identify the quenching mechanism of LVF-CF and NRF-CF and determination of the binding site and binding constant and thermodynamic parameters and nature of binding force.

2. LITERATURE REVIEW

This chapter deals with the literature review associated to the fluoroquinolones, their mechanism of action and resistance, photophysical properties, and solvent-drug interactions. The discussion started with the fluoroquinolones effectiveness in preventing different bacteria related diseases, mechanism by which these drugs kill bacteria and how the bacteria develops resistance to the fluoroquinolones drug. Moreover, the photophysical properties and solvent effects on various drugs previously studied and information it provides for the pharmaceutical development of drugs were discussed. In addition, review related to caffeine, its interaction with several drugs, effects of caffeine-drug interaction on pharmacokinetic properties such as drug adsorption, metabolic activities, drug distribution, and excretion are involved.

The chapter also deals with basic considerations of the interaction of light with matter by classical and semi-classical theory. The basic idea of electromagnetic theory, Maxwell's equations and wave equation in isotropic media are discussed using classical electromagnetic theory to show the various optical phenomena exhibited by medium in the first two section. In the next section the light interaction with molecular system in the ground and excited state briefly discussed. The time dependent Schrodinger equation has been solved to relate, the theoretical expressions that are important in UV-Vis spectroscopy. In addition, theory behind the photophysical parameters, general and specific solute-solvent interaction and fluorescence quenching due to molecules interaction obtained from fluorescence measurements are discussed. The theoretical concept behind the computational methods to model the structure and properties of molecules are also offered under this chapter.

2.1. Fluoroquinolones, Mechanism of Action, and Resistance

2.1.1. Fluoroquinolones

Fluoroquinolone (FQ) are derived from the quinolone family of antibiotics (Márquez-Lázaro et al., 2021; Matchette et al., 2007). They differ from quinolones by the replacement of the eighth carbon atom of the backbone with a nitrogen atom and the addition of a fluorine atom at the sixth position that give them more potent antibiotic action and a broader spectrum of activity (Redgrave et al., 2014). All compounds of FQs contain the oxygen at C-4 and carboxylic acid side chain at C-3, both of which have now been found to be essential to antibacterial activity of the drugs (Chuang et al., 2020).

FQs are drugs widely prescribed as antibiotic because they are effective to prevent and treat infection diseases. The drugs have broad medicinal spectrum antibacterial activity, strong tissue penetration and produce few adverse reactions (Márquez-Lázaro et al., 2021; Matchette et al., 2007). These antibiotics have excellent potency for the treatment of various bacterial infections such as upper and lower respiratory infections, sexually transmitted diseases, and some skin, bone, soft tissue infections and community acquired pneumonia (Fish, 2001; Viola et al., 2004). Besides their classical anti-bacterial activities, FQs also display diverse typical biological profiles such as anti-cancer (Sharma et al., 2020), anti-tubercular (Stojanović et al., 2020), anti-malarial (Matchette et al., 2007), and anti-HIV (Sekgota et al., 2017) properties that play a pivotal role in the development of new drugs. They also provide side effects including gastrointestinal reactions, central nervous system reactions, Geno toxicity, photo-toxicity, and some minor adverse effects (Sárközy, 2001).

The fluoroquinolone drugs Levofloxacin and Norfloxacin Figure 1(a) and 1(b) respectively are among the famous fluoroquinolone drugs frequently prescribed for patients. They also contain a carboxylic acid that required for antimicrobial activity (Park et al., 2002). A fluorine atom at position 6 on those drugs carboxylic acid nucleus enhances the efficacy of these compounds against gram-negative pathogens and broadens the spectrum of activity against gram-positive pathogens. A basic nitrogen containing moiety enhances tissue penetration and reduces the central nervous system toxicity (Sárközy, 2001).

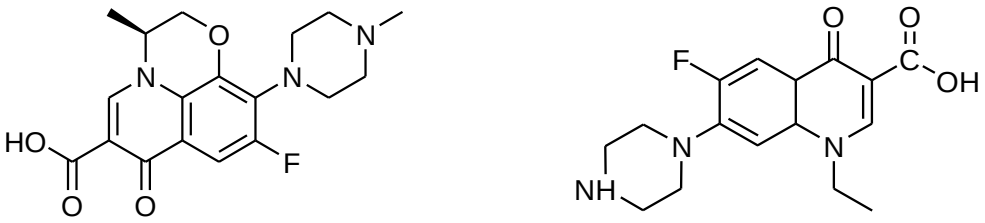

a) b)

Figure 1. Chemical structure of (a) Levofloxacin and (b) Norfloxacin.

2.1.2. Fluoroquinolones Drugs Mechanism of Action and Resistance

LVF and NRF drugs inhabit bacteria by stopping two enzymes involved in bacterial DNA synthesis, both of which are DNA topoisomerases that human cells lack. They are essential for bacterial DNA replication, and thus enabling these agents to be both specific and bactericidal (Fàbrega et al., 2009; Sárközy, 2001). DNA topoisomerases are responsible for separating the

strands of duplex bacterial DNA, inserting another strand of DNA through the break, and then resealing the originally separated strand (Fàbrega et al., 2009; Sharma et al., 2020). DNA gyrase is an enzyme found only in bacteria and it introduces negative super helical twists in the bacterial DNA double helix ahead of the replication, thereby catalysing the separation of daughter chromosomes. (Fàbrega et al., 2009; Sharma et al., 2020). Whereas, Topoisomerase IV enzyme is responsible for decantation that is, removing the inter linking of daughter chromosomes, thereby allowing segregation into two daughter cells at the end of a round of replication (Fàbrega et al., 2009; Karampela & Dalamaga, 2020).

LVF and NRF are interact with the DNA gyrase and topoisomerase IV of bacteria to create conformational changes that result in the inhibition of normal enzyme activity (Gao et al., 2019). As a result, the new drug-enzyme DNA complex blocks progression of the replication fork, thereby inhibiting normal bacterial DNA synthesis and ultimately resulting in rapid bacterial cell death (Sharma et al., 2009). The targeting of either DNA gyrase or topoisomerase IV fluoroquinolones varies with bacterial species and specific fluoroquinolone. However, as a broad generalization, the significant target in Gram-negative bacteria is DNA gyrase, whereas in Gram-positive microorganisms topoisomerase IV is preferentially targeted (Sissi et al., 2001). When either DNA gyrase or topoisomerase IV induces transient double-strand DNA breaks, they first bind covalently to the DNA to form enzyme-DNA complexes before breaking the bound DNA, passing another segment of DNA through this break, and re-joining the original DNA segment (Aldred et al., 2013; Jeffrey, 2014). When a fluoroquinolone drugs are present, the complex is transformed into a drug-enzyme-DNA complex in which the topoisomerase is trapped with the bound DNA (Hooper, 2001; Mohd et al., 2010).

Antibiotic resistance is one of the most pressing global concerns in medicine, with highly resistant pathogens of many species proving difficult to treat (Redgrave et al., 2014). Fluoroquinolone resistance develops through two main mechanisms: changes in the drug target enzymes and in access to the drug target enzymes. Alterations in the drug target enzymes may be sub-classified as mutations in DNA gyrase and mutations in topoisomerase IV (Hooper & Jacoby, 2015). These mutations differ among the bacterial types in terms of their relative impact on fluoroquinolone resistance development (Fàbrega et al., 2009; Sárközy, 2001). Alterations in DNA gyrase occur most commonly in fluoroquinolone resistant Gram-negative bacteria and may affect either the gyrase A or gyrase B subunits (Hooper, 2001; Redgrave et al., 2014). Mutations in the gyrase A subunit tend to cluster in a region known as the quinolone resistance determining region (Tanaka, 1983). The most common mutations in this region are

believed to cause resistance through decreased drug affinity for the altered gyrase-DNA complex. Gyrase B mutations occur less commonly than gyrase A mutations(Hooper, 2001). Alterations in gyrase B also tend to confer lower levels of resistance than do gyrase A mutations (Fàbrega et al., 2009; Hooper & Jacoby, 2015; Tanaka, 1983).

DNA gyrase mutations both in the gyrase A and gyrase B subunits, also occur in Gram-positive bacteria; however, as DNA gyrase typically serves as a secondary target to topoisomerase IV in these bacterial species, the relative importance of these mutations is questionable (Fàbrega et al., 2009; Tanaka, 1983). DNA gyrase appears to be the primary target for Gatifloxacin and Moxifloxacin in pneumonia (Lorenzo et al., 2009; Tanaka, 1983). Furthermore, in fluoroquinolone resistant Gram-positive bacteria, alterations in either subunit of DNA gyrase have typically been found only in the presence of concomitant topoisomerase IV mutations. Topoisomerase IV mutations have been most extensively studied in fluoroquinolone resistant Gram-positive bacteria (Hooper & Jacoby, 2015; Tanaka, 1983).

2.2. Fluoroquinolone Photophysical Properties

In addition to their pharmaceutical applications as antibacterial agents, FQs are also fluorescent drugs that have also been used as luminescent probes for various analytical and bioanalytical purposes (Sciscenko et al., 2021). These enable us to understand and examine photophysical properties of the drugs which can provide the electronic properties, geometrical structure, and the mechanism of reaction of these drugs with light (Desai et al., 2016; Kian et al., 2019). Photophysical properties of FQs have been also extensively studied over the last decade partly because of the discovery of photophysical properties provide information about drugs structural change, and their photo toxicity properties (Kian et al., 2019).

Due to its intrinsic fluorescence photophysical properties, Norfloxacin photophysical properties have been comprehensively studied in different pH conditions. As the study confirms, the change in photophysical properties of NRF observed because of the intramolecular charge transfer (ICT) process taking place from the nitrogen on piperazinyl ring to the aromatic fluoroqulinone system (Lorenzo et al., 2008; H. Zhang et al., 2019). The photophysical properties of antibacterial drug Moxifloxacin (Lorenzo et al., 2008; Viola et al., 2004), Danofloxacin (Ma, 2018) and Sarafloxacin antibiotic (Li et al., 2012) are also investigated. All investigation indicates the dipole moment, quantum yield, Oscillator strength of the drugs are varied in different environments. Change in those photophysical properties of the drug molecules indicates the structural change of the molecules that can bring side effects,

affects the effectiveness of the drugs and can reveal complex formation (Li et al., 2012; Lorenzo et al., 2009).

In addition, antibiotic fluoroquinolone drug namely Norfloxacin and Ofloxacin photophysical properties have been investigated in bio mimicking environments formed by bile salts. As the study indicates, the photophysical enhancement and fall of particular species are sensitive to the excitation wave length in bile salt aggregates (Park et al., 2002; Thakur et al., 2012). Recently, the photophysical properties of Ciprofloxacin in some amino acids was also studied by fluorescence spectroscopy and result shows the drug is intrinsically a highly fluorescent molecule, its photophysical properties are altered by acid as compared to aqueous solution (Paul et al., 2017; Polishchuk et al., 2012).

2.3. Solvent Drug Interaction

The effect of solvent on the absorption and fluorescence characteristics of drug molecules has been a subject of extensive research (Raikar et al., 2006). Excitation of a molecule by photon causes a redistribution of charges leading to conformational changes in the excited state. This can result in increase or decrease of dipole moment of the excited state as compared to ground state. The dipole moment of an electronically excited state of a molecule is important property that provides information on the electronic and geometrical structure of the molecule in short lived state. Knowledge of the excited-state dipole moment of electronically excited molecules is quite useful in designing nonlinear optical materials (Khadem Sadigh et al., 2017), elucidating the nature of the excited states and in determining the course of photochemical transformation (Kumar et al., 2001; Sharma et al., 2021a).

Moreover, the interactions between drug molecules and their surrounding media are important in biological applications. In biological systems, drugs interact with media like aqueous solution, acids, molecules such as proteins and other externally taken beverages. The type and degree of interactions are controlled by functional groups of the drugs (Zakerhamidi et al., 2017). It should be noted that, the polarity parameters of drug materials originate from their chemical structure, activity of functional groups in the molecular structure and the type of molecular interactions (Kumari et al., 2017). The functional groups activity and applicability of drug based on the molecular structure change and interactions with environments. The conventional analysis methods provide information about the structure of the material, but the polarity parameters can provide valuable information about the chemical structure and interactional behaviour of functional groups of drug material (Kian et al., 2019).

The chemical structure of FQs contains several proton binding sites such as carboxyl, carbonyl and amine groups. As a result of those functional groups, the acid-base properties of FQs are influenced by physicochemical characteristics of the solvents (De Guidi et al., 2011). Study report shows FQs and Naphthyridones provide completely different antibacterial responses and chemical properties as the physicochemical properties of solvents are changed (Rubinstein, 2001). For these matter the behaviour of Ciprofloxacin in different solvents were studied and the result specifies that the drug molecule absorption and emission spectra has been show a bathochromic shift and the excited state energy can be highly reduced or relaxed by the polar solvent molecules (Alizadeh et al., 2012). In addition, the fluorescence properties of Ofloxacin, and Norfloxacin were studied in H_2O-CH_3OH (methanol) and H_2O-CH_3CN (acetonitrile) mixed solvent and the result shows the drugs were very sensitive to the solvents (Cuquerella et al., 2006). The spectral shift is indication of geometrical structural change of the drugs.

2.4. Caffeine and its Interaction with Different Drugs

Caffeine (1, 3, 7-trimethylxanthine) from dietary sources mainly coffee, tea and soft drink is probably human kind most widely consumed drug. It is naturally found in leaves, seeds or fruits of 63 plant species (Carrillo & Benitez, 2000). The intake of caffeine is so much a part of dietary habits that one occasionally looks at its consumption as a health concern. The popularity of caffeine is related to central nervous system stimulant properties, which are manifested as elevated mood, decreased fatigue and increased capacity for work (Benvenga et al., 2008; Vanattou Saïfoudine et al., 2012). Consuming about 400 mg of caffeine (accounts for 2 to 3 cups of coffee) per day is considered safe as reported by the US Department of Agriculture as well as the European Food Safety Authority (Nawrot et al., 2003).

Caffeine (Figure 2) can interact with drug and may make our drug less effective, cause unexpected side effects or increase the action of a particular drug. Some drug interactions can even be harmful (Lasswell et al., 1984; Vanattou Saïfoudine et al., 2012). Previous infrared radiation (IR) investigation of caffeine interaction with non-steroidal anti-inflammatory drugs such as Ibuprofen, Aspirin, Paracetamol and indomethacin shows complex formation between the molecules that can influence the pharmacodynamics properties of the drugs (Constantinos, 2022, Khalil, 1996). In addition, an experimental and computational investigation of Caffeine interaction with sulfamethoxazole drugs clearly indicates the complex formation between the molecules (Kesimili, et al., 2003).

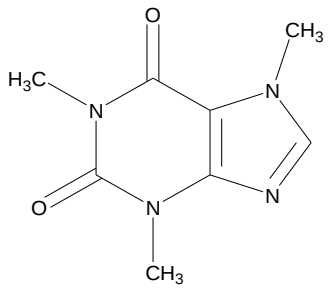

Figure 2. Chemical structure of caffeine

The consumption of caffeinated beverages whether it be in the form of energy drinks, diet drinks or coffee is almost popular and often perceived as harmless by patients. However, recent investigation on Caffeine-clozapine interaction shows the interaction provide toxicity (Yartsev & Peisah, 2021). The Toxicity or effects of the drug-Caffeine interaction are mainly because of the pharmacokinetic properties of the drug altered. Although tolerance develops many of the pharmacological effects of caffeine, tolerance may be overwhelmed by the nonlinear accumulation of caffeine when its metabolism becomes saturated (Carrillo & Benitez, 2000; Yartsev & Peisah, 2021). The following sections summarize how the interaction of the drug and caffeine affects the pharmacokinetic properties of the drugs.

2.4.1. Effect of Caffeine on Pharmacokinetics of Drugs

Caffeine is the most known compound which has a pharmacokinetic interaction with many drugs (Krishna et al., 2013; Persky, 2005). Patients as well as healthy people throughout the world are starting and finishing their days with cups of coffee, tea and other source of caffeine. Even though caffeine has many profits to our body, there is also a clinically significant pharmacokinetic interaction between caffeine and many important over the counter as well as prescription medications (Carrillo & Benitez, 2000). The pharmacokinetics of drugs can be affected via different mechanisms such as altering the absorption, distribution, excretion, and induction or inhibition of metabolizing enzymes (Belayneh & Molla, 2020).

2.4.2. The Effect of Caffeine on Absorption of Drugs

Caffeine can affect the absorption process of drugs by changing the dissolution profile, changing the gastrointestinal (GI) pH, affecting the sink condition of the GI membrane and blood, affecting the GI emptying time, formation of complex, and inhibiting glucose-6-phosphatase. Caffeine interacts with different drugs by a dipole-dipole force or hydrogen bonding between the polarized carbonyl groups of caffeine and the hydrogen atom of drugs(Carrillo & Benitez, 2000; Krishna et al., 2013). It forms more soluble complexes with

several drugs which have organic acid anions. But, sometimes less soluble complexes of drugs with some other organic acids are formed. Caffeine forms hydrogen bonded complexes with various drugs which have a proton donor functional group: phenol, phenol l derivatives, and aliphatic alcohols. For instance, with the addition of caffeine, the solubility of p-amino benzoic acid rises linearly due to complexation (Fukasawa et al., 2006).

Coffee and other caffeine containing products are found to interfere with the pharmacokinetic profile of citalopram oxalate (selective serotonin reuptake inhibitor). The in vitro and in vivo study on the release showed that the absorption of citalopram oxalate decreased by the formation of complexes between the drug and caffeine. This complex formation reduced the bioavailability of citalopram oxalate tablets by 33.15% (in vitro) and 28% (in vivo) by decreasing the dissolution of the citalopram tablet (Krishna et al., 2013). Another in vitro investigation report revealed that, the reduction in effectiveness of neuroleptics and tricyclic drugs as a result of their interaction with caffeine/caffeinated beverages (Lasswell et al., 1984). The intestinal absorption of both inorganic and organic compounds could be decreased by caffeine. For instance, about 39 - 90% of iron absorption is reduced when a cup of coffee as well as other caffeinated beverages is taken with an iron rich meal (Garcıa-Casal et al., 1998). Due to this, coffee and other beverages containing caffeine should be separated from iron-containing foods or supplements (Fukasawa et al., 2006).

Caffeine is also a known stimulant of gastric acid secretion by activating several taste type 2 bitter receptors (TAS2Rs) due to its bitter taste. This leads to a decrease in the gastric pH by increasing the hydrochloric acid secretion (Liszt et al., 2017). The production of excess hydrochloric acid in the stomach can affect the extent of drug absorption through acid degradation of the drug, conversion of the drug substance into an insoluble form, and by altering the drug's rate of dissolution (Wendl et al., 1994).

The rate of drug degradation by the acid catalysed process is pH dependent, thus, a little change in pH can have a great impact on the amount of drug that survives gastric transit. In addition to its acidic nature, caffeine also stimulates the hyper secretion of hydrochloric acid in the stomach. As a result, this highly acidic stomach contents are easily passed into the small intestine more rapidly than normal. This may lead to a decrease in the pH of the intestinal environment which affects the absorption of several basic drugs (Nehlig, 2022). For example, a drop of one pH unit reduces the amount of active midazolam drug by 75% after drinking two to three cups of coffee. Generally, increased gastric acid secretions in the stomach results in

faster dissolution of basic drugs which makes the absorption rate of such drugs by twenty times faster (Liszt et al., 2017).

2.4.3. The Effect of Caffeine on Distribution of Drugs

After absorption from different sites of administration directly into the bloods stream, a drug distributes into the interstitial and intracellular fluids of the whole body part. This process involves passing of a number of physiological barriers which partly depends on physicochemical properties of the individual drugs (Liguori et al., 1997; Schmidt & Fanchamps, 1974). The most important physiological factors which affect drug distribution are blood tissue partitioning and availability of different barriers which prevent the distribution of drugs (Gilman's, 1985; Schmidt & Fanchamps, 1974). Blood-tissue partitioning refers to the relative binding ability of a drug to plasma proteins and tissue macromolecules that limits the concentration of free drug. Blood-brain barrier (BBB)is the most common barrier affects drug distribution to the central nervous system(Granados-Soto et al., 2011).

Previous study revealed that caffeine protects the BBB breakdown by keeping the expression levels of tight junction proteins. These proteins bind the cells of the BBB closely to each other to avoid unwanted molecules, even extremely lipophilic drugs, crossing into the central nervous system (Tran & Yijun Zhang, 2015; Weiser & Weigmann, 2019). The stabilization of BBB by caffeine has great implications during therapeutic interventions of neurological disorders in two ways. First, caffeine can prevent the opening of the BBB which might hinder the passage of important drugs into CNS including drugs with high lipophilic nature(Tran & Yijun Zhang, 2015; Willson, 2018). On the other hand, coffee can prevent the passage of different toxic substances to CNS by strengthening the junction of the BBB. Because of this, it is important to limit ingestion of coffee by patients taking drugs acting in the CNS; for instance, drugs used for Alzheimer treatment such as donepezil (Tran & Yijun Zhang, 2015).

2.4.4. The Effect of Caffeine on Metabolism of Drugs

Enzymes (mostly liver enzymes) that are secreted over time to protect the body from exogenous chemicals are responsible for most of drug metabolism reactions (Schmidt & Fanchamps, 1974). The metabolites are mostly less pharmacologically active or generally inert. Metabolism also usually makes the drugs more water soluble so that they can be easily excreted (Franklin, 2003). Coffee is one of the factors which affect drug metabolism by affecting metabolizing enzymes in different ways(Das et al., 2019; Granados-Soto et al., 2011).

The dominant and most abundant enzyme that is responsible of metabolizing caffeine is a CYP450 liver enzyme also called CYP1A2 (Urry et al., 2016). This enzyme also has a key role for the metabolism of several clinically important medications. When caffeine and drugs that are metabolized by CYP1A2 are administered together, computing for the same enzyme is common (Barcelos et al., 2020). Consequently, the availability of enzymes to metabolize drugs is decreased as it is saturated by caffeine. In other word, caffeine and drugs act as a metabolic inhibitor to each other which lead to the decreased rate of elimination of drugs (Weiser & Weigmann, 2019).

A study done on healthy adult male albino rabbits to assess the effect of caffeine on the anticoagulation activity of warfarin revealed that caffeine significantly inhibits the metabolism of warfarin by saturating enzymes which is responsible of metabolizing it (Fish, 2001). Because of this, ingestion of caffeine increased the plasma concentration of warfarin which leads to enhanced anticoagulant effects(Weiser & Weigmann, 2019). This result suggests that health professionals should advise patients to stop the frequent use of coffee and other caffeine-rich products during warfarin therapy (Granados Soto et al., 2011).

2.4.5. The Effect of Caffeine on the Excretion of Drugs

Immediately after being absorbed into the systemic circulation, drugs are removed from the body either unchanged by the process of excretion or converted to metabolites. Most drugs and drugs metabolites are removed by the kidney as it is the most important organ for excretion (Schmidt & Fanchamps, 1974). Some drugs and metabolites are excreted either in the bile or secreted directly into the intestinal tract and not reabsorbed (Carrillo & Benitez, 2000). There are different mechanisms in which caffeine affects the excretion of some drugs. One of the main side effects of consuming too much caffeine is frequent urination (Franklin, 2003).

The mechanism of caffeine to increase urination is by increasing the glomerular blood pressure within capillaries in the kidney. Due to this mechanism, caffeine increases the blood filtration which leads to an increase in urine formation (Liguori et al., 1997). This can cause the body to become quite easily and quickly depleted of some of the nutrient essential for maintaining good health and some medications. Minerals that can become depleted very easily include calcium, magnesium, sodium, phosphate, and potassium (Barcelos et al., 2020; Urry et al., 2016). A hormone called antidiuretic hormone is responsible to regulate urine production in the body. Based on the condition of body dehydration and the need to retain water, the body releases this hormone which concentrates the urine to save body fluids (Fukasawa et al., 2006). Coffee

causes much production of dilute urine by inhibiting the antidiuretic hormone (Osswald et al., 1997). The study done in Czech Republic also showed that even moderate daily intake of coffee at the dose up to 400 mg daily may be associated with adverse outcomes, like bone status and calcium balance (Ženata et al., 2019).

As one observational study on women showed that for every 150 mg of caffeine ingested (equivalent to one to two cup of coffee), there was a loss of 15mg of calcium every hours after the consumption of caffeine. This study also showed that women who consumed more than 300mg of caffeine had lost more bone in the spine than women who consumed less amount of caffeine (Liguori et al., 1997). In addition, more hip fractures occurred in these women than those who avoid caffeine or drink in moderation. Water-soluble vitamins such as the B vitamins (B1 and B12), magnesium, sodium, chloride, and water can be also depleted as a result of the fluid loss due to the diuretic effect of caffeine (Ženata et al., 2019).

2.5. Theory of Light Matter Interaction

Spectroscopy is the study of the interaction of electromagnetic radiation (EMR) with matter. Classically, light matter interactions are a result of an oscillating electromagnetic field resonantly interacting with charged particles in the matter, most often bound electrons. We observe these processes either through changes to the light induced by the matter, such as absorption or emission of new light fields. This section deals with basic considerations of the interaction of light with matter by classical and semi-classical theory. The basic idea of electromagnetic theory, the quantities expresses the phenomena of light interaction with molecular system in the ground and excited state briefly discussed. The time dependent Schrodinger equation has been solved to relate transition diploe moment with the molar extinction coefficient. In the last section, the theoretical concept used in the computational techniques are also presented.

2.5.1. Maxwell's Equations and the Wave Equations

The static and dynamic microscopic characteristics of electromagnetic field or radiation interaction with material media is described by four Maxwell's Equations (Milonni & Eberly, 2010). They are the basis for the most fundamental description of electric and magnetic fields of light. The Maxwell's equation for a dielectric medium with no free electric charges or currents, are described as Eq. (2.1- 2.4) (Fowles, 1975; Milonni & Eberly, 2010).

$$\vec{\nabla} \times \vec{E} = -\frac{\partial \vec{B}}{\partial t} \tag{2.1}$$

$$\vec{\nabla}.\vec{D} = \rho \tag{2.2}$$

$$\vec{\nabla}.\vec{B} = 0 \tag{2.3}$$

$$\vec{\nabla} \times \vec{H} = \frac{\partial \vec{D}}{\partial t} + \vec{J} \tag{2.4}$$

Where $\vec{E}$ is the electric field strength, $\vec{H}$ is the magnetic field strength, $\vec{B}$ is the magnetic induction. The electromagnetic-matter interaction nature at a given point are described by the quantities such as electric charge per unit volume (ρ), the magnetic dipole moment per unit volume or magnetization ($\vec{M}$), polarization or the electric dipole moment per unit volume $(\vec{P})$, and the current density or electric current per unit area ($\vec{J}$). The material response expressed by material relation as shown in Eq. (2.5-2.6).

The electric displacement ($\vec{D}$) is defined by

$$\vec{D} = \varepsilon_0 \vec{E} + \vec{P} \tag{2.5}$$

The magnetic intensity vector H is given by,

$$\vec{B} = \mu_0 (\vec{H} + \vec{M}) \tag{2.6}$$

Where μ_0 is, the permittivity of free space and ε_0 is permeability in vacuum. For non-magnetic and non-conducting media, the volume density of electric charge and magnetization are zero. Thus the Maxwell's equations expressed in Eq. (2.1) to (2.3) take the following form (Fowles, 1975; Patel, 2019).

$$\vec{\nabla} \times \vec{E} = -\mu_0 \frac{\partial \vec{H}}{\partial t} \tag{2.7}$$

$$\vec{\nabla} \times \vec{H} = \varepsilon_0 \frac{\partial \vec{E}}{\partial t} + \frac{\partial \vec{P}}{\partial t} \tag{2.8}$$

$$\vec{\nabla}.\vec{E} = 0 \tag{2.9}$$

$$\vec{\nabla}.\vec{H} = 0 \tag{2.10}$$

The general wave equation for electric field can be obtained by using the second order linear partial differential of Maxwell's equations for the description of waves by taking the curl of Eq. (2.7) and time derivative of Eq. (2.8) and rejecting the magnetic field (Fowles, 1975; Milonni & Eberly, 2010). Thus,

$$\vec{\nabla}\times(\vec{\nabla}\times\vec{E})+\frac{1\partial^2\vec{E}}{c^2\partial t^2}=-\mu\frac{\partial^2\vec{P}}{\partial t^2} \tag{2.11}$$

By general identity of vector calculus the first left hand side of Eq. (2.11) can be expressed as follows (Milonni & Eberly, 2010).

$$\vec{\nabla}\times(\vec{\nabla}\times\vec{E})=\vec{\nabla}(\vec{\nabla}.\vec{E})-\vec{\nabla}^2\vec{E} \tag{2.12}$$

Substituting Eq. (2.12) in to Eq. (2.11) one finds

$$\vec{\nabla}^2\vec{E}-\vec{\nabla}(\vec{\nabla}.\vec{E})-\frac{\partial^2\vec{E}}{c^2\partial t^2}=\frac{\partial^2\vec{P}}{\varepsilon_0 c^2\partial t^2} \tag{2.13}$$

Eq. (2.13) is a partial differential equation with the term on the right side a source term shows the presence of polarization within the medium. It tells us how the electric field depends on the electric dipole moment density P of the medium.

Where,

$$\mu_0\varepsilon_0=\frac{1}{c^2} \tag{2.14}$$

Where c represents the velocity of light in vacuum ($3\times10^8 m/s$). The way in which the propagation of light is affected by the source is revealed by the solution of the wave equation when the source term is included. For non-conducting (a neutral isotropic dielectric media) the polarization term is important. This term leads to an explanation of many optical effects including dispersion and absorption (Milonni & Eberly, 2010). We will be particularly interested in transverse fields (also called solenoidal or radiation fields), which satisfy

$$\vec{\nabla}.\vec{E}=0 \tag{2.15}$$

The wave equation of radiation fields expressed on Eq. (2.13).

$$\vec{\nabla}^2\vec{E}-\frac{\partial^2\vec{E}}{c^2\partial t^2}=\frac{\partial^2\vec{P}}{\varepsilon_0 c^2\partial t^2} \tag{2.16}$$

However this (Eq. 2.16) cannot be done solely with in the frame work of Maxwell's equations, since polarization is the property of the material media. We need to know how a dipole moment density is produced in the medium. For this purpose in the next section, a theory of dielectric media will be introduced. First, however this section would be completed with a discussion of the solution of the Maxwell's equation in vacuum, where a wave equation (2.11), does not contain the polarization term (Fowles, 1975; Milonni & Eberly, 2010; Patel, 2019). In the absence of any medium the right-hand side of Eq. (2.16) is zero and we have the "homogeneous" wave equation.

$$\vec{\nabla}^2\vec{E} - \frac{\partial^2\vec{E}}{c^2\partial t^2} = 0 \tag{2.17}$$

For a wave propagating in the z-direction in free space the solution of wave equation becomes

$$\vec{E}(\vec{z},t) = \vec{\varepsilon}E_0\cos(wt - kz) \tag{2.18}$$

Where, the wave vector and phase velocity are defined as follows

$$\kappa_0^2 = \frac{\omega_0^2}{c^2} \tag{2.19}$$

$$u_p = \frac{\omega}{\kappa_0} = c \tag{2.20}$$

2.5.2. Propagation of Light in Isotropic Dielectric

Isotropic dielectrics are medium whose polarization always has a direction that is parallel to the applied electric and a magnetic fields which does not depend on the direction of the electric field. When light propagate through them, their polarization expressed in terms of simple Lorentz model. Lorentz oscillator model is model of a classical atom, in which the electron is harmonically bound to the nucleus (Fowles, 1975; Patel, 2019).

The classical theory satisfactorily treats many important features of the interaction of light with matter by adopting the hypothesis that an electron exert a binding force on nucleus. This hypothesis states that an electron in an atom responds to light, as if it was bound to its atom or molecule by simple spring (Milonni & Eberly, 2010). The goal of this model is to use Newton's second law to obtain the motion of the electron, and can then be used to obtain expressions for the dipole moment, polarization, susceptibility, and dielectric constant. As a consequence, the

electron can be imagined to oscillate about the nucleus and this leads to the following equation of motion (Fowles, 1975; Milonni & Eberly, 2010; Patel, 2019) described on Eq. (2.21).

$$m\frac{d^2\vec{x}}{dt^2} = -e\vec{E}(\vec{R},t) - K\vec{x} \tag{2.21}$$

Where K is the spring constant and Eq. (2.21) is called Newton's second law. As a result of applied electric filed on the dielectrics substance, individual electron is displaced by some distance x from its original location, consequently each atom has a dipole moment. If the density of atoms is signified by N, then the density of dipole moment is N times the individual dipole moment of each atom (Milonni & Eberly, 2010). Hence, the polarization density induced in the medium by the field is given by:

$$\vec{P} = N\vec{p} = Ne\vec{x} \tag{2.22}$$

The dependence of electric field on dipole moment density of the medium is here clearly observed on Eq. (2.16) and Eq. (2.21), telling us how the electron displacement depends up on the electric field whereas Eq. (2.22) links these two basic equation by relating polarization to displacement (Fowles & Lynch, 1968; Kawano & Kitoh, 2001). The electron oscillator model thus ties the Maxwell's equations with Newton's law of motion. Solution of these coupled equations provide information about provide mutual interaction of light and matter. Further, if atoms or molecules of the medium absorb radiation energy while it transits through the materials, the strength of EMR would be reduced. To account for the absorption of radiation in the electron oscillator model, it must be assumed that the oscillator is subject to a frictional force in addition to the applied field. This absorption can be more explained by the assumption of Lorentz electron oscillator of Eq. (2.21). The classical damped harmonic oscillators due to bound electron modify Newton's force of Eq. (2.21) can be given as follows (Fowles & Lynch, 1968; Milonni & Eberly, 2010).

$$m\frac{d^2\vec{x}}{dt^2} = -e\vec{E}(\vec{R},t) - K\vec{x} + \vec{F}_{fric} \tag{2.23}$$

Since the assumption is compatible with the idea of frictional drag, and a frictional damping force is proportional to the velocity of the electron, and some proportionality constant designated by γ. Therefore the differential equation of the motion becomes (Belay, 2011; Milonni & Eberly, 2010).

$$m\frac{d^2\vec{x}}{dt^2}+m\gamma\frac{d\vec{x}}{dt}+K\vec{x}=-e\vec{E} \tag{2.24}$$

In order to find trial solution for Eq. (2.24), let us consider the assumption that the electric field varies harmonically with the time and the motion of electron has also similar harmonic time dependence $\vec{x}=e^{i\omega t}$, thus, substitution of this field into Eq. (2.24) results in.

$$(-m\omega^2-i\omega m\gamma+K)\vec{x}=e\vec{E} \tag{2.25}$$

Therefore, the polarization described on Eq. (2.22) would be given by

$$\vec{P}=\frac{Ne^2/m}{-m\omega^2-i\omega m\gamma+K}\vec{E} \tag{2.26}$$

A more significant way of writing Eq. (2.26) is in which the equation of resonance frequency of bound electrons have been written. Thus Eq. (2.26) can be written as:

$$\vec{P}=\frac{Ne^2/m}{\omega_0^2-\omega^2-i\omega\gamma}\vec{E} \tag{2.27}$$

Apart from Lorentz model, classical electrodynamics proves that polarization is related to the electric field $\vec{E}$ as Eq. (2.28).

$$\vec{P}=\varepsilon_0(\varepsilon_r-1)\vec{E}=\varepsilon_0\chi\vec{E} \tag{2.28}$$

The relative dielectric constant is related to refractive index n by

$$n=\sqrt{\varepsilon_r} \tag{2.29}$$

Substituting Eq. (2.29) into Eq. (2.28) and comparing it with Eq. (2.27) yields

$$n^2-1=N\frac{e^2}{\varepsilon_0 m(\omega_0^2-\omega^2-i\omega\gamma)} \tag{2.30}$$

For gaseous media at not too high pressures the refractive index n is nearly 1. Hence $n^2-1\approx 2(n-1)$ which is sufficiently accurate for the most purpose and the above equation can be reduced to (Brooks, 2013)

$$n=1+N\frac{e^2}{2\varepsilon_0 m(\omega_0^2-\omega^2-i\omega\gamma)} \tag{2.31}$$

In order to make clear about the physical implication of Eq. (2.31) or the complex index of refraction, let us separate its real and the imaginary part as follows:

$$n = n' - i\kappa \tag{2.32}$$

For electromagnetic wave

$$\vec{E} = E_0 \exp[i(\omega t - kz)] \tag{2.33}$$

Passing through a medium in the z direction, with the refractive index n has same frequency as in vacuum or $\omega_n = \omega_0$ but the wave vector becomes $k_n = k_0 n$ and inserting this into Eq. (2.33). gives,

$$\vec{E} = E_0 e^{-k_0 kz} e^{i(\omega t - k_0 n' z)} \tag{2.34}$$

In Eq. (2.31), the imaginary part $\kappa(\omega)$ of the complex refractive index n describes the absorption of electromagnetic wave. At penetration depth the amplitude of $E_0 e^{-k_0 kz}$ decreases to 1/e of its value at $z = 0$. On the other hand, the real part $n'(\omega)$ represents the dispersion of the wave that means the dependence of the phase velocity $u(\omega) = \dfrac{c}{n'(\omega)}$ on the frequency. The intensity which is $I \alpha E^* x E$ then decrease as (Fowles, 1975; Milonni & Eberly, 2010):

$$I = I_0 e^{-2\kappa k_0 z} = I_0 e^{-\alpha z} \tag{2.35}$$

Where the absorption coefficient $\alpha = 2k_0\kappa = \dfrac{4\pi\kappa}{\lambda_0}$ is proportional to the imaginary part of the complex refractive index. The frequency dependent α and n using the above equation as the real and imaginary parts becomes.

$$\alpha = \frac{Ne^2 \omega_0 \gamma \omega}{c\varepsilon_0 m[(\omega_0^2 - \omega^2)^2 + \gamma^2 \omega^2]} \tag{2.36}$$

$$n' = 1 + \frac{Ne^2(\omega_0^2 - \omega^2)}{2\varepsilon_0 m[(\omega_0^2 - \omega^2)^2 + \gamma^2 \omega^2)} \tag{2.37}$$

The above two equations are the Kramers-Kronig dispersion relation and they are the absorption and dispersion of the complex refractive index (Demtröder, 2010). In addition, from the above equations the real and imaginary part of dielectric constant, susceptibility can also be obtained, however since classical way of interaction of light with matter are not our interest

we move to the next section where the interaction of light with matter is treated by semi-classical approach (Brooks, 2013; Milonni & Eberly, 2010).

Thus, in the next sections the absorption and emission of light by molecular system would be presented by semi-classical approach in which the radiation incident upon an atom is described by a classical electromagnetic plane wave and the molecules, on the other hand, it is treated quantum mechanically. For molecular system instead of absorption coefficient the absorption cross-section and molar extinction coefficient were used to express the phenomena of absorption and these are discussed in detail in the next two sections.

2.5.3. Absorption and Emission of Radiation

The phenomena that well express electromagnetic radiation interaction with molecular systems are absorption and emission of fluorophore. As a result of light absorption, molecules transition happened from initial state to the other states. To discuss transition in molecular states the time dependent Schrodinger equation is applicable. It allows calculating the atomic scale phenomena as a function of time as well as space. Thus, in the next section the general solution for time dependent Schrodinger equation will be derived.

2.5.3.1. The Time Dependent Schrodinger Equation

The quantitative study of the interaction of electromagnetic radiation with matter can be done using a simple semi-classical model. In this approach, the electromagnetic radiation is treated classically, while the transition dipole moment of the molecule are obtained by solving the time-dependent Schrödinger equation and the equations is compared with the experimentally measured quantities (Brooks, 2013; Razum, 1989).

When an electromagnetic radiation is exposed to molecules for limited time, the oscillating electric field of a radiation disturbs the potential energy of the molecule and scape it from its initial stationary state and it undergoes in to another stationary states. (Fowles & Lynch, 1968; Sonnessa & Wilson, 1967). The radiation field causes transitions in the atom. This means that the Eigen-functions of the atom become time-dependent. Let $\hat{H}^0$ is the quantum mechanical Hamiltonian in the absence of radiation field on the molecular system. Considering two level system of a molecule with $|k_i\rangle$, and $|m_i\rangle$ state, the time independent Schrodinger equation in the x direction given by Eq. (2.37) and can take the following form (Fowles & Lynch, 1968; Milonni & Eberly, 2010; Parisi & Auletta, 2000).

$$\hat{H}^0\psi_k^{(0)}(x) = E_k^{(0)}\psi(_k^{(0)}(x) \tag{2.37}$$

Where, $\psi_k^{(0)}(x)$ is wave function and $E_k^{(0)}$ is the energy of unperturbed system of molecules. In contrast, if $\hat{H}^{'}$ is the Hamiltonian operator due to interaction between the system and radiation, the time dependent Schrodinger equation can be written as follows to point out the state change with time (Belay, 2011; Milonni & Eberly, 2010).

$$i\hbar\frac{\partial\psi}{\partial t} = \hat{H}^{'}\psi \tag{2.38}$$

The Schrödinger equation during irradiation time becomes the sum of unperturbed Hamiltonian of the free atom plus the perturbation operator.

$$i\hbar\frac{\partial\psi}{\partial t} = (\hat{H}^{'} + \hat{H}^0)\psi \tag{2.39}$$

Where the general state wave function expressed as a linear superposition of

$$\psi(x,t) = \sum c_k \exp(-iE_k^{(0)}t/\hbar)\psi_k^{(0)}(x) \tag{2.40}$$

For two level systems Eq. (2.40) reduces to a sum of two terms, according to the following

$$\psi(x,t) = c_k(t)\psi_k^{(0)}e^{-\frac{iE_k t}{\hbar}} + c_m(t)\psi_m^{(0)}e^{-\frac{iE_m t}{\hbar}} \tag{2.41}$$

The coefficient $c_k(t)$ and $c_m(t)$ represents the time dependent probability amplitudes of the two atomic states of k and m (Demtröder, 2010). Therefore, the value of $|c_k(t)|^2$ can be used to determine the probability of finding the system in the level $|k_i\rangle$ at time t. Obviously, the relation of $|c_k(t)|^2 + |c_m(t)|^2 = 1$ holds at time t, if the decay into other level is neglected. If we insert Eq. (2.40) in to Eq. (2.39), it yields (Brooks, 2013; Razum, 1989).

$$i\hbar\frac{d}{dt}\sum c_k(t)\exp(\frac{-iE_k^{(0)}t}{\hbar})\psi_k^{(0)} = (\hat{H}^0 + \hat{H}^{'})\sum c_k \exp(-iE_k^{(0)}t/\hbar)\psi_k^{(0)} \tag{2.42}$$

For two level states Eq. (2.42) becomes the following, where the relation in Eq. (2.37) has been used to cancel equal terms on both sides and a multiplication by conjugate with $\psi_k^*(n=k,m)$ and spatial integration result in the following two equations (Brooks, 2013).

$$\frac{d}{dt}(c_k(t)) = -\frac{i}{\hbar}\{c_k(t)\hat{H}_{kk}^{'} + c_m(t)\hat{H}_{km}e^{\frac{i(E_k - E_{m)t}}{\hbar}}\} \quad (2.43)$$

$$\frac{d}{dt}(c_m(t)) = -\frac{i}{\hbar}\{c_m(t)\hat{H}_{mm}^{'} + c_k(t)\hat{H}_{mk}e^{\frac{-i(E_k - E_{m)t}}{\hbar}}\} \quad (2.44)$$

with the spatial integral

$$\hat{H}^{'}_{mk} = \int \psi_k^* \hat{H}^{'} \psi_m d\tau = -e\vec{E}\int \psi_k^* \vec{r}\, \psi_m d\tau = -\vec{E}.\vec{\mu}_{km} \quad (2.45)$$

$$\vec{\mu}_{km} = -e\int \psi_k^* \vec{r}\, \psi_m d\tau \quad (2.46)$$

The above Eq. (2.46) is the atomic transition dipole moment. It depends on the wave functions ψ_k and ψ_m of the two states is determined by charge distribution in these state (Demtröder, 2003; Sonnessa & Wilson, 1967). The rate at which a system can be transformed from one stationary to another under the influence of perturbing effect described in Eq. (2.43) and (2.44). They are the basic equations which must be solved to obtain the probability amplitudes of $c_k(t)$, and $c_m(t)$ (Brooks, 2013). To further proceed with Eq. (2.43) and (2.44), it is necessary to be more specific about the perturbation. Thus, in the next section some features of the interaction between the electric field and molecular system would be treated.

2.5.3.2. Interaction of EMR with Molecular System

The mechanism of interaction between electromagnetic radiation and molecules relies on the interaction between the oscillating electric and magnetic fields of the radiation with the electric or magnetic dipole moment of a molecules. Thus, a molecular system can experience a force as a consequence of the electrostatic interaction between its electric dipole moment and the oscillating electric field. The oscillating electric field of the radiation can disturb the energy of the molecule and allow it to escape from its initial stationary state, which is characterized by quantum number k (Belay, 2011; Milonni & Eberly, 2010). In the semi-classical description, the radiation incident upon an atom is described by a classical electromagnetic plane wave shown in Eq. (2.47).

$$\vec{E} = E(\frac{e^{i\omega t} + e^{-i\omega t}}{2}) \quad (2.47)$$

To provide energy difference, the field has to be applied on the dipole moment and is responsible for the Hamiltonian change as a result of radiation falls on the system. The change in the Hamiltonian is therefore given by Eq. (2.48) (Fowles & Lynch, 1968).

$$\hat{H}' = -\vec{E}.\vec{\mu} = -E.\mu\cos\theta \tag{2.48}$$

Where, θ is the angle between the electric field and the dipole moment. For a polarized electromagnetic radiation traveling along the x direction, the perturbed Hamiltonian amplitude of the electric field when substituting Eq. (2.47) into (2.48) becomes(Brooks, 2013; Fowles & Lynch, 1968):

$$\hat{H}' = -E_x^0\mu_x\cos(2\pi\nu t) = -E_x^{(0)}(\frac{e^{i\omega t}+e^{-i\omega t}}{2})\mu_x \tag{2.49}$$

Where, $\omega = 2\pi\nu$ and $\vec{E}_x^0$ is the maximum amplitude of the electric field assuming that the dipole and the electric radiation field are parallel. In a weak field approximation where the atoms are in the lower state which implies $c_k(t) = 1$ and $c_m(t) = 0$ at $t = 0$, the field amplitude to be sufficiently small for the time $t < T$ and the population of $\vec{E}_m$ remains small compared with that of $\vec{E}_k$. Therefore Eq. (2.43) and (2.44) become (Belay, 2011; Patel, 2019).

$$\frac{d}{dt}(c_k(t)) = 0 \tag{2.50}$$

$$\frac{dc_m}{dt} = \frac{i}{2\hbar}E_x^{(0)}\left\langle\psi_m^{(0)}\middle|\mu_x\middle|\psi_k^{(0)}\right\rangle[e^{it(\omega+\omega_{mk})}+e^{it(\omega_{mk}-\omega)}] \tag{2.51}$$

Where,

$$\left|\vec{\mu}_{xkm}\right| = \int_0^t\left\langle\psi_m^{(0)}\middle|\mu_x\middle|\psi_k^{(0)}\right\rangle dx \tag{2.52}$$

Using $c_k(0) = 1$ and $c_m(0) = 0$ as precondition, the integration provides,

$$c_k(0) = 1 \tag{2.53}$$

$$c_m(t) = \frac{E_x^0\left|\mu_{xkm}\right|}{2}[\frac{e^{it(E_m-E_k-h\nu)}-1}{E_m-E_k-h\nu}+\frac{e^{it(E_m-E_k+h\nu)}-1}{E_m-E_k+h\nu}] \tag{2.54}$$

The point of concern viewed here is the process in which the system goes from lower energy level k to higher energy level m. For suck kinds of energies arrangement, the denominator of the first term of Eq. (2.54) becomes very small making the first term dominating when the radiation frequency is such that:

$$h\nu = E_m - E_k \tag{2.55}$$

In contrast, the second term of Eq. (2.54) is essential for emission phenomena, because of the energy in the state m is greater than that of state k. Therefore, for assumed energy level pattern Eq. (2.54) reduces to (Fowles, 1975; Milonni & Eberly, 2010):

$$c_m(t) = \frac{E_x^0|\mu|}{2}[\frac{e^{it(E_m - E_k - h\nu)} - 1}{E_m - E_k - h\nu}] \tag{2.56}$$

The transition probability of absorption from k to m state becomes

$$c_m^*(t)c_m(t) = E_0^2|\mu|^2\left(\frac{\sin^2(\frac{E_m - E_k - h\nu)t}{2\hbar}}{(E_m - E_k - h\nu)^2}\right) \tag{2.57}$$

The total probability of a transition to state m is found by summing the infinitesimal probabilities over the various frequencies. Since the energy density in an electromagnetic wave is given by, $u = \frac{E_0^2\varepsilon_0}{2}$ the calculated transition probabilities is proportional to the energy density of the incoming radiation.

If we consider a situation in which the incoming radiation is electromagnetic waves of many frequencies, it is the best to replace u with energy density in the range $\mathrm{d}\omega$ (that means $\mathrm{u} = \mathrm{d}\omega d\rho$ and integrate over the frequency spectrum. Moreover, since the term in the bracket is sharply peaked about $\omega = \omega_{mk}$ while $\rho(\omega)$ is slowly varying we can move ρ outside of the integral (Belay, 2011; Milonni & Eberly, 2010).

$$c_m^*(t)c_m(t) = \frac{2\rho(\omega)}{\varepsilon_0\hbar^2}|\mu_{xkm}|^2\int\sin^2\frac{(\omega_{mk} - \omega/2)t}{(\omega_{mk} - \omega)^2}d\omega \tag{2.58}$$

Integrating, Eq. (2.58) yields

$$c_m^*(t)c_m(t) = \frac{\rho(\omega)}{\varepsilon_0 \hbar^2}\left|\mu_{xkm}\right|^2 \tag{2.59}$$

According to Eq. (2.59), the probability transition of the molecule due to irradiation is proportional to the transition dipole moment, the intensity of the radiation, and the time of irradiation. It is important to note that, the integration of Eq. (2.58) is carried out using the following integration technique (Li & Thumm, 2020).

$$\int \sin^2 \frac{ax}{x^2} dx = \pi a \tag{2.60}$$

For instance the number of transition to m state per second or rate of transition probability becomes

$$\frac{d(c_m^* c_m)}{dt} = \frac{\pi\rho(\omega)}{\varepsilon_0 \hbar^2}\left|\mu_{xkm}\right|^2 \tag{2.61}$$

Where $\rho = \frac{(E_x^0)^2}{2\pi}$. Further the differentiation of the transition probability with respect to time and extension of the complete procedure for isotropic radiation components for the three components of the radiation and one can write:

$$\frac{d(c_m^* c_m)}{dt} = \frac{\pi\rho(\omega)}{3\varepsilon_0 \hbar^2}\left|\mu_{km}\right|^2 \tag{2.62}$$

Eq. (2.62) is the proportion of variation of the system because of absorption under the perturbing effect of the oscillating electric field of the radiation and it is usually written with Einstein's coefficient of induced absorption so that Eq. (2.62) becomes (Brooks, 2013; Demtröder, 1996).

$$\frac{d(c_m^* c_m)}{dt} = B_{km}\rho \tag{2.63}$$

Moreover, to generalize the theoretically derived equations it is left to compare the derived expression with experimental results on the amount of radiation absorbed. Therefore in the next sections the experimentally visible quantities through spectroscopic technique such as, the molar extinction coefficient, Oscillator strength, absorption coefficient and other parameters are related to the parameter which reflects the detail molecular properties of the system, namely

the transition integral (Brooks, 2013; Demtröder, 1996; Razum, 1989) are related for the experimental and theoretical view.

2.5.3.3. Comparison of Theoretical Quantities and Experimental Result

In order to relate theoretical concepts with experimental results on the amount of radiation absorbed, now we are going to compare theoretical concepts with measurable quantities. The optical absorption coefficient which indicates how far light of some wavelength irradiate in to the sample can penetrate or the penetration depth of the radiation before it can be absorbed expressed in Eq. (2.36) related to the molar decadic absorption coefficient which can obtained from radiation absorption by Eq. (2.64) (Belay, 2011; Milonni & Eberly, 2010).

$$\alpha(v) = \ln(10)\varepsilon(v)c \tag{2.64}$$

Using Eq. (2.65), in to Eq. (2.35) for diluted sample and short path length it provides

$$I = I_0(1 - \ln(10)\varepsilon cl) \tag{2.65}$$

If we differentiating both side of Eq. (2.66) we will get:

$$-dI = I_0 \ln(10)\varepsilon c dl \tag{2.66}$$

Where the concentration (c)

$$c = \frac{N}{N_a} \tag{2.67}$$

In the above expression, N is the number density and N_a is Avogadro's number. Substitution of Eq. (2.67) in to (2.66) we get Eq. (2.68) which contain experimental quantities.

$$-dI = \varepsilon \frac{N}{N_a} I_0 \ln(10) dl \tag{2.68}$$

For the theoretical expression, if $\frac{d(c_m^* c_m)}{dt}$ is the rate of probability for a single molecule changes as a result of absorption of radiation under perturbing effect of electric field radiation then $\frac{d(c_m^* c_m)}{dt} Ndl$ is the number of molecules excited in with energy absorption hv_{mk} so the loss in intensity becomes (Banwell, 1983; Panigrahi & Mishra, 2019).

$$-dI = \frac{d(c_m^* c_m)}{dt} Nh\nu_{mk} dl \tag{2.69}$$

The rate of probability can be described by comparing Eq. (2.68) with Eq. (2.69) and can be expressed as follows.

$$\frac{d(c_m^* c_m)}{dt} = \frac{\varepsilon(\nu) c\rho \ln(10)}{N_a h\nu} \tag{2.70}$$

Where $I_0 = \rho c$. Assuming that the energy density is not varied through out the bands, the whole rate of probability of absorption band can be determined by integrating over the entire frequency range. Hence, the total rate of transition probability is given by Eq.(2.71) (Banwell, 1983; Panigrahi & Mishra, 2019).

$$\frac{c\rho \ln(10)}{N_a h} \int \frac{\varepsilon(\nu) d\nu}{\nu} = \frac{|\mu_{km}|^2 \rho}{6\varepsilon_0 \hbar^2} \tag{2.71}$$

In the absorption region, total intensity of the band is achieved by determining ε(ν) and usually determined by integrating the area under the graph. Therefore, the integrated absorption coefficient due to the transition can be expressed as (Banwell, 1983; Brooks, 2013; Razum, 1989).

$$I_A = \int \frac{\varepsilon(\nu) d\nu}{\nu} = \frac{2\pi^2 N_a |\mu_{km}|^2}{3\ln(10) c\varepsilon_0 h} = S \frac{|\mu_{km}|^2}{3} \tag{2.72}$$

Where, $S = 2.9352 \times 10^{60} C^{-1} mol^{-1}$. Eq. (2.72) relates the experimentally measured molar decadic absorption coefficient with the quantum mechanical expression of the transition dipole moment. The transition dipole moment is a vector that depends on both ground and excited states wave functions and couples the transition to the electric field of light. Therefore the transition dipole momemt can be determined using Eq. (2.73)(Belay, 2011).

$$|\mu_{km}|^2 = \frac{3}{S} \int \frac{\varepsilon(\nu)}{\nu} d\nu \tag{2.73}$$

The Einstein's coefficients (A and B): A_{km} is the first-order rate coefficient for spontaneous emission $k \leftarrow m$ and the B coefficients (induced absorption and emission) are given by (Abraha et al., 2016).

$$B_{mk} = {A_{km}}/{8\pi hcv^3} \tag{2.74}$$

The integrated molar extinction coefficient can be correlated with B Einstein's coefficient by (Belay, 2011).

$$B_{km} = B_{mk} = \frac{\ln 10}{hN_0} \int \frac{\varepsilon(v)}{\tilde{v}} dv \tag{2.75}$$

On the other hand, oscillator strength (f) is considered as the other useful parameter providing the intensity of transition. It is the relative strength of electron transition and providing average number of electrons per atom that can be excited by incident radiation. It is related to the molar extinction coefficient by Eq.(2.76) (Georgakopoulou et al., 2004).

$$f = 4.32x10^{-9} \int \varepsilon(v) dv \tag{2.76}$$

Integrated absorption coefficient (α_t) is a useful parameter that is obtained from sum of absorption coefficient for all frequencies. In the frequency range v and $v+dv$, it can be expressed as (Belay, 2010).

$$\alpha_t = \int \alpha dv \tag{2.77}$$

The integrated absorption cross-section (σ_t) which is related to absorption coefficient at a single frequency for N number of molecules per unit volume can be expressed by the following relation as given by Eq. (2.78). It indicates a measure of probability of an absorption of molecules (Vinet & Zhedanov, 2010).

$$\sigma_t = \frac{1}{N} \int \alpha dv \tag{2.78}$$

Where α indicates absorption coefficient of the molecules.

2.5.4. Phenomena of Fluorescence

The other important phenomena that express the light molecular system interaction is the emission of light by molecules. When a molecule absorbs light in the visible or ultraviolet range of the spectrum, it is excited from the electronic ground state to an excited state. The excited molecules release their energy either by spontaneous or induced emission or by collisional deactivation. The emitted light is called fluorescence (Gonçalves, 2021; Milonni &

Eberly, 2010). Fluorescence is a transition from first excited state to the ground state, which is spin allowed according to the rules of quantum mechanics. Fluorescence can be detected with very high sensitivity even from single molecules and it is also used in a large number of chemical and biochemical applications. Sensitive fluorescence detection relies on the fact that the emitted light usually has a longer wavelength than the intense light used for excitation, which can therefore be suppressed by filters or monocromators (Royer, 1995; Strickler & Berg, 1962).

The energy emitted from a fluorescent species is typically lower than the absorbed energy. This difference between absorption and fluorescence wavelength maxima is known as Stokes shift (Congrave, 2018; Lakowicz, 2006). Stock shift can happen as a result of the excited state decays via internal conversion (IC), molecular reorientation, and excited state reaction in to the lowest level (Lakowicz, 2006; Milonni & Eberly, 2010). Solvent relaxation or molecular reorientation effect occurs in solvents through interactions between the fluorophore and the dipole moment of the solvents (Lakowicz, 2006; Valeur, 2001).

The processes that occur between the absorption and emission of light are generally explained by the Jablonski diagram and are often used as basic idea for expressing light absorption and emission (Jabłoński, 1935). The excitation of molecules using light of suitable wavelength that can be considered as an immediate process happen at time scales of $\leq 10^{-15}$ s. Then the molecules be present in one of the many vibrational levels of an excited singlet state (Figure 3) (Lakowicz, 2006). The excited state of most organic molecules can be separated into singlet states (S_1) and trip let states (T_n), where all electrons in the molecule are spin paired or one set of electron spins is unpaired, respectively (Gutiérrez et al., 2019). The probability of finding the molecule in one of the possible excited singlet states, depends on the transition probabilities and the excitation wavelength. In other words, the occupation of singlet states is controlled by the interaction of the electron involved in the transition with the electric field of the excitation light (Milonni & Eberly, 2010).

Upon excitation to higher excited singlet states, molecules relax through IC to higher vibrational levels of the first excited singlet state S_1 or S_2. Molecules residing in higher vibrational levels will quickly (10^{-10} - 10^{12} s) fall to the lowest vibrational level of this state via vibrational relaxation by losing energy to other molecules through collisions (Itagaki, 2000). From the lowest lying vibrational level of the first excited singlet state, the molecule might be excited into higher singlet states by absorption of a second photon. The efficiency of the process

depends on the absorption spectra transition strengths of the higher excited states involved that is whether absorption into higher excited singlet states is in resonance with the excitation light (Lakowicz, 2006).

Depending on the molecular structure, radiative depopulation of S_1 might occur by spontaneous emission of a fluorescence photon. According to the Franck-Condon principle, the transition to higher excited vibrational levels of S_0 is followed by vibrational relaxation until thermal equilibrium, according to the Boltzmann distribution is reached. Both vibrational relaxation and internal conversion cause heating of the solvent, which thus offers an elegant method to determine the fluorescence quantum yield of fluorophores via measurement of the solvent temperature of related parameters, for example, the refractive index. Generally speaking, loose and floppy molecules exhibiting several rotational and vibrational degrees of freedom will seriously exhibit lower fluorescence intensity (Lakowicz, 2006; Xu et al., 2012). The spin of an excited electron can also be reversed by intersystem crossing, usually leaving the molecule in the first excited triplet state T_n. In most organic dyes intersystem crossing is fairly inefficient as a spin forbidden process, even though the triplet state is of lower electronic energy than the excited singlet state (Xu et al., 2012).

The probability of intersystem crossing increases if the vibrational levels of the two states overlap. For example, the lowest singlet vibrational level can overlap one of the higher vibrational levels of the triplet state.

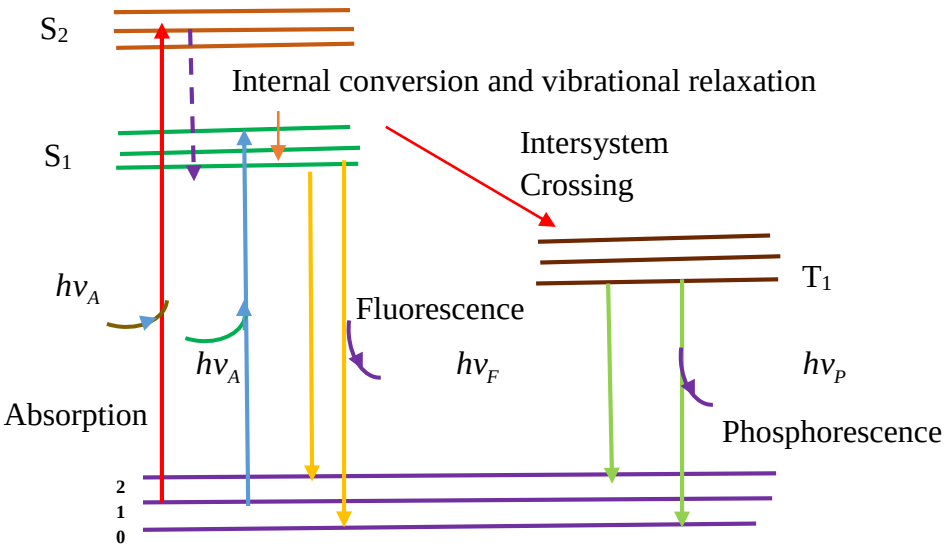

Figure 3. Schematic of Jablonski Diagram

Overall, the intersystem crossing efficiency strongly depends on the nature of the fluorophore and the transition probabilities (Zhang et al., 2019; Zhao et al., 2019). A molecule in a high vibrational level of the triplet state can lose energy through collisions with solvent molecules (vibrational relaxation) leaving it at the lowest vibrational level of the triplet state. It can then again undergo intersystem crossing to a high vibrational level of the electronic singlet ground state, where it returns to the lowest vibrational level through vibrational relaxation(Zhang et al., 2020). As in the case of singlet states, triplet states can be excited into higher excited triplet states T_1 by absorption of a second photon. Because the triplet/singlet transition is also spin forbidden, triplet-state lifetimes can last up to 100s, in comparison with the 10^{-7} - 10^{-9} s average lifetime of an excited singlet state and causes phosphorescence(Royer, 1995; Valeur, 2001).

Emission of a fluorescence photon from the vibrational ground state of the first excited singlet state constitutes a spontaneous process that contains information about the environment of the fluorophore and its interactions (Sadigh et al., 2016). For example, the fluorescence emission spectrum and its maximum contain information about the polarity of the solvent, whereas the fluorescence lifetime and fluorescence quantum yield directly reflect photophysical properties and transient quenching interactions of the fluorophore with other molecules (Sadigh et al., 2016). Therefore in the next sections, the information that are obtained from fluorophore and parameters that can be determined from fluorescence spectra are discussed in detail.

2.5.5. Photophysical Properties

Photophysical properties describe the photoexcitation and any process that does not involve any chemical change. These properties are such as excitation wavelength, emission wavelength, quantum yield, lifetime, rate of radiative decay, rate of non-radiative decay, oscillator strength, transition dipole moments, and so on.

The fluorescence quantum yield (φ_f) is the most important characteristics of fluorophore. Quantum yield is the number of emitted photons relative to the number of absorbed photons (Lakowicz, 2006). There are many non-radiative processes that can reduce the fluorescence quantum yield. The reduction in fluorescence efficiency/quantum yield depends in a complicated fashion on the molecular structure of the dye (Royer, 1995). Fluorescence quantum yield can be measured either by the absolute method or relative method. Because of the experimental difficulties associated with attempting to obtain absolute φ_f values, the

measurement of relative φ_f values seems more appropriate to determine quantum yield. Relative φ_f measurements are achieved using the comparative method and calculated by comparing the fluorophores fluorescence intensity to another sample of known quantum yield (the reference) as described in Eq. (2.79) (Glusko et al., 2011).

$$\varphi_f = \varphi_r \frac{I_f A_r n_f^2}{I_r A_f n_r^2} = \frac{k_r}{k_r + k_{nr}} \tag{2.79}$$

Where, I is the integrated emission intensity and φ_f , φ_r are the fluorescence quantum yield of the unknown and standard, A is the absorbance at excitation wavelength and n is the refractive index of the solvents.

The other photophysical properties of fluorophores is the rate of radiative decay (k_r) which significantly depends on the environments. It can be theoretically predicted from the well-known Stickler-Berg [Eq. (2.80)], which has its foundations in Einstein's spontaneous emission rate and Planck's black body radiation law (Strickler & Berg, 1962).

$$k_r = \frac{1}{\tau_0} = 2.88x10^{-9} n^2 \frac{\int F(v)dv}{\int F(v)v^{-3}dv} \int \frac{\varepsilon(v)}{v} dv \tag{2.80}$$

Where $F(v)$ is the fluorescence intensity, $\varepsilon(v)$ is the molar extinction coefficient, v is the wavenumber, n is the refractive index, and τ_0 is the natural lifetime. For the ideal case of a negligible Stokes shift and a perfect mirror image relationship of absorption and fluorescence spectrum, Eq. (2.80) simplifies to (Strickler & Berg, 1962).

$$k_r = 2.88x10^{-9} n^2 (v)_{av}^2 \int \varepsilon(v)dv \tag{2.81}$$

Excited state lifetime or the average time the molecule spends in the excited state to come back to the ground state is also another important parameters and determined using Eq. (2.82 or 2.83) (Pal et al., 2003).

$$\tau_f = \tau_0 \varphi_f \tag{2.82}$$

Or

$$\tau_f = \frac{1}{k_r + k_{nr}} \tag{83}$$

Where k_{nr} represents non radiative decay and it comprises all possible competing deactivation pathways, such as internal conversion, intersystem crossing, or other intra and intermolecular quenching mechanisms. Very high quantum yields that are close to unity can be observed when the non-radiative decay rate is small. The quantum yield of phosphorescence is typically low because the decay rate k_r is small compared to the non-radiative decay rate k_{nr} (Gonçalves, 2021).

2.5.6. Solvent Polarity Effects

Solvent polarity have great effects on the absorption and emission spectral properties of molecules. The molecules are normally excited to the first singlet state vibrational level and the extra vibrational energy is quickly released to the solvent. Thus, the polarity of the solvent shift the emission peak wavelength to lower energy due to stabilization of the excited state by solvent molecules (Kian et al., 2019). As the solvent polarity is increased, this effect becomes larger, resulting in emission at lower energies or longer wavelengths. In general, only fluorophores that are themselves polar display a large sensitivity to polar solvents (Reichardt, 1994; Rotkiewicz et al., 2004). Nonpolar molecules, such as un-substituted aromatic hydrocarbons, are much less sensitive to solvent polarity (Lakowicz, 2006).

The average fluorescence lifetimes (1–10 ns) are typically much greater than the time required for solvent relaxation. For fluid solvents at room temperature, solvent relaxation occurs in 10-100 ps. For this reason, the emission spectra of fluorophores are representative of the solvent relaxed state (Jabłoński, 1935; Royer, 1995). Light absorption of molecules takes about 10^{-15}s, which is very short time as compared to the time for motion of the fluorophore or solvent. Hence, the absorption spectra are less sensitive to solvent polarity as the molecule is exposed to the same local environment in the ground and excited states. However, the emitting fluorophore molecules are exposed to the relaxed environment, which contains solvent molecules oriented around the dipole moment of the excited state(Kumar et al., 2005; Lakowicz, 2006).

2.5.6.1. General and Specific Solvent Effects

The analysis of solvent dependent emission spectra appears very complex due to variety of interactions occurring that can result in spectral shifts. The effect of solvent polarity observed on the spectral shift raised due to general and specific solute solvents interactions (Lakowicz, 2006).

The concept of general solvent effects provides a useful framework for consideration of solvent dependent energy variation. The interactions between the solvent and fluorophore affect the energy difference between the ground and excited states. The energy difference is a property of the refractive index (n) and dielectric constant (ε) of the solvent, and is described by the Lippert-Mataga equation (Lippert, 1955; Mataga et al., 1956), Bakhshiev's equation (Bakhshiev et al., 1969), Kawski-Chamma-Viallet equation (Kian et al., 2017) and Reichardt equation (Reichardt, 1994). The equations are an approximation in which the polarizability of the fluorophore and higher order terms are neglected. These equations describes the Stokes shift in terms of the changes in dipole moment which occur upon excitation, and the energy of a dipole in solvents of various dielectric constant (ε) or refractive index (n).

Investigation on solvatochromic through general solvent effects confirms the opposite properties of ε and n on the Stokes shift (Lakowicz, 2006). An increase in n will decrease the energy loss, whereas an increase in ε results in a larger difference between v_a and v_f. The refractive index is a high frequency response and depends on the motion of electrons within the solvent molecules, which is essentially instantaneous and can occur during light absorption. In contrast, the dielectric constant (ε) is a static property, which depends on both electronic and molecular motions, where the latter being solvent reorganization around the excited state (Bayliss, 1950; Lakowicz, 2006). This electron redistribution results in a decrease in the energy difference between the ground and excited states (Bayliss, 1950; Bayliss & Mcrae, 1954).

To determine the ground and excited state dipole moments of a molecule by general solvent effects, the equation relating the difference and sum of absorption (v_a) and fluorescence (v_f) wavenumbers to solvent polarity functions are given by Eq. (2.84-2.86) (Kian et al., 2017, Desai, 2016 et al.,).

Lippert-Mataga equation (Lippert, 1955; Mataga et al., 1956)

$$v_a - v_f = mf(\varepsilon_r, n) + const \tag{2.84}$$

Bakhshiev's equation (Bakhshiev et al., 1969)

$$v_a - v_f = m_1 f(\varepsilon_r, n) + const. \tag{2.85}$$

Kawski-Chamma-Viallet Equation (Kawski, 2002; Kian et al., 2019)

$$v_a + v_f = -m_2 f(\varepsilon_r, n) + 2g(n) + const. \tag{2.86}$$

Where, $f(\varepsilon_r, n)$ and $g(n)$ are the solvent polarity functions, dependent on the dielectric constant ε_r and the index of refraction *n*. The parameters m, m_1 and m_2 described in Eq. (2.84-2.86) are determined from the slopes of Eq. (2.84), Eq. (2.85) and Eq. (2.86) respectively and are related to ground and excited-state dipole moment using the following equations.

$$m = \frac{2(\mu_e - \mu_g)^2}{hca^3} \tag{2.87}$$

$$m_1 = \frac{2(\mu_e - \mu_g)^2}{hca^3} \tag{2.88}$$

$$m_2 = \frac{2(\mu_e^{\ 2} - \mu_g^{\ 2})}{hca^3} \tag{2.89}$$

The parameters μ_e is the excited and μ_g is ground state dipole moments of the solute molecule, c is the speed of light in vacuum, h is Planck's constant and a is Onsager cavity radius of the solute molecule and determined as (Edward, 1970; Suppan, 1983).

$$a = \left(\frac{3M}{4\pi\delta N} \right)^{1/3} \tag{2.90}$$

Where, M is the relative molecular mass of the solute molecules, N is Avogadro's number and δ is the density assuming that the molecules are spherical. The solvent polarity function used in the Lippert-Mataga equation can be determined by (Lippert, 1955).

$$f(\varepsilon_r, n) = \frac{\varepsilon_r - 1}{2\varepsilon_r + 2} - \frac{n^2 - 1}{2n^2 + 1} \tag{2.91}$$

Substituting Eq. (2.91) into Eq. (2.84), one finds the following Lippert-Mataga equation (Mataga et al., 1956).

$$v_a - v_f = m\left(\frac{\varepsilon_r - 1}{2\varepsilon_r + 2} - \frac{n^2 - 1}{2n^2 + 1} \right) + const \tag{2.92}$$

From the slope m of the graph of $v_a - v_f$ versus Lippert-Mataga solvent polarity function, change in the dipole moment expressed as Eq. (2.93).

$$\Delta\mu = \mu_e - \mu_g = \left(\frac{mhca^3}{2}\right)^{1/2} \tag{2.93}$$

The solvent polarity functions used in Bakhshiev's and Kawski-Chamma-Viallet Equation are expressed in Eq. (2.94) and (2.95) according to (Bilot & Kawski, 1962; Kawski et al., 2002).

$$f(\varepsilon_r, n) = \frac{2n^2+1}{2\left(n^2+2\right)}\left(\frac{\varepsilon_r - 1}{\varepsilon_r + 2} - \frac{n^2-1}{n^2+2}\right) \tag{2.94}$$

$$g(n) = \frac{3}{2}\left(\frac{n^4-1}{\left(n^2+2\right)^2}\right) \tag{2.95}$$

When Eq. (2.94) is substituted into Eq. (2.85) we get Bakhshiev's Eq. (2.96) (Bakhshiev et al., 1969).

$$\nu_a - \nu_f = m_1 \frac{2n^2+1}{n^2+2}\left(\frac{\varepsilon_r - 1}{\varepsilon_r + 2} - \frac{n^2-1}{n^2+2}\right) + const \tag{2.96}$$

Similarly, when Eq. (2.94) and (2.95) are substituted into Eq. (2.86), we can get the Kawski-Chamma-Viallet Eq. (2.97) (Bilot & Kawski, 1962).

$$\nu_a + \nu_f = -m_2\left(\frac{2n^2+1}{n^2+2}\left(\frac{\varepsilon_r - 1}{\varepsilon_r + 2} - \frac{n^2-1}{n^2+2}\right)\right) + 3\left(\frac{n^4-1}{\left(n^2+2\right)^2}\right) + const \tag{2.97}$$

If the symmetry of the investigated solute molecule remains unchanged during electron excitation the following expressions are obtained on the basis of Eq. (2.88) and (2.89).

$$\mu_g = \frac{|m_2 - m_1|}{2}\left(\frac{hca^3}{2m_1}\right)^{\frac{1}{2}} \tag{2.98}$$

$$\mu_e = \frac{|m_2 + m_1|}{2}\left(\frac{hca^3}{2m_1}\right)^{\frac{1}{2}} \tag{2.99}$$

$$\frac{\mu_e}{\mu_g} = \frac{|m_2 + m_1|}{|m_2 - m_1|}\mu_g \; for(m_2 > m_1) \tag{2.100}$$

The dipole moments can also be determined using other method that is based on the empirical solvent polarity scale (E_T^N). The idea was initially expressed by Reichardt (Reichardt, 1994) and developed by Ravi (Ravi et al., 1995). The method is based on solvatochromic properties of Betaine dye, correlated with the polarization and hydrogen bonding effect, and is expressed as.

$$\nu_a - \nu_f = 11307.6\left[\left(\frac{\Delta\mu}{\Delta\mu_B}\right)^2\left(\frac{\mathrm{a_B}}{\mathrm{a}}\right)^3\right] E_T^N + \mathrm{const} \tag{2.101}$$

Where $\Delta\mu_B = 9\,\mathrm{Debye}$ is the change in dipole moment and $\mathrm{a_B} = 6.2A$ is the Onsager radius for Betaine dye, $\Delta\mu$ and a are the corresponding quantities for molecule of interest, and E_T^N given by.

$$E_T^N = \frac{E_T(30)_{solvent} - E_T(30)_{TMs}}{E_T(30)_{water} - E_T(30)_{TMs}} = \frac{E_T(30)_{solvent} - 30.7}{32.4} \tag{2.102}$$

In this case TMS represents Tetramethylsilane known as a non-polar solvent $(E_T^N = 0)$ and using water as a highly polar solvent $(E_T^N = 1)$. The change in dipole moment is determined from the slope of the linear plot of $\nu_a - \nu_f$ versus E_T^N of Eq. (2.101) described as.

$$\Delta\mu = \mu_e - \mu_g = \sqrt{\frac{m \times 81}{\left(\frac{6.2}{\mathrm{a}}\right)^3 11307.6}} \tag{2.103}$$

Specific solute solvent interactions are produced by one or a few neighbouring molecules and are determined by the specific chemical properties of both the fluorophore and solvent. It can be due to hydrogen bonding, preferential solvation, acid–base chemistry, or charge-transfer interactions, to name a few (Petrov et al., 2002; Petrov et al., 2001). The spectral shifts due to such specific interactions can be substantial, and if not recognized, limit the detailed interpretation of fluorescence emission spectra. In addition to hydrogen fluorophore interactions, many fluorophores can form an internal charge transfer (ICT) state, or a twisted internal charge transfer (TICT) state. For instance, suppose the fluorophore contains both an electron-donating and an electron-accepting group. Following excitation there can be an increase in charge separation within the fluorophore. If the solvent is polar, then a species with charge separation (the ICT state) may become the lowest energy state (Lakowicz, 2006).

2.5.7. Fluorescence Quenching

Emission of a fluorophore can be affected by other species in the same solution. A commonly observed effect is quenching, which results in reduced emission intensity and shorter fluorescence lifetimes. Fluorescence quenching is a process of decreasing the fluorescence intensity due to energy transfer, ground state complex formation, collisional between the molecules and excited state reactions (El-Mossalamy et al., 2011; Mrkalić et al., 2021). It has been used as common experiment to determine the location of fluorescent probes in macromolecules based on the accessibility of fluorophores to quenchers. Quenching requires molecular contact between the fluorophore and quencher (Lakowicz, 2006). The fluorescence intensity quenching mechanism can be divided into three categories in general: static, dynamic, and mixed. Static quenching occurs when the drug and the quencher form a ground state complex. In contrast, dynamic quenching occurs when molecules collide in the transition to the excited state rather than direct interaction between drug and ligand. The mixed type of quenching is a combination of static and dynamic quenching that occurs when a fluorophore collides with a quencher as well as the complex is formed between fluorophore and quencher(Wang et al., 2016; Zhang et al., 2017).

2.5.7.1. Static Quenching

Static quenching occurs as a result of complex formation between a fluorescent molecule or fluorophore and a fluorescence quencher (Van De Weert & Stella, 2011). The resulting complex is not fluorescent leading to a decrease in the overall measured intensity as there is less free fluorophore in the system. In static quenching the dependence of the fluorescence intensity upon quencher concentration is easily derived by consideration of the association constant for complex formation and is given by (Lakowicz, 2006).

$$Ksv = \frac{[F-Q]}{[F][Q]} \tag{2.104}$$

Where, $[F]$is the uncomplexed fluorophore concentration, $[F-Q]$is the concentration of the complex, and $[Q]$ is the concentration of quencher. If the complexed molecule is not fluoresce, then the division of the fluorescence that remains is given by the fraction of the total fluorophores that are not complexed to complexed$\left(F_0 \diagup F\right)$. Therefore, the whole concentration of fluorophore intensity $[F_0]$ is given as (Lakowicz, 2006).

$$[F_0] = [F] + [F - Q] \tag{2.105}$$

Up on substitution of (2.105) into (2.104) yields.

$$Ksv = \frac{[F_0] - [F]}{[F][Q]} = \frac{[F_0]}{[F][Q]} - \frac{1}{[Q]} \tag{2.106}$$

Rearrangement of Eq. (2.106) yields

$$\left[\frac{F_0}{F}\right] = 1 + K_S[Q] \tag{2.107}$$

$$\left[\frac{F_0}{F}\right] = 1 + k_q \tau_0 [Q] \tag{2.108}$$

Where k_q the quenching rate constant, τ_0 is fluorescence life time in the absence of quencher, F_0 and F are the fluorophore fluorescence intensity in the absence and presence of quencher respectively, $[Q]$is initial concentration of quencher, and $[K_{SV} = k_q \tau_0]$ is the Stern-Volmer constant. The Quenching data are usually obtained from plots of $\left(F_0 / F\right)$ versus $[Q]$. This is because $\left(F_0 / F\right)$ is expected to be linearly dependent upon the concentration of quencher.

A linear Stern-Volmer plot is generally indicative of a single class of fluorophores, all equally accessible to quencher. If two fluorophore populations are present, and one class is not accessible to quencher, then the Stern-Volmer plots deviate from linearity toward the x-axis. Unless additional information is provided, fluorescence quenching data obtained by intensity measurements alone can be explained by either dynamic or static processes (Lakowicz, 2006).

The binding site and binding constant of interacting molecules can be calculated using the modified double logarithm regression (Ferrie et al., 2017).

$$\log\left[\frac{F_0 - F}{F}\right] = \log k_a + n\log\left([Q] - [D](\frac{F_0 - F}{F_0})\right) \tag{2.109}$$

Where, k_a is the binding constant and n is the binding site, [Q] and [D] are the total concentrations of quencher (caffeine) and drugs (LVF and NRF) respectively. The plot of

$\log(F_0 - F)/F$ vs $Log([Q] - [D](F_0 - F)/F_0))$ give a straight line that intercepts on the y-axis representing the binding constant (k_a) and slope indicates the binding site (n) per molecule.

2.5.7.2. Collisional Quenching

Collisional quenching raises from diffusive encounters between the molecules and quencher during the excited state's lifetime. It is a time dependent process and happens while the excited-state molecules are deactivated due to interaction with some other molecules in the solution, which is called the quencher. The fluorescence quenching in dynamic quenching, can occur due to energy transfer, excited state electron transfer, proton transfer, excited state complex and spin orbit coupling (heavy atom effect) (Lakowicz, 2006).

It is important to recognize that, observation of a linear Stern-Volmer plot does not prove that collisional quenching of fluorescence has occurred. Static quenching can also results in linear Stern-Volmer plots. Static and dynamic quenching can be distinguished by their differing dependences on temperature and viscosity measurements. Higher temperatures result in faster diffusion and hence larger amounts of collisional quenching. Higher temperature will typically result in the dissociation of weakly bound complexes, and hence smaller amounts of static quenching (Alizadeh et al., 2012; Lakowicz, 2006).

2.5.8. Thermodynamic Parameters and Nature of Binding Force between Molecules

Investigating the thermodynamic parameter of interacting molecules is highly important since it provide information about the responsible force for the interaction and nature of their binding (Van De Weert & Stella, 2011). When small molecules bound to biologically macromolecules, the interaction force like electrostatic force, van der Waals force, hydrophobic force and hydrogen bond are promoting the interaction (Khashkhashi-Moghadam et al., 2022). To acquire further insight about the interaction of molecules and the thermodynamic parameters such as enthalpy (ΔH), entropy (ΔS) and Gibbs free energy change (ΔG) Van't Hoff Eq. (2.110) is used. The value of ΔG provides information of the reaction process and the sign of ΔH and ΔS gives idea of the force associated with it (Rout et al., 2020).

$$\ln k_a = -\frac{\Delta H}{RT} + \frac{\Delta S}{R} \tag{2.110}$$

The Gibbs free energy change at a given temperature is calculated using

$$\Delta G = RT \ln k_a = \Delta H - T\Delta S \tag{2.111}$$

Where R is gas constant, T is experimental temperature and k_a is the binding constant at corresponding temperature.

2.6. Computational Theory

There are different methods engaged to correctly model different systems, including quantum mechanical methods, force field simulations, ab initio methods, density functional theory (DFT), and combinations of them. Each approaches have their own weaknesses and strengths and the selection of method employed based on various considerations, like size of system to be studied, computational resources, and the nature of the problem to be studied or question asked (Horn, 2003; Skoromnik et al., 2017).

Of course, all computational techniques relies on calculating the energy of a system from some initial condition, and then try to minimise the energy of the system by altering various parameters. This is most easily visualised for geometry optimisation of a molecule, where the molecular structure is altered until an energy minimum is found. But, the basic principle applies regardless of the highest level of theory with the largest basis set in an excited state calculation. All the calculation used in different methods are based on the multi electron system consideration (Dorohoi et al., 2020).

2.6.1. Multi Electron System

The interaction of N electrons system with a laser field can be described by its wave function $\psi(r,t)$ at $(r = [r_1 .....r_N])$ which obeys the time-dependent Schrodinger equation. The physical system wave function is an essential quantity which provides almost a whole picture of the system. The wave-function is a solution of Eq. (2.112) (Horn, 2003; Mora, 2019).

$$\hat{H}\psi(r,t) = i\hbar \frac{\partial \psi(r,t)}{\partial t} \tag{2.112}$$

Where, H is Hamiltonian described in the form of

$$H(r,t) = T(r) + V_{ee}(r) + V_{ne}(r) + V_{laser}(r,t) \tag{2.113}$$

In Eq. (2.113), $T(r)$ is the electrons kinetic energy which in turn determined by

$$T(r) = \frac{1}{2}\sum_{i=1}^{N} \nabla_i^2 \tag{2.114}$$

The second term denoted $V_{ee}(r)$ is the electron-electron interaction which has the form

$$V_{ee}(r) = \sum_{i<j=1}^{N} \frac{1}{|r_i - r_j|} \tag{2.115}$$

In addition, $V_{ne}(r)$ corresponds to the nuclear-electron interaction given by

$$V_{ne}(r) = \sum_{i,k}^{N} \frac{Z_k}{|r_i - R_k|} \tag{2.116}$$

Where, R_k is the position and Z_k is the charge of the kth nucleus.

The last term of Eq. (2.113) $V_{laser}(r,t)$ includes the interaction between the electrons and the applied laser expressed as Eq. (2.117)(Marques & Gross, 2004).

$$V_{laser}(r,t) = E_0 f(t) \sin(\omega t)\left(\sum_{i=t}^{N} r_i . \hat{n}\right) \tag{2.117}$$

Where, ω is the frequency of the laser, $\hat{n}$ is the polarization direction, E_0 is the amplitude of the electric field, and $f(t)$ is the envelope of the pulse of the field.

However multi electron system Schrodinger equation describes the system completely, it is computationally expensive to solve for wave function in the case of larger systems. Thus up to now it is impossible to exactly solve the multi electron Schrodinger equation for systems with more than two electrons interacting with intense laser pulses in a reasonable amount of time. The best alternative approach to approximately solve multi-electron systems is Density Functional Theory (DFT) (Sharma et al., 2021b).

2.6.2. Hohenberg-Kohn Variation Theorem

In the DFT approach, electrons interact with one another and with an 'external potential. To describe the interactions the basic concept of DFT begin from Hohenberg-Kohn (HK) theorem which states that the external potential given by (Horn, 2003).

$$V_{ext} = V + T = \sum_{i=1}^{N} u(r_i) + \frac{1}{2} \sum_{i,k,i\neq k}^{N} \frac{1}{|r_i - r_j|} \tag{2.118}$$

If the system is a function of the electron density $\rho(r)$, the ground state of a system can be determined by its electronic density given as.

$$\rho_{gs}(r) = N \sum_{\sigma} \int dx_2 ... \int dx_N \left| \psi_{gs}(r, \sigma, x_2 .... x_N) \right| \tag{2.119}$$

We can show this by considering a ground state wave function, $\psi(r)$ with an electron density for an external potential $V(r)$, with a Hamiltonian H and energy E, and another ground state wave function $\psi'(r)$. The corresponding second external potential $V'(r)$ with a Hamiltonian H' and energy E', gives the same electron density $\rho(r)$. Due to the variational principle we can then say that (Horn, 2003; Marques & Gross, 2004; Skoromnik et al., 2017).

$$\langle \psi | H | \psi \rangle < \langle \psi' | H | \psi' \rangle = \langle \psi' | H' | \psi' \rangle + \langle \psi' | H - H' | \psi' \rangle \tag{2.120}$$

$$\langle \psi | H | \psi \rangle < \langle \psi' | H | \psi' \rangle = E' + \int V(r) - V'(r) \rho(r) dr \tag{2.121}$$

Which gives the following

$$E < E' + \int V(r) - V'(r) \rho(r) dr \tag{2.122}$$

Also for the case of the primed and un-primed indices being reversed

$$E' < E + \int V'(r) - V(r) \rho(r) dr \tag{2.123}$$

If we then add equations (2.121) and (2.122) we get the following contradiction

$$E + E' < E' + E \tag{2.124}$$

Which is clearly a contradiction. So we realize that, the external potential $V(r)$ is indeed a unique functional of the ground state electron density $\rho(r)$. In other words, the ground state wave function $\psi_{gs}(r)$ is a functional of the ground state density $\rho_{gs}(r)$, so it can be written as:

$$\psi_{gs}(r) = \psi_{gs}[\rho_{gs}(r)] \tag{2.125}$$

Where, square brackets denote functional dependence. Then this leads to the fact that any observable corresponding to the ground state is also a functional of the density $\rho_{gs}(r)$.

$$O[\rho_{gs}(r)] = \langle \psi_{gs}[\rho_{gs}(r)] | O | \psi_{gs}[\rho_{gs}(r)] \rangle \tag{2.126}$$

2.6.3. Density Functional Theory and the Kohn-Sham Equations

Density functional theory is a method that uses the energy density instead of the wave function to model molecular systems. Based on the HK theorem it has been established that the observables of a system are functional of the density $\rho_{gs}(r)$, we therefore need to consider ways to solve for the density. This can be done using the Kohn-Sham equations. Consider a system of non-interacting particles with a Hamiltonian given by(Horn, 2003; Muchmore, 2004):

$$\hat{H}_s = \hat{T} + \hat{V}_s = \sum_{i=1}^{N} (-\frac{\nabla_i^2}{2} + v_s(r_i) \tag{2.127}$$

Where v_s is an arbitrary external potential. We can write the associated total energy of the system as a functional given by:

$$E_{vs}[\rho] = T_s[\rho] + \int d^3 r \rho(r) v_s(r) \tag{2.128}$$

While $\rho(r)$ is the system electron density. Since the particles are non-interacting, a slater determinant can be used to approximate the ground state wave function $\psi_{gs}(r)$ of the N-particle system(Horn, 2003; Skoromnik et al., 2017).

$$\psi_{gs}(r) = \frac{1}{\sqrt{N!}} \begin{vmatrix} \phi_1(r_1) & \phi_1(r_2) & \phi_1(r_3) & \dots & \phi_1(r_N) \\ \phi_2(r_1) & \phi_2(r_2) & \phi_2(r_3) & \dots & \phi_2(r_N) \\ \vdots & \vdots & \vdots & \vdots & \vdots \\ \phi_N(r_1) & \phi_N(r_2) & \phi_N(r_3) & & \phi_N(r_N) \end{vmatrix} \tag{2.129}$$

Where, the orbitals $\phi_i(r)$ are solutions to the single particle Schrodinger equation

$$-\frac{1}{2}\nabla^2 \phi_i(r_i) + V_s(r_i)\phi_i(r_i) = \varepsilon_i \phi_i(r)_i \tag{2.130}$$

The ground state density of the *N* electron system is given by

$$\rho_{gs}(r) = \sum_{i=1}^{N} |\phi_i(r)|^2 \tag{2.131}$$

In this case, the HK theorem applies and there exists a one to one mapping between the grounds state density $\rho(r)$ and the potential $v_s(r)$. The energy of the system is given by(Horn, 2003).

$$E_{s,gs}[\rho] = T_s[\rho_{gs}] + \int dr\rho(r)v_s(r) = \sum \int dr\phi_i^*(r) + \int dr\rho(r)v_s(r) \tag{2.132}$$

Now, consider a system of interacting particles with an external potential denoted by $v(r)$. The ground state density $\rho(r)$ for this system can be obtained from the ground state density of a system of non-interacting particles with a potential denoted by $v(r)$. This turns the problem of solving a multi electron Schrodinger equation into multiple non-interacting single particle Schrodinger like equations. In turn, this greatly reduces the computational costs needed to numerically solve such systems. For a system of interacting particles, the energy functional is given by (Horn, 2003).

$$E[\rho_{gs}] = T_s[\rho_{gs}] + V_H[\rho_{gs}] + E_{xc}[\rho_{gs}] + V[\rho_{gs}] \tag{2.133}$$

The second term $V_H[\rho_{gs}]$ is the Hartree energy (classical coulomb energy) which is given by

$$V_H[\rho_{gs}] = \frac{1}{2}\int dr \int dr' \frac{\rho_{gs}(r)\rho_{gs}(r')}{|r-r'|} \tag{2.134}$$

The exchange correlation energy $E_{xc}[\rho_{gs}]$ given by

$$E_{xc}[\rho_{gs}] = T[\rho_{gs}] - T_s[\rho_{gs}] + U[\rho_{gs}] - \frac{1}{2}\int dr \int dr' \frac{\rho_{gs}(r)\rho_{gs}(r')}{|r-r'|} \tag{2.135}$$

Taking the derivative of the exchange correlation energy, gives the correlation potential

$$V_{xc}[\rho_{gs}] = \frac{\delta E_{xc}}{d\rho_{gs}} \tag{2.136}$$

This potential has an unknown form, but can be approximated for different systems. For a system of interacting particles the variation principle with respect to the electron density results in (Horn, 2003; Marques & Gross, 2004; Skoromnik et al., 2017).

$$0 = \frac{\delta T_s[\rho_{gs}]}{\delta \rho_{gs}} + \frac{\delta V[\rho_{gs}]}{\delta \rho_{gs}} + \frac{\delta V_H[\rho_{gs}]}{\delta \rho_{gs}} + \frac{\delta E_{xc}[\rho_{gs}]}{\delta \rho_{gs}} \tag{2.137}$$

Similarly, for non-interacting particles the variation principle with respect to density yields

$$\frac{\delta E_{xc}[\rho_{gs}]}{\delta \rho_{gs}} = 0 = \frac{\delta T_s[\rho_{gs}]}{\delta \rho_{gs}} + \frac{\delta V[\rho_{gs}]}{\delta \rho_{gs}} \tag{2.138}$$

Comparing the variation principle for both the interacting and non-interacting system, we get

$$v_s(r) = v_{ext}(r) + v_H(r) + v_{xc}(r) \tag{2.139}$$

This implies that the density of an interacting system within an external potential $v_{ext}(r)$ can be determined by solving the Schrodinger equation for many non-interacting particles in a potential $\psi_{gs}(r)$ only if the exchange-correlation potential is known. Based on this assumption, the orbitals of the non-interacting system can be obtained by solving the Kohn-Sham equation, given by(Horn, 2003; Marques & Gross, 2004)

$$-\frac{1}{2}\nabla^2\phi_i(r) + v_s(r)\phi_i(r) = \varepsilon_i\phi_i(r) \tag{2.140}$$

The electron density of the interacting system can then be obtained via

$$\rho(r) = \sum_{i=1}^{N} |\phi_i(r)|^2 \tag{2.141}$$

The KS equations must be solved self-consistently because both the terms $v_H(r)$ and $v_{xc}(r)$ depend on the density $\rho(r)$, which depends on the orbitals $\phi_i(r)$, which in turn depend on $v_s(r)$. Due to this, the calculation starts with an initial guess for the electron density $\rho(r)$, then the potential $v_s(r)$ is obtained, which leads to a solution of the KS equation $\phi_i(r)$, which then yields a new density $\rho(r)$ (Capaz, 2014; Marques & Gross, 2004). This process is repeated until the system converges to the correct ground state density. Once convergence is obtained, then observables for the system can be calculated.

2.6.4. Time-Dependent Density-Functional Theory (TDDFT)

An extension of DFT beyond the static potential is TDDFT, which considers the system being subjected to a time dependent external potential, typically for laser-molecule interactions, of

the form of Eq. (2.117) (Capaz, 2014; Marques & Gross, 2004; Muchmore, 2004). There are several assumptions made in this description.

i. The field is treated classically since at high intensities field has large photon density.
ii. The dipole approximation is used, which holds when the wavelength of the laser field is larger than the size of the system.

The electromagnetic field is treated as purely electric field, and its magnetic component can be neglected for the considered range of laser frequencies and intensities. In the case of a time dependent external potential, the Runge-Gross theorem states that there is a one-to-one mapping between the electron density $\rho(r,t)$ and the external potential $v(r,t)$. Therefore, instead of solving a many body time dependent Schrodinger equation, the density can be found by using the time dependent Kohn-Sham equation given by Eq. (2.142) (Capaz, 2014; Horn, 2003; Marques & Gross, 2004).

$$-\frac{1}{2}\nabla^2\phi_i(r,t)+v_{ks}(r,t)\phi_i(r,t)=i\frac{\partial}{\partial t}\phi_i(r,t) \tag{2.142}$$

Where, for the time-dependent case, the external potential includes the potential from the laser field and is of the form

$$v_{ks}(r,t)=v_{ext}(r)+v_H(r)+v_{xc}(r)+v_{laser}(r,t) \tag{2.143}$$

The density of the interacting system can be obtained from the time dependent Kohn-Sham orbitals (2.144) (Horn, 2003; Marques & Gross, 2004).

$$\rho(r,t)=\sum_{i=1}^{N}\left|\phi_i(r,t)\right|^2 \tag{2.144}$$

The function given in Eq. (2.144) is the density of all interact electrons and nucleus that are used in density functional theory to determine computational parameters such as the dipole moments, HOMO energy, LUMO energy, oscillator strength and many other.

3. MATERIALS AND METHODS

3.1. Chemicals and Solvents

Levofloxacin and Norfloxacin drugs, Caffeine, Methylene blue, Hydrochloric acid, Monobasic (Na2HPO4), and dibasic (NaH2PO4) sodium phosphate were purchased from Sigma-Aldrich Company and used without further purification. Caffeine was used as a quencher to observe the effects that it bring on levofloxacin and Norfloxacin drugs. Monobasic (Na2HPO4), and dibasic (NaH2PO4) sodium phosphate were used to prepare buffer to control the pH of caffeine-drug mixture whereas hydrochloric acid used to wash materials. Methylene blue used as a reference sample to determine the quantum yield of Levofloxacin and Norfloxacin drugs. The polar solvents (Distilled Water, Methanol, Ethanol, Ethyl Glycol, and Ethyl Acetate) and non-polar solvents (Chloroform, Dichloromethane, and Isopropanol) are used and all are spectroscopic grade. The polar and non-polar solvents were used to investigate the effects of solvents on drugs.

3.2. Apparatus and Instruments

In this research the laboratory apparatus used for the experiment are such as, Oven, Volumetric Flasks, measuring Cylinders, Pipettes, Magnetic stirrer with hot plate, Spatula, Thermometer, Beakers, Aluminium foil and Cuvette are some of them. The mass of LVF, NRF, Methylene blue and Caffeine were measured by digital balance with accuracy of 0.0001g.

The absorption spectra was measured by double beam UV/vis spectrometer (An ISO 9001 model, India) using quartz cuvette of 1cm length in the wavelength region of 200-400 nm at room temperature. Steady state emission spectra were carried out using Cary Eclipse Fluorescence Spectrophotometer (Agilent, Malaysia). Emission spectra of the drugs measured in the wavelength regions of 350-600 nm, at 290 nm excitation wavelength and 10 nm slit width. The Fourier transform infrared (FTIR) spectra were measured in the wavenumber of 400-4000 cm^{-1}.

3.2.1. Basic Components of UV/Vis Spectrophotometry and Working Principles

UV/Vis spectroscopy is an analytical technique that measures the amount of discrete wavelengths of UV or visible light that are absorbed by or transmitted through a sample in comparison to a reference or blank sample. This property is influenced by the sample composition and potentially providing information on what is in the sample and its

concentration. The UV/Vis absorption spectroscopic use common basic components including a source of energy, a means for isolating a narrow range of wavelengths or monocromator, a detector for measuring the signal, and a signal processor that displays the signal in a form convenient for the analyst (Demtröder, 2003). Fig. 4 shows the basic component and working principle of UV-Vis absorption spectrophotometer.

For instruments employing two lamps, a tungsten or halogen lamp is commonly used for visible light whereas a deuterium lamp is the common source of UV light. During operation in the ultraviolet range, M_1 is used to allow radiation from deuterium lamp to strike diffraction grating. In the same way for the task in the near infrared and visible ranges, source M_1 reflects the radiation from tungsten lamp onto diffraction grating, and it blocks the radiation from deuterium lamp. The light from the M1 reaches diffraction grating by passing through first slit width. The diffraction grating is an optically reflecting surface with a large number of parallel grooves. The radiation is then dispersed at the grating to produce the spectrum. The rotational position of the grating effectively selects a segment of the spectrum, and reflecting this segment to optical filter through the second slit .The slits are used to allow the amount of light that is able to enter the spectrometer for processing.

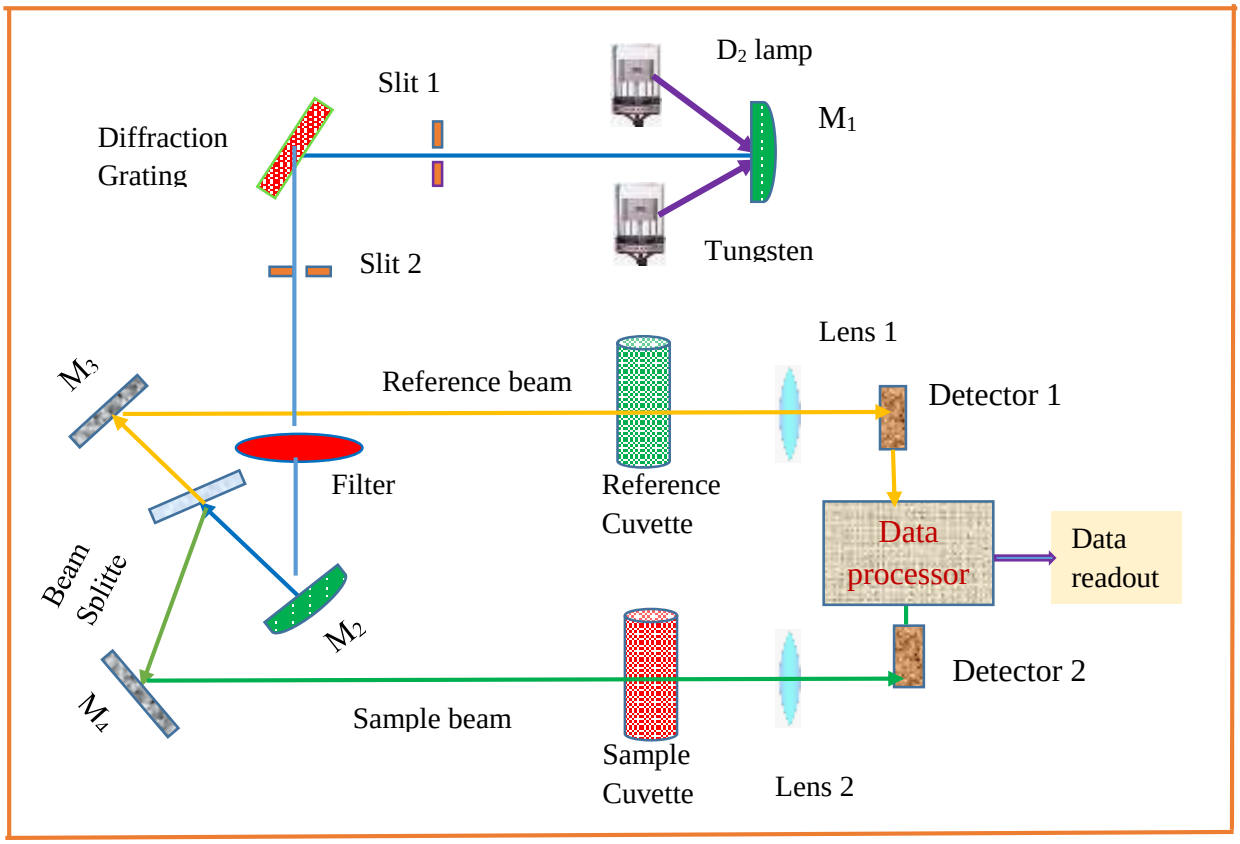

Figure 4. Schematic view of a UV-Vis absorption spectrometer (M represents Mirror)

Light passed through M_2 is divided in two parts of similar intensity with a half mirror splitter. One part travels via the cuvette having the solution of sample to be examined in transparent solvent. Second beam or reference beam, travels via similar cuvette having only solvent. Reference and sample solution containers have to be transparent towards passing beam. Then the detector detects intensity of light transmitted by cuvettes and sends this data to a meter to record and display the values. Electronic detectors calculated and compare the intensities of light beams(Milonni & Eberly, 2010; Razum, 1989).

3.2.2. Fluorescence Spectrophotometer Basic Components and Working Principles

Fluorescence spectrophotometer uses beam of light that excite the electron in a molecule of certain compound and cause them to emit a light. The main components of a fluorescence spectrophotometer are such as light source, excitation and emission monocromator, detectors and signal processor (Fig.5). Knowing characteristics of these components allows to understand capabilities and limitations of fluorescence spectrophotometer (Lakowicz, 2006).

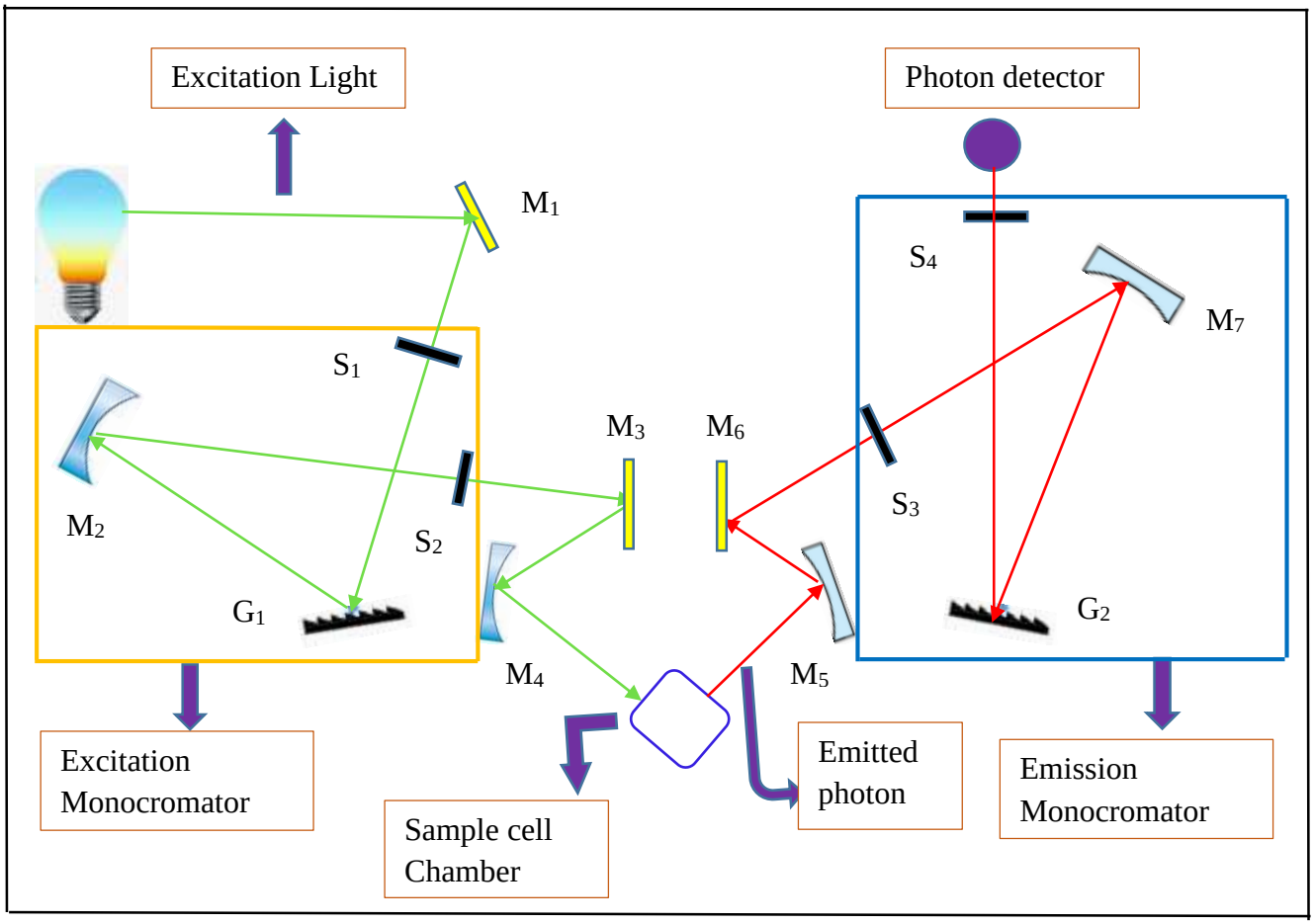

Figure 5. Schematic view of a fluorescence spectrometer (M is Mirror, S is Slit and G represent Grating)

The typical light source used in a fluorescence spectrophotometer is a high pressure xenon arc lamp. The bulb of this lamp includes xenon at high pressure that is excited to higher level by the electrical arc established by the current running through the electrodes. Light from xenon lamp entering excitation monocromator. The excitation monocromator utilizes diffraction grating, mirror and slits at the entrance and at the output and operated to select the light of particular wavelength and reject the rest of excitation spectrum.

The Light emitted from the sample which is longer wavelength than the excitation is filtered by emission monocromator. This select the wavelength of the light that reaches the detector which is typically a photon counting photomultiplier tube (PMT). PMT detectors are capable of detecting single photon so it is important that any unwanted is effectively rejected by the monocromator to avoid any background on the emission spectrum. The excitation and emission path are set at an angle of 90^0 to each other to minimize the fraction of excitation light entering the emission arm.

3.2.3. Fourier Transform Infrared (FTIR) Spectroscopy

FTIR measures the absorption of infrared radiation (IR) made by each bond in the molecule and as a result gives spectrum which is commonly designated as absorbance/transmittance versus wavenumber (cm^{-1}). For the determination of functional groups in a molecule, it must be IR active (i.e., molecule having a dipole moment). When the IR radiation interacts with the covalent bond of the materials having an electric dipole, the molecule absorbs energy, and the bond starts back and forth oscillation. Therefore, the oscillation which caused the change in the net dipole moment of the molecule should absorbed infrared radiations. The plot of measured infrared absorbance light intensity versus its property such as energy range expressed in wavenumber (cm^{-1}) is called an infrared spectrum. The IR spectrum is recorded in absorbance mode, which measures the amount of light absorbed by a sample (Sharma et al., 2018; Tran & Yijun Zhang, 2015).

3.3. Experimental Methods

3.3.1. Method of Stock Solution Preparation

The LVF and NRF drugs bought from the market and grounded to reduce its size physically using mortar and pestle to tiny particles and stored in polythene bottle until used. An accurately weighed amount of LVF (0.0072g) and NRF (0.0064g) drugs powder by electronic balance was dissolved in different 100ml solvents to prepare stock solution of $2\times10^{-4}M$. The

solutions were stirred for 10 minutes using magnetic stirrer to increase the solubility of the drug in solvents solution. Then, the solution was filtered using what man filtration paper to reduce the suspended particles. On the other hand the stock solution of Caffeine were prepared in water using similar procedure in order to investigate the fluorescence quenching mechanism of Caffeine with LVF and NRF drugs.

3.3.2. Method of Measuring Effects of Solvent Polarity on LVF and NRF Drugs

To observe the effects of solvent polarity on LVF and NRF drugs, the stock solution of LVF and NRF of $2\times10^{-4}M$ were prepared in polar and non-polar solvents. The stock solution diluted until concentration reaches: absorbance < 1 au for absorption and absorbance < 0.1 au for the fluorescence spectra measurement and kept in dark room to avoid self-reabsorption and other effects. Then UV/Vis absorption and emission measurement were taken immediately and the data obtained was analysed using Origin software. The values of the solvent polarity functions were calculated from relative permittivity, refractive index of the solvents and empirical solvent polarity parameters as shown in Table 2.

3.3.3. Method of Measuring Optical Transition Probability of LVF and NRF Drugs

To determine the optical transition probability of the drugs, LVF of concentration $1.5\times10^{-5}M$ were prepared in solvents like Chloroform, Dichloromethane and Methanol. Similarly, NRF with concentration of $1.5\times10^{-5}M$ were prepared in Chloroform, Isopropanol, and Methanol. Then UV/Vis measurement were taken. The parameters such as oscillator strength, transition dipole moments, Einstein A and B coefficients and integrated absorption cross-sections were calculated by integrating molar extinction coefficients and absorption coefficient in 25000-50000 cm^{-1} wave number regions. These can be achieved by recalculating the absorption versus wavelength measurement obtained from UV-Vis-spectrometer.

3.3.4. Method of Measuring Photophysical Properties of LVF and NRF Drugs

In order to investigate the photophysical properties of drugs in different solvents, solutions of LVF and NRF with $4\times10^{-6}M$ were prepared from the stock solution for both absorption and emission measurement. To eliminate the possibility of re-absorption and inner filter effects, the fluorescence data were corrected for absorption of excitation light and emitted light and kept in dark room to avoid other effects. Also to observe the effects of concentration on the photophysical properties of LVF and NRF drugs, LVF of varied concentrations $2.4\times10^{-6}M - 1.68\times10^{-5}M$ and NRF $2.4\times10^{-6}M - 1.3\times10^{-5}M$ prepared in water. Then for the

sample prepared in different solvents and concentration, the UV/Vis absorption and emission measurement were immediately taken. To probe the quantum yield of LVF and NRF drugs in different solvents and concentration, methylene blue dye used as a reference sample and prepared in ethanol based on reference (Glusko et al., 2011). The quantum yield then determined using comparative method.

3.3.5. Method of Measuring Fluorescence Quenching

To study the interaction of LVF and NRF with caffeine, LVF of solution $C = 8.8\times10^{-6}M$ and NRF $C = 1.2\times10^{-5}M$ were prepared in sodium phosphate buffer from stock solution for UV/Visible absorption and steady state fluorescence measurement. The drugs were dissolved in a buffer solution to maintain constant pH (6.8). Then stock solution of caffeine $2.4\times10^{-3}M$ prepared in deionized water. The fluorescence spectra of LVF and NRF containing caffeine were obtained by successive addition of caffeine of different concentration $(1.27\times10^{-4} - 1.40\times10^{-3}M)$ to fixed amount of LVF and NRF solution. The mixture of LVF-CF and NRF-CF shake to arrive uniform solution before measurement was taken. Temperature effects on the complexes were examined at 298K, 308K and 318K by putting the mixed solution of drugs and caffeine on magnetic stirrer with hot plate for 10minutes. The temperature of the samples was measured by thermometer and controlled using ice bath to keep the temperature constant. The UV/vis electronic absorption spectra of the complex solution measurement were prepared and obtained by similar procedures at room temperature. For FTIR the samples were prepared in a solution form and converted to powder by evaporating water.

3.4. Computational Method

To understand the electronic structure and electronic properties of LVF and NRF, computational work was performed employing Gaussian 09 software. The outputs of the optimized structure were used to visualize HOMO-LUMO structure and total density matrix with electrostatic potential map (TDM-ESP) of the LVF and NRF molecules. The HOMO-LUMO energy band gap, the dipole moments, electron charge density distribution, oscillator strength and electrostatic potential of the molecules were computed using semi-empirical methods PM6, DFT-B3LYP-3-21G, and DFT-B3LYP-6-31G respectively. Time dependent DFT (TDDFT) with basis set 6-31G is used to calculate the excited state dipole moment. All the calculations were performed after optimizing the geometry of the molecule in the ground state (Frisch et al., 2009).

4. RESULTS AND DISCUSSION

4.1. Solvatochromic Effects

4.1.1. Effects of Solvent Polarity on Absorption and Emission Spectra of Levofloxacin and Norfloxacin Drugs

The electronic absorption and emission spectra of molecules in solvents provide reliable information about solvation effects on the ground and excited states (Bozkurt et al., 2017). Fig. 6a, b and 7a, b shows the normalized absorption and fluorescence emission spectra of LVF and NRF in different polar and non-polar solvents, respectively. The absorption spectrum of LVF exhibited different double absorption band spectra with maximum absorption at around 275-325 nm and minor absorption band seen between 325-350nm which vary with the polarity of the solvents. Similarly, NRF revealed main peak band appeared around 250-300 nm and weak band seen between 300-350 nm. The change in the solvent polarity can bring about change in the energy gap between the ground and singlet excited states, consequently leading to variation in the position, intensity and shape of the absorption bands (Patil et al., 2019; Soltani et al., 2020). Hence, the absorption spectra of the two drugs showed a blue shift with increasing solvent polarity. This is because the increase of solvent polarity causes a blue shift in the $n \rightarrow \pi^*$ absorption of carbonyl compounds (Bratkowska et al., 2020). In addition, *n* state is more easily stabilized by polar solvent effects such as hydrogen bonding, so in going from non-polar solvents to polar solvents there is a blue shift.

On the other hand, the emission spectra of the drugs contain only one band. The graph shows red shifts upon going from nonpolar solvent to polar solvents and these are due to the fact that the excited states of LVF and NRF are more stabilized in polar solvent than non-polar solvents (Basavaraja et al., 2016; Manohara et al., 2013). The shift of the fluorescence emission peak towards longer wavelengths is caused by the marked difference between the excited state and ground state charge distribution of the drugs, and this results in a stronger intermolecular interaction with polar solvents in the excited state (Kian et al., 2020; Zhao et al., 2021). The largest peak emission shifts in different solvents are 44 nm and 39 nm for LVF and NRF respectively as shown in Table 1. Larger shifts of the emission spectra were observed when compared to the shifts of the absorption spectra. The reason is that absorption of light occurs in about 10^{-15} s, a time too short for motion of the fluorophore or solvents molecules. Hence, the absorption spectra are less sensitive to solvent polarity.

In contrast, the emitting fluorophore is exposed to the relaxed environment, which contains solvent molecules oriented around the dipole moment of the excited state (Kian, et al., 2017). This is due to the length of time of fluorescent molecules remain in the excited state provides an opportunity for interactions with other molecules in solution (Lakowicz, 2006).

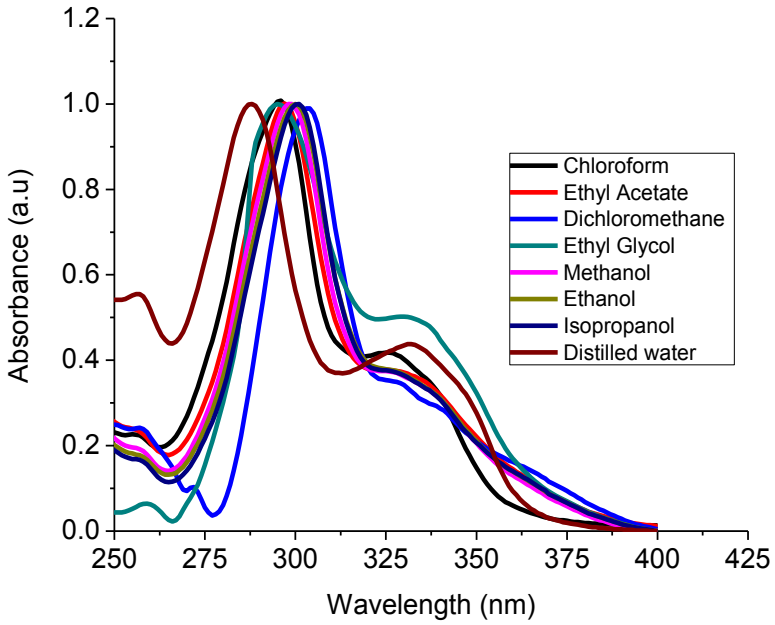

a)

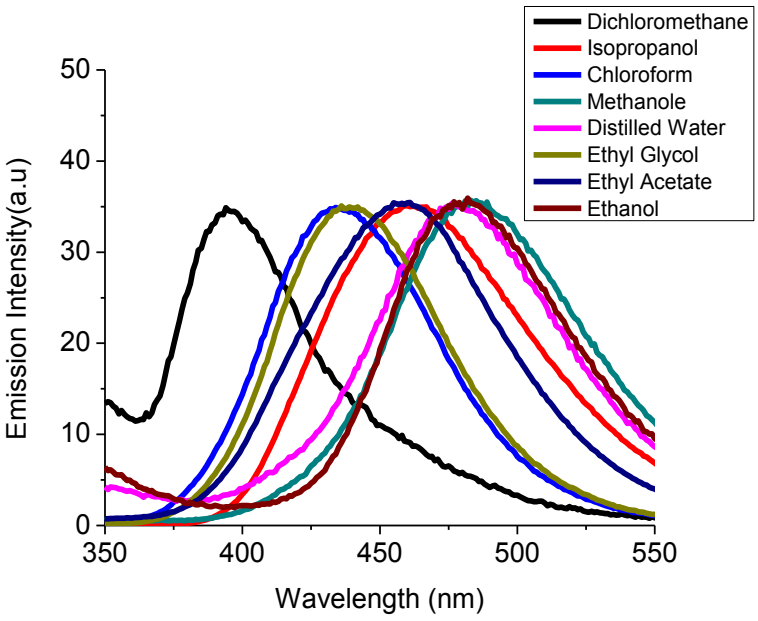

b)

Figure 6. (a) UV/vis absorption spectra and (b) Emission spectra of LVF in solvents with different solvent polarities.

In general, a large emission shift shows that the excited state geometry of the compounds is different from the ground state geometry and the dipole moment increases during excitation. In such cases, the relaxed excited state S_1 will be energetically stabilized relative to the ground state S_0 and a significant red shift of the fluorescence will be observed (Siddlingeshwar et al., 2011).

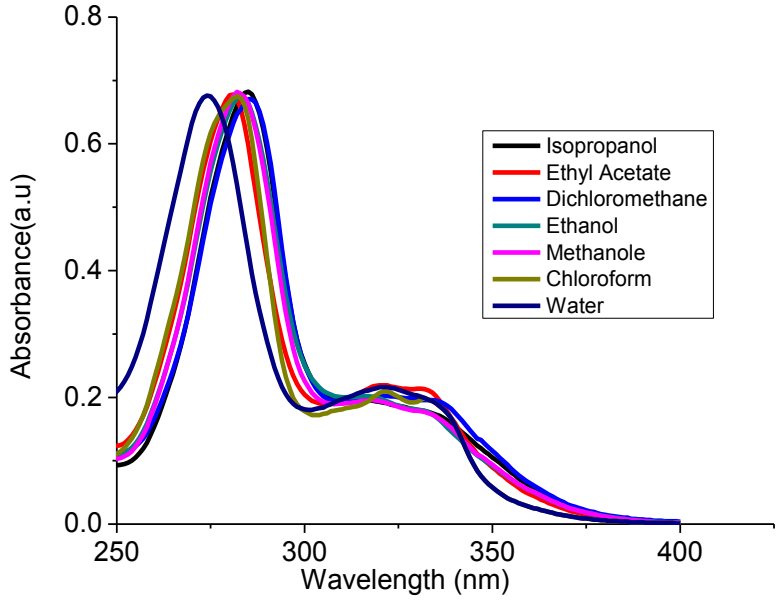

a)

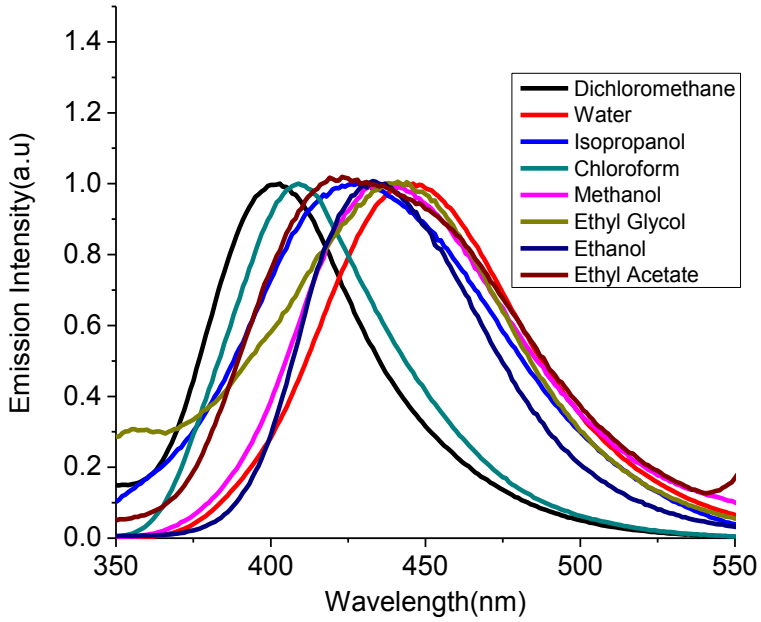

b)

Figure 7. (a) UV/vis absorption spectra and (b) Emission spectra of NRF in solvents with different solvent polarities.

As shown in Table 1, the largest and smallest values of the wavenumbers of the emission peaks of LVF and NRF were observed in water (polar solvent) and dichloromethane (nonpolar solvent) respectively. These indicated that, both LVF and NRF have strong intermolecular interaction with polar solvents in the excited state. Large Stokes shifts were observed for both LVF and NRF antibiotic drugs (Table 1) and this can be an indication of intramolecular charge transfer (ICT) occur as result of excitation (Sabahi et al., 2020; Sharma et al., 2021a). Previous work confirms that, large Stokes shift seen on fluoroquinolones antibiotic drugs in aqueous solution are explained through intramolecular charge transfer from the (N1) Piperazinyl group to the main ring of the molecule (Cuquerella et al., 2006).

On another hand, a large magnitude of Stokes shift indicates that, the excited state geometry could be different from that of the ground state associated with a variation of the charge distribution upon excitation. Therefore, it is reasonable to assume specific interactions involving the carbonyl groups and solvent molecules (Benazzouz et al., 2016). In order to investigate the solvent effects on the charge distribution characteristics of drug molecules, ground and excited state dipole moments of LVF and NRF were calculated and described in the next section.

Table 1. Peaks of the absorption and emission spectra of LVF and NRF in solvents with different polarity

Solvent	Norfloxacin		Levofloxacin	
	$v_a(cm^{-1})$	$v_f(cm^{-1})$	$v_a(cm^{-1})$	$v_f(cm^{-1})$
Chloroform	35460.99	24626.90	33783.78	22782.68
Dichloromethane	34965.03	24812.05	32894.74	22373.37
Isopropanol	35087.72	23588.80	33222.59	20966.12
Ethanol	35335.69	23093.09	33222.59	20788.29
Methanol	35460.99	22885.39	33444.82	20704.79
Distilled Water	36496.35	22727.27	34722.22	21415.00
Ethyl Acetate	34722.22	24862.36	33444.82	21689.15
Ethyl Glycol	34602.08	22672.07	33898.30	20833.33

4.1.2. Evaluation of Dipole Moments

In another attempt, to evaluate the dipole moments, the spectral shift, the differences of absorption and emission wavenumbers of the LVF and NRF obtained from experimental investigation. The Dipole moment is one of the important physical parameters of any organic molecules, which describe the distribution of electrons quantitatively. In the excited state, the dipole moment of the molecule is changed due to redistribution of electron density relative to ground state. The change of the dipole moment is influenced the nature of the surrounding media/solvent and the type of solute solvent interactions (Patil et al., 2019).

To understand the solvatochromic effects of LVF and NRF drugs, the absorption and emission spectra are correlated to solvent polarity functions and empirical solvent polarity parameter. The solvent polarity functions are calculated and presented in Table 2.The ground and excited state dipole moments of LVF and NRF were estimated from the slope of the Lippert-Mataga Eq. (2.84), Bakhshiev's Eq. (2.85), the Kawski-Chamma-Viallet Eq. (2.86), and the Reichardt Eq. (2.101) fitted to the experimental data. Fig. 8a and b are the graphs of $\nu_a - \nu_f$ versus $f(\varepsilon_r, n)$ for LVF and NRF using Bakhshiev's equation respectively. The statistical analysis of the graphs for both drugs has good linearity with high correlation coefficients. The higher correlation coefficient values suggest better linearity for these methods.

Table 2. Calculated values of solvent polarity functions in different solvents

Solvents	n	ε_r	$f_{Bac}(\varepsilon_r, n)$	$f(\varepsilon_r, n) + 2g(n)$	$f_{LM}(\varepsilon_r, n)$	E_T^N
Chloroform	1.445	4.81	0.3714	0.9634	0.1486	0.253
Dichloromethane	1.424	8.93	0.4745	1.0295	0.203	0.321
Isopropanol	1.3776	19.9	0.7786	1.2923	0.2762	0.546
Ethanol	1.3616	24.5	0.8126	1.3348	0.2886	0.654
Methanol	1.33	32.7	0.8542	1.3041	0.308	0.762
Distilled Water	1.3325	80.1	0.9138	1.3636	0.3203	1.000
Ethyl Acetate	1.372	6.02	0.4895	0.9955	0.2001	0.221
Ethyl Glycol	1.4382	37.7	0.8394	1.4334	0.2720	0.790

Similarly, Fig. 9a and b are the graphs of $v_a + v_f$ versus $f(\varepsilon_r, n) + 2g(n)$ obtained using Kawski-Chamma-Viallet equation with good correlation coefficients. The slopes, intercepts, and correlation coefficients of LVF and NRF are summarized in Table 3. In some case deviation of data point from linearity were observed in the graph $v_a - v_f$ versus $f(\varepsilon_r, n)$ and $v_a + v_f$ versus $f(\varepsilon_r, n) + 2g(n)$.

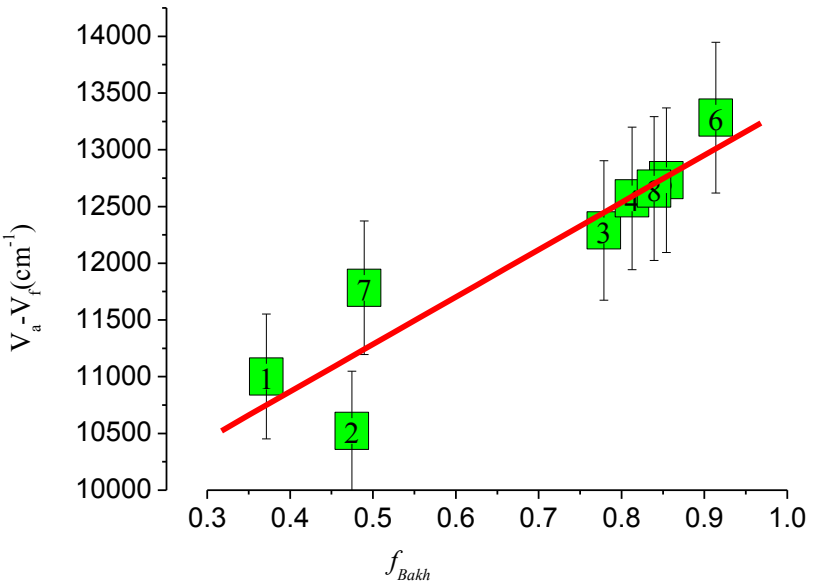

a)

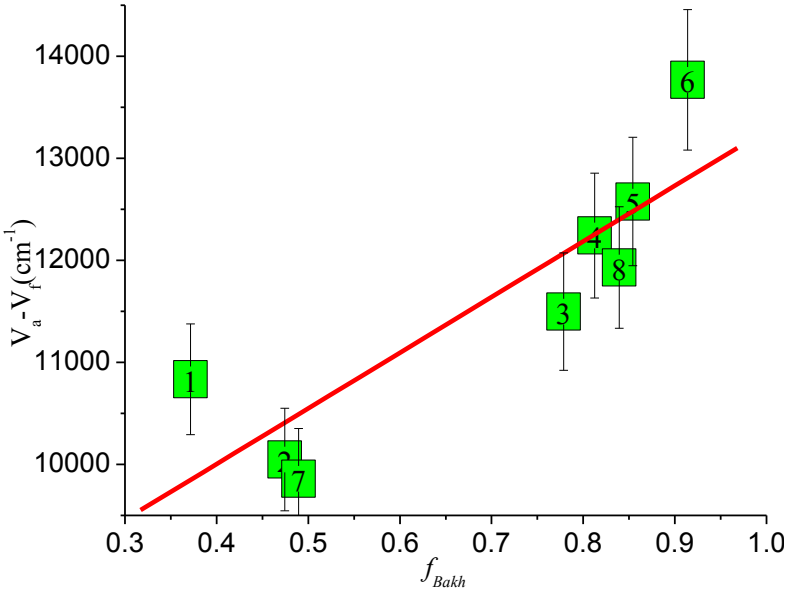

b)

Figure 8. Plot of $v_a - v_f$ versus $f_{Bac}(\varepsilon_r, n)$ using Bakhshiev's equation for (a) LVF and (b) NRF in different solvents (1. Chloroform, 2.Dichloromethane, 3. Isopropanol, 4. Ethanol, 5. Methanol, 6. Distilled Water, 7. Ethyl Acetate and 8. Ethyl Glycol)

This is probably due to specific solute-solvent interactions (for example hydrogen bond formation and the tendency of polar solvent molecules to form aggregates of two or more molecules) that are not taken into consideration in all the above mentioned theories. Therefore, it indicates the extent of interactions between the solute and solvent molecules (Fatma et al., 2021; Patil et al., 2021; Walki et al., 2021).

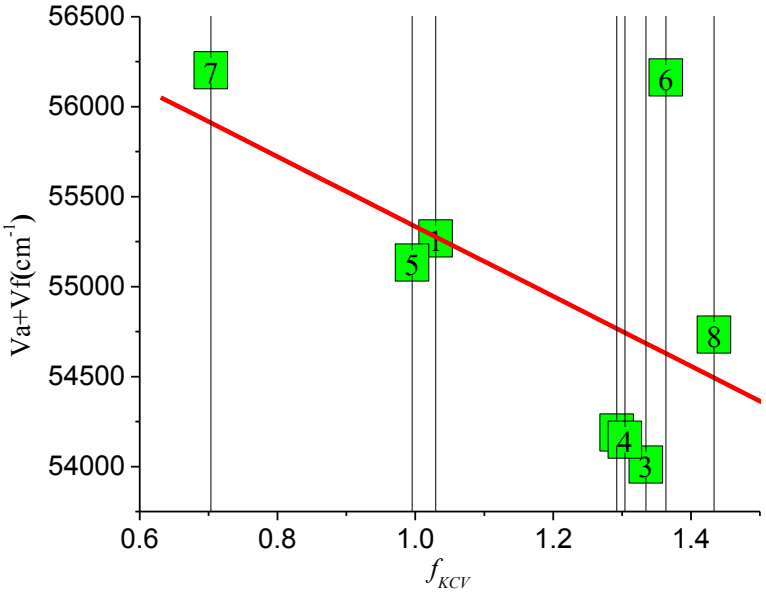

a)

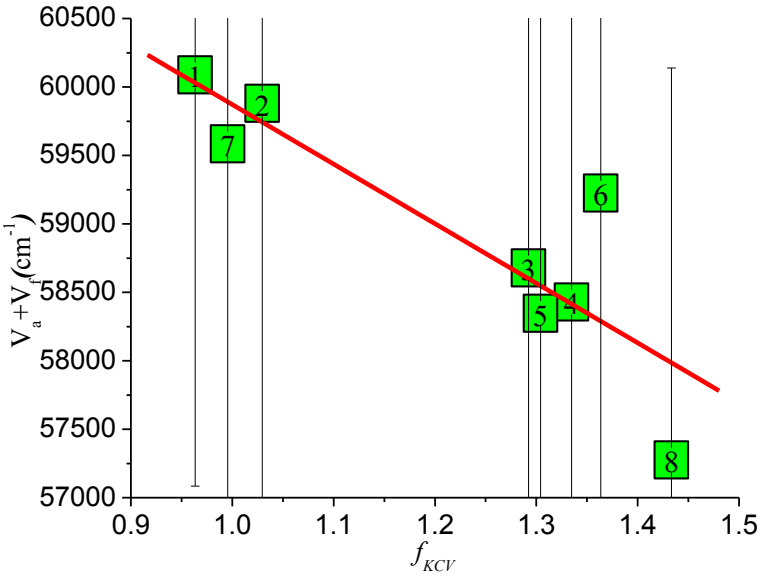

b)

Figure 9. Plot of $v_a + v_f$ versus $f(\varepsilon_r, n) + 2g(n)$ using Kawski-Chamma-Viallet equation for (a) LVF and (b) NRF in different solvents (1. Chloroform, 2.Dichloromethane, 3.Isopropanol, 4. Ethanol, 5. Methanol, 6. Distilled Water, 7. Ethyl Acetate and 8.Ethyl Glycol)

From the slope of the graphs and using Eq. (2.98) and (2.99) the ground and excited state dipole moments of LVF and NRF were determined by assuming that the dipole moments are almost parallel and the results are depicted in Table 4.The calculated results indicates that, the excited state dipole moment is larger than the ground state dipole moment indicating that the probe compounds are significantly more polarized in the excited state than in the ground state. More of, the excited state strong interactions between solute and polar solvent molecules may be lead to appearance of high dipole moments changes as compare to non-polar solvents (Melavanki et al., 2021; Sabahi et al., 2020).

Table 3. Statistical analysis of the correlations of solvent spectral shifts of LVF and NRF

	Slope(cm^{-1}) (r^2)	Intercept (cm^{-1})	Correlation Coefficient
Bakhshiev's Correlation			
Levofloxacin	5938	7707	0.93
Norfloxacin	5899	7152	0.87
Kawski-Chamma-Viallet			
Levofloxacin	3463	58669	0.79
Norfloxacin	4999	64848	0.86
Lippert-Mataga Correlation			
Levofloxacin	19464	6858	0.87
Norfloxacin	27749	4312	0.85
Reichardt Correlation			
Levofloxacin	3140	10373	0.91
Norfloxacin	4858	8738	0.95

In addition, large excited state dipole moment leads to a change in the distribution of charge densities of solute solvents (Kian, et al., 2017a). On the other hand, the ground and excited state dipole moments that are estimated by different methods are not similar due to the fact that different assumption and simplification are applied in each method (Morosanu et al., 2019). It is also noted that the value of the ground and excited state dipole moments of LVF and NRF are not similar. The variation in the value of dipole moment may be due to structural difference of the two compounds (Benazzouz et al., 2016). The change in dipole moments ($\Delta\mu$ = 13.6, 16.4 D) obtained using Lippert-Mataga Eq. (2.93) are larger than the value obtained by other

methods. This is due to the fact that Lippert-Mataga equation neglected polarizability of the solute molecules (Bratkowska et al., 2020). Previously it has also been reported that the change in dipole moment obtained using Lippert-Mataga equation is larger than the values calculated by other methods (Belay, 2010; Belay, Libnedengel, et al., 2016).

Table 4. Calculated value of dipole moments in Debye (D), and Onsager cavity radius (a) obtained from experimental and theoretical work for LVF and NRF

Comp.	a[a]	μ_g[b]	μ_e[c]	μ_e[d]	μ_g[e]	μ_e[f]	$\Delta\mu$[g]	$\Delta\mu$[h]	$\Delta\mu$[i]	$\frac{\mu_e}{\mu_g}$[j]
LVF	4.57	1.57	5.97	4.58	7.539	5.277	4.4	13.6	3.01	3.79
NRF	4.6	0.95	7.16	6.03	7.921	6.813	6.21	16.4	5.08	7.54

a. Calculated value of Onsager cavity radius in angstrom
b. Experimental μ_g value calculated by Eq. (2.98)
c. Experimental μ_e value calculated by Eq. (2.99)
d. Experimental μ_e value calculated from empirical solvent polarity function
e. Theoretical μ_g values obtained by employing DFT B3LYP-3-21G
f. Theoretical μ_e values obtained by employing DFT B3LYP-6-31G
g. $\Delta\mu$ calculated from Eq. (2.98) and (2.99)
h. $\Delta\mu$ calculated from Eq. (2.93)
i. $\Delta\mu$ calculated from Eq. (2.103)
j. Ratio of excited and ground states' dipole moments found by Eq. (2.100)

The other important method to estimate the dipole moments depends on the empirical solvent polarity scale E_T^N (Muddapur et al., 2014; Reichardt, 1994). It correlates better with the solvatochromic data than the traditionally used bulk solvent polarity functions. In E_T^N, the error associated with the estimation of the Onsager cavity radius is reduced and the empirical polarity scale also includes intermolecular interactions along with solvent polarity. Fig 10a and 10b are the graphs of $(\nu_a - \nu_f)$ versus E_T^N for LVF and NRF, respectively. The statistical results indicate that, very high correlation coefficients (R = 0.91 and 0.95) were obtained for LVF and NRF, respectively. The good linearity of E_T^N with the Stokes shift indicates that the inclusion

of both the solute-solvent interaction as well as H-bonding interaction in the empirical polarity scale. As it can be seen from the results of all models, the first excited state dipole moment of Reichardt is larger than the ground state dipole moment. The difference in dipole moments seen in two electronic states can be the indication of ICT (Sadigh et al., 2016; Melavanki et al., 2021; Sıdır & Sıdır, 2011).

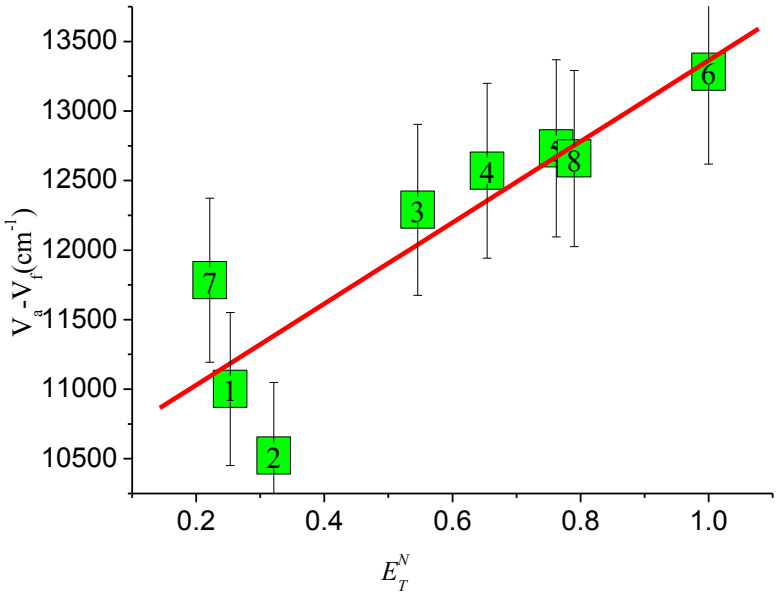

a)

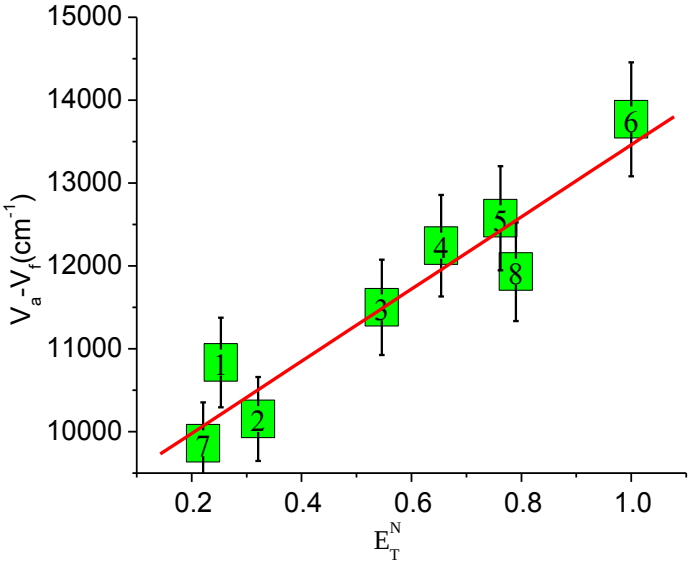

b)

Figure 10. Plot of $v_a - v_f$ versus E_T^N for Reichardt equation (a) LVF and (b) NRF in different solvents (1. Chloroform, 2.Dichloromethane, 3. Isopropanol, 4. Ethanol, 5. Methanol, 6. Distilled Water, 7. Ethyl Acetate and 8.Ethyl Glycol)

In general, the dipole moments of the different states of a molecule are important parameters which reveal information about the electronic and geometrical structures of the molecule. Investigating the ground and electronically excited state dipole moments of a molecule provides elucidation of the excited state nature and reflects the charge distribution in the molecule (Melavanki et al., 2021). It is also used to predict the regions of electrophilic and nucleophilic reactivity in some photochemical reactions.

Since both the pharmacological activities and the ground and excited state dipole moments of the molecule is sensitive to the molecular structure and geometry, small changes in dipole moments can be indicative of different pharmacological activities of the drugs (Khadem Sadigh et al., 2016; Kian, et al., 2017a). Therefore, investigation of spectral properties and dipole moment of LVF and NRF drug molecules in wide variety of solvents especially in aqueous and alcoholic media can be extended to biological systems. Indeed, the obtained results about molecular interactions can indicate completely the behaviours of LVF and NRF drugs in body system.

4.1.3. Quantum Chemical Calculation

Fig 11 a-c shows the HOMO-LUMO structures, the optimized structure with the dipole moment vector and the total density matrix with the electrostatic potential map (TDM-ESP) for LFV and NRF obtained using the semi-empirical method MP6, DFT-B3LYP-3-21G and DFT-B3LYP-6-31G respectively. It shows the spatial distribution of the electron cloud in three dimensions. The three methods provided similar results in which the electron clouds are mainly distributed on the molecular skeleton of the aromatic benzene ring of the drugs. Electron clouds are also present on the functional groups attached to the benzene ring.

The values of ground and excited state dipole moments of the selected molecules were calculated from the optimized structure using DFT. The ground state dipole moments obtained from the semi-empirical method PM6, DFT B3LYP-3-21G and DFT B3LYP-6-31G are larger than the experimental results. For example the ground state dipole moments obtained using DFT B3LYP-3-21G are $\mu_g = 7.539D$ and $\mu_g = 7.921D$ for LVF and NRF respectively, and are larger than the experimental results as shown in Table 4. The reason for such difference may be that the experimental method is affected by solvent and environmental effects (solute-solvent interaction), whereas the theoretical calculation is performed for a free molecule (Sidir et al., 2016; Sidir & Gülseven Sidir, 2015).

Comp.	HOMO	LUMO	Optimized Structure	TDM-ESP
LVF				
NRF				

a)

Comp.	HOMO	LUMO	Optimized Structure	TDM-ESP
LVF			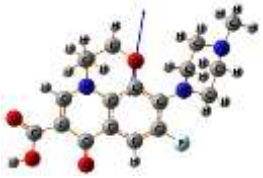	
NRF	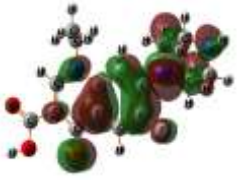	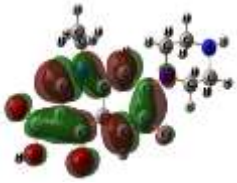		

(b)

Comp.	HOMO	LUMO	Optimized Structure	TDM-ESP
LVF		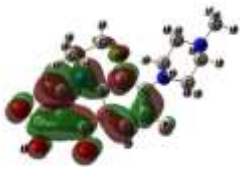		
NRF				

(c)

Figure 11.The HOMO-LUMO structures, optimized structure with dipole moment vector and total density matrix with electrostatic potential map (TDM-ESP) for LFV and NRF using (a) Semi-empirical method MP6, (b) DFT-B3LYP-3-21G and (c), DFT-B3LYP-6-31G.

In addition, dipole moments obtained by the theoretical method are larger than experimental results due to theoretical dipole moments depending on charge densities obtained from Eigen functions of the molecular orbital approximations. Also the quantum chemical methods usually yield an exaggerate electrons distribution in molecules and make them more polar than in reality (Manohara et al., 2013). Recent work on 5-methyl-benzofuran-3-yl-acetic acid hydrazine also indicated that the ground state dipole moment obtained by chemical calculation is larger than the excited state dipole moment (Maridevarmath et al., 2019). On the other hand the excited dipole moments obtained using the three methods are similar to the experimental value (5.970 and 7.160 D). The excited state dipole moment of LVF and NRF are 6.350, 6.939; 4.716, 6.20 and 5.277, 6.813 D using Semi-Empirical method PM6, TD-SCF-DFT-B3LYP-3-21G and TD-SCF-DFT-B3LYP-6-31G, respectively.

Investigation of frontier molecular orbital is important to realize the optical and electrical properties of molecules, since the energy gap between HOMO and LUMO governs the kinetic stability, chemical reactivity, optical polarizability, chemical hardness and softness of the molecule (Bratkowska et al., 2020). The molecule with large HOMO-LUMO gaps is generally stable and unreactive while ones with small gaps are highly reactive (Ivan et al., 2020; Morosanu et al., 2019). The HOMO-LUMO energy band gap of LVF and NRF compounds calculated are 0.146, 0.157 and 0.151, 0.162 eV using DFT-B3LYP-6-31G and 3-21G respectively. The HOMO-LUMO band gap energy of the two drugs are small compared to other aromatic compounds reported by (Belay, 2011; Libnedengel, et al., 2016) and this indicates that, the drugs are highly reactive or an electron of the HOMO orbital can easily be excited to the LUMO orbital (Sharma et al., 2021b; Uv et al., 2017). A difference in the electronic distribution was also noticed on the HOMO-LUMO molecular orbital plots of LVF and NRF as shown in Fig. 12. A higher electronic distribution was observed on the HOMO orbital level as compared to LUMO orbital.

The total density matrix with electrostatic potential map (TDM-ESP) is another crucial tool used to understand the hydrogen bonding interactions and the electrophilic and nucleophilic sites, and the charge distribution in a given molecule. Identifying these nucleophilic and electrophilic regions are essential to design non-linear optical materials (Akshaya et al., 2016). The purpose of the TDM-ESP analysis also gives a clue where the intermolecular interactions are formed within the molecule.

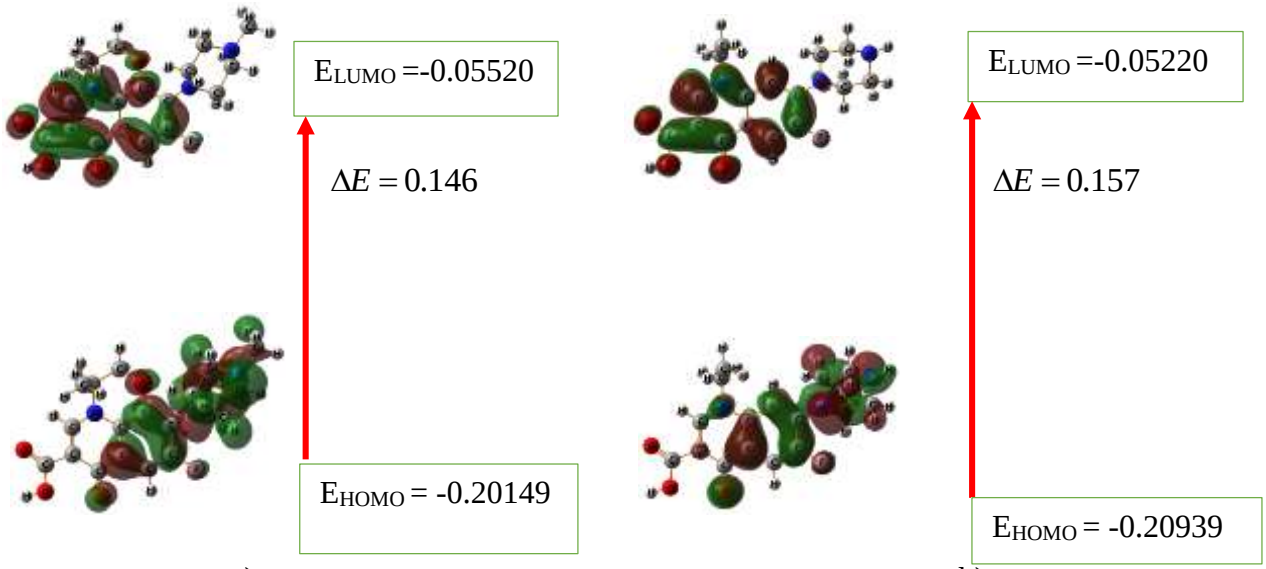

Figure 12. The HOMO-LUMO energy, band gap energy and structure of (a) LVF and (b) NRF using DFT-B3LYP-6-31G.

The electrostatic potential map plot of LVF and NRF shown in Fig.13 a, b. The electrostatic potential map of LVF and NRF are represented in red and blue colour. Blue colour represents a positive phase that corresponds to a nucleophilic region and red colour represents a negative phase corresponds to an electrophilic region (Patil et al., 2019). According to these calculated results, the 3D diagram TDM-ESP map shows that the negative potential sites are on oxygen atoms for electrophilic attack as well as the positive potential sites are around the Nitrogen atoms for nucleophilic attack symptoms.

Figure 13. Total density matrix with electrostatic potential map (TDM-ESP) of (a) LVF and (b) NRF

In addition, the UV/vis absorption spectra, the excitation energies and their corresponding oscillator strengths are determined using TD-SCF-DFT-B3LYP-6-31G since it determines these better than other methods (Allouche, 2011; Krawczyk, 2015). The result obtained

indicates that, at different excitation wave length the oscillatory strength of both LVF and NRF drugs are varied. The numerical values are shown in Table 5. The HOMO-LUMO structures and UV/vis spectra are shown in Fig 14. The excitation energy variation cause the oscillator strength of the drugs to be changed.

Comp.	HOMO	LUMO	UV-Vis. Spectra
LVF			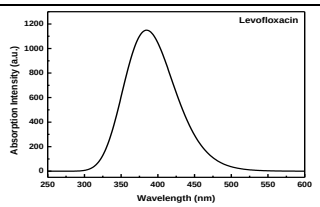
NRF			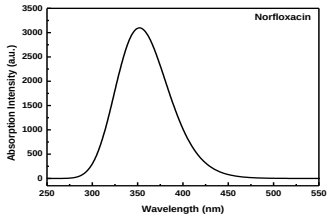

Figure 14. HOMO-LUMO structures and UV/vis spectra of LVF and NRF determined using TD-SCF-DFT-B3LYP-6-31G.

Table 5. The UV/visible absorption wavelengths and corresponding oscillator strengths determined using TD-SCF-DFT-B3LYP-6-31G.

Compound.	λ_1 (nm)	λ_2 (nm)	λ_3 (nm)	E_1 (eV)	E_2 (eV)	E_3 (eV)	S_1	S_2	S_3
LVF	416.4	394.0	386.3	2.9773	3.1467	3.2098	0	0.0262	0.0003
NRF	390.2	360.2	359.1	3.1773	3.4424	3.4529	0.0003	0.0118	0.0609

E_1- Excited State 1 energy and corresponding wavelength λ_1, oscillator strength S_1

E_2- Excited State 2 energy and corresponding wavelength λ_2, oscillator strength S_2

E_3- Excited State 3 energy and corresponding wavelength λ_3, oscillator strength S_3

4.2. Optical Transition Probability of LVF and NRF

The optical transition probabilities are useful for understanding the nature and strength of its molecular interaction in liquid solutions, in order to characterize the electron transition probabilities and interpret the absorption spectra of the compound (Ataklti et al., 2016; Belay & Gholap, 2009b; Keyeta & Gholap, 2011). Determination of these properties are also essential for direct experimental application in the emission, absorption and dispersion, and in providing

stringent test of atomic and molecular structure calculation in theoretical works (Belay, 2010; Belay & Gholap, 2009a). The optical transition probability such as transition dipole moments, Einstein A and B coefficients, oscillator strength, integrated absorption cross-section, were determined in different solvents using Eq. (2.73, 2.75, 2.76, 2.77) respectively and the results are shown in Table 6.

In this investigation, the oscillator strength of LVF and NRF in distilled water was calculated by absorption measurements. It was related to the molar extinction coefficient by using Eq. (2.76). The calculated oscillator strength of both LVF and NRF are larger in methanol as compared to other solvents as shown in Table 6. Increased oscillator strength can be due to absorption gets faster in solvents with high polarity and it is proportional to probability of a photon absorption based on polarity of the molecules (Zhang et al., 2020). The other important parameters like transition dipole moments, absorption coefficient, Einstein A and B coefficients also indicates both LVF and NRF have less transition probability in non-polar solvents and high transition probability in polar solvents at room temperature (Table 6). It is due to Einstein coefficients and absorption cross section are large where the atom inside a host medium are increasing for monochromatic field induced absorption rate in the given angular frequency range (Milonni & Eberly, 2010) . A similar trends were observed on recent study of coumarinyl and anthracene also shows high absorption coefficient and transition dipole moment in polar solvents (Fahmy et al., 2018).

Table 6. Optical transition probability of Levofloxacin and Norfloxacin

Drug	Solvents	Concentration (mole/L)	A	f	$\int \varepsilon dv$ (L/mol. cm) x10^{8}	$\int \alpha dv$ (cm^{-2})	δ_t(cm/molecule)x10^{-15}	B_{km}(s/kg) x10^{-12}	μ_{km}(C.cm) x10^{-28}	A_{km} (s^{-1}) x10^{-8}
LVF	Chloroform	1.5x10^{-5}	0.16	0.26	0.60	893.1	98.9	0.99	13.4	1.9
	Methanol	1.5x10^{-5}	0.34	0.44	1.02	1795	146	2.07	19.1	3.8
	DCM	1.5x10^{-5}	0.26	0.28	4.62	708.0	78.4	0.91	12.5	1.7
NRF	Chloroform	1.5x10^{-5}	0.18	0.21	0.57	859.1	95.1	0.91	12.8	2.0
	Methanol	1.5x10^{-5}	0.36	0.38	0.88	1782	147	1.50	16.2	2.6
	Isopropanol	1.5x10^{-5}	0.14	0.25	0.59	879.0	97.0	0.99	13.2	2.1

4.3. Photophysical Properties

4.3.1. Effects of Solvent Polarity on Photophysical Properties of LVF and NRF Drugs

The effect of solvent polarity on the photophysical properties of LVF and NRF were determined at room temperature and the results are listed in Table 7. The fluorescence quantum yield (φ_f) obtained using Eq. (2.79) indicates that, solvent polarity has significant effects on the quantum yield of LVF and NRF. This effect is due to reorientation of solvent around the solute which may affects the fluorescence spectra of the drugs (Woldegiorges et al., 2021). The effect of solvent polarity function (Δf) on φ_f are shown in Table 7. Higher φ_f of drugs were observed in non-polar solvents as compared to polar solvents and these can be due to absence of solute solvent interaction in non-polar solvents related to polar solvents and as the result the drugs undergoes fast radiative decays (Nad & Pal, 2001). In addition, it was also observed that φ_f of LVF is greater than NRF and this can be due to the structural differences of the LVF and NRF drug molecules (Bozkurt et al., 2017).

Moreover, in order to get an insight about the excited state dynamics of the drugs molecules, the fluorescence life time (τ_f) of LVF and NRF in different solvents are also calculated using Eq. (2.82) and the result are shown in Table 7. A change in the microscopic environment of the solvent shows profound effect on its fluorescence life time properties. The obtained results indicated there will be variation of the fluorescence life time with the solvent polarity. The variation in fluorescence life time is due to the drug molecules have different nature and interaction with the solvent molecules (Panja, 2021). Fluorescence lifetimes are also affected by the conformational stability of the molecule in the excited state which depends on the orientation polarizability of the surrounding solvent and other specific interactions (Sabahi et al., 2020).

Based on the fluorescence quantum yield and lifetime measurements, the values of rate constant for the decay of the excited state through radiative decay (k_r) and non-radiative decay (k_{nr}) in different solvent polarity are determined by using Eq. (2.80 or 2.83) and shown in Table 7. The result indicates that, the rate of non-radiative value were large in polar solvents relative to non-polar solvents. Less rate of non-radiative decay observed is possible because of the emission is from locally excited state in non-polar solvents and specific solvent interaction such as hydrogen bond and intermolecular charge transfer can be raised in the polar solvents

(Lakowicz, 2006). It could be observed that the values of both k_r and k_{nr} strongly depends on the type of solvent used.

The non-radiative rate constant can be also expressed in terms of the energy gap law after making due allowance for changes in the solvent reorganisation energy. As it is confirmed from the effects of solvent polarity on LVF and NRF emission spectra (section 4.1), red shift were observed in polar solvents compared to non-polar solvents. This was occurred as result of excited state of LVF and NRF molecules are more stable in polar solvents which decrease emitting molecules due to solute solvents molecules interactions or reaction. Hence, the non-radiative decay become large in polar solvents.

Table 7. Photophysical properties of Levofloxacin and Norfloxacin in different solvents

Solvent	Solvent polarity (Δf)	Levofloxacin				Norfloxacin			
		φ_f	$k_r \times 10^8$ (s^{-1})	$k_{nr} x10^8$ (s^{-1})	$\tau_f (ns)$	φ_f	$k_r \times 10^8$ (s^{-1})	$k_{nr} x10^8$ (s^{-1})	$\tau_f (ns)$
Chloroform	0.1486	0.47	3.76	4.89	0.13	0.22	2.96	1.06	0.07
Isopropanol	0.2762	0.12	5.17	38.6	0.02	0.19	3.81	1.66	0.49
Ethanol	0.2886	0.22	0.70	24.5	0.31	0.02	0.85	4.70	0.02
Water	0.3203	0.31	2.22	48.6	0.14	0.12	0.85	7.27	0.12

4.3.2. Concentration Dependent Photophysical Properties of LVF and NRF

Concentration dependent photophysical properties of LVF and NRF such as quantum yield, and fluorescence life time graphs are shown in Fig.15 and Fig.16 respectively. The result obtained clearly shows that, as the concentration of the drugs increasing, the quantum yield drastically reduced in the studied concentration range. In contrast, the fluorescence life time is increasing. The rapid decrease in quantum yield and increase in fluorescence life time at higher concentrations can be mainly attributed to the formation of dimers and higher aggregates which have a zero or very small fluorescence quantum yield (Al-Tememee et al., 2013; Antina et al., 2021). The competition between increasing dimer absorption and decreasing monomer absorption with increasing concentration plays a comparable role in decreasing quantum efficiency (Panja, 2021). Previous findings confirms that due to increase in concentration, the formation of dimer play a great role in decreasing quantum yield because of self-quenching of fluorescence intensity (Al-Tememee et al., 2013).

In this study, we employed solutions of LVF and NRF with varied concentration 2.4×10^{-6} – $1.68x10^{-5}M$ and 2.4×10^{-6} – $1.3\times10^{-5}M$, respectively, to investigate the effects of drug concentration on their emission spectra. Fig. 17 and 18 show the variation of emission spectra with the change in concentration and from the graphs it can be witnessed that the fluorescence intensity is linearly increasing at low concentration of LVF and NRF drugs. The linear increase of fluorescence intensity at lower concentration of LVF and NRF could be result of no aggregation formed (Itagaki, 2000).

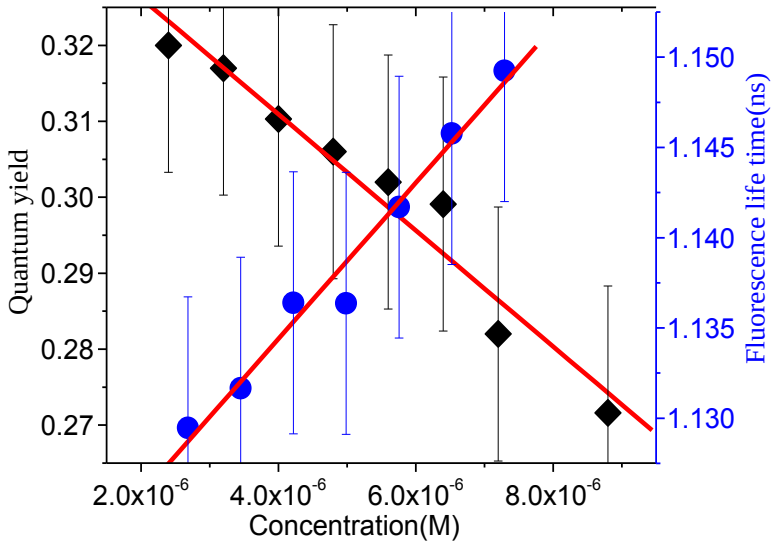

Figure 15. Quantum yield and fluorescence life time versus concentration of LVF

However, the emission intensity of LVF start to decrease when the concentration reaches beyond $1.68x10^{-5}M$. This may be due to the effect of high concentration reabsorption or inner filter effects and collisional quenching of the sample can happen. Something possibly occur with fluorescence or other emission processes is that emitted photons can be reabsorbed by ground state molecules (Biral Silva et al., 2021; Rodríguez & San Román, 2013). This is a particular problem of S_1-S_0 emission transition and the fluorescence intensity measured at the detector may actually start to drop (Montero et al., 1990).

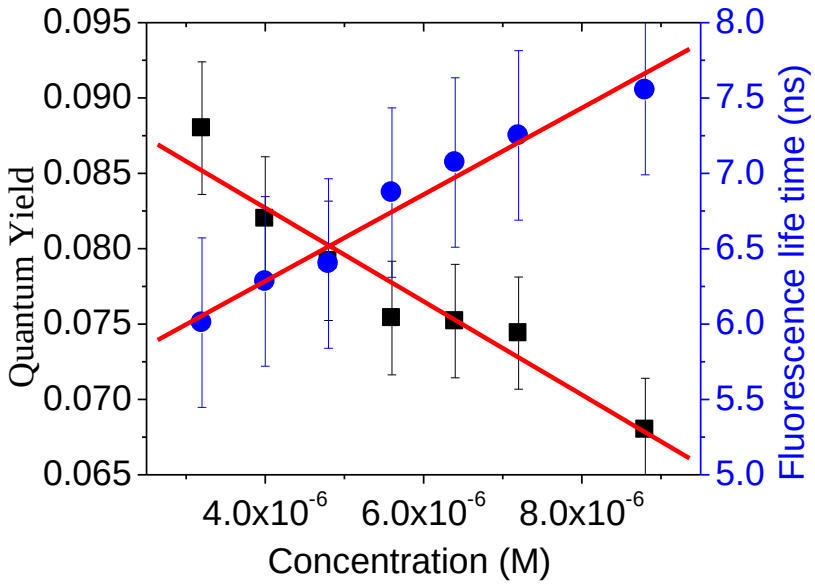

Figure 16. Quantum yield and fluorescence life time versus concentration of NRF

Any increment of concentration also affects the number and force of collisions taking place in the solution and influence the magnitude of the fluorescence emission. Collisions promote radiation less decay and loss of extra energy as heat, so more collisions or more forceful collisions will promote radiation less decay and reduce fluorescence emission (Itagaki, 2000; Robeson & Tilton, 1995).

In addition, at large drugs concentration, peak emission spectra of Fig. 17, and 18 indicated relatively slight blue shift. More of, the inset graph of Fig. 17, and 18 losses linearity at higher drug concentration. These confirms that there is formation of aggregation of the drugs molecules at higher concentration which indicates self-quenching of the drugs molecules (Rodríguez & San Román, 2013). Previous study confirms that deviations in photophysical properties of the drug molecules are one way to verify aggregation formation. When concentration increases, aggregation is perceived and loss of linearity in the relations between emission intensity versus sample concentration happen (Biral Silva et al., 2021).

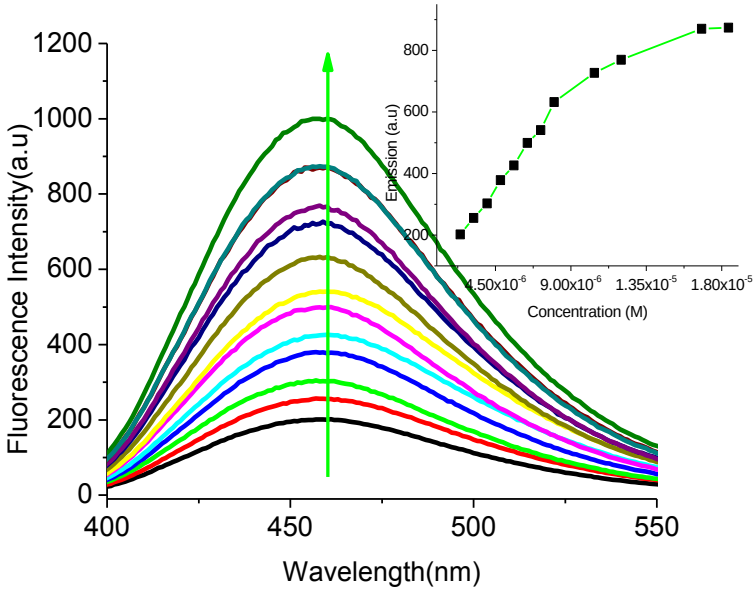

Figure 17. Emission spectra versus wavelength spectra of LVF in $(2.4\times10^{-6}, 3.2\times10^{-6}$ $4.0\times10^{-6}, 4.8\times10^{-6}$, $5.6\times10^{-6}, 6.4,\times10^{-6}$, $7.2\times10^{-6}, 8.0\times10^{-6}$, 1.04×10^{-5}, 1.2×10^{-5}, and $1.68\times10^{-5})$ M concentration

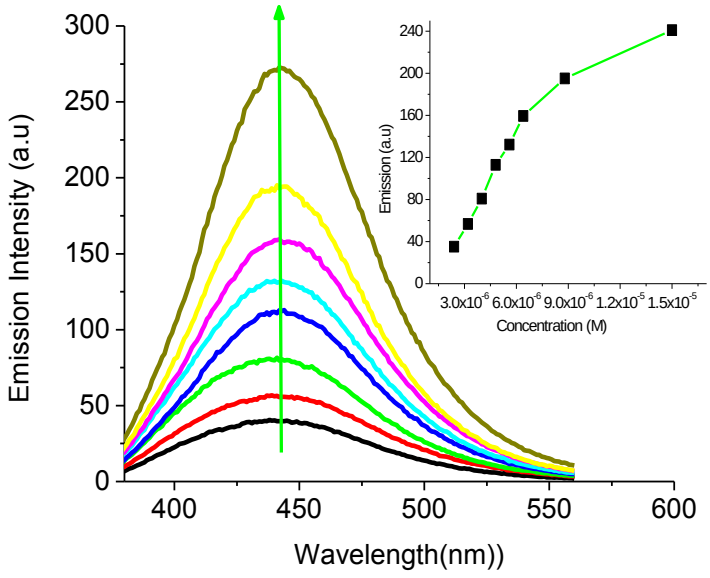

Figure 18. Emission spectra versus wavelength spectra of NRF in $(2.4\times10^{-6}, 3.2\times10^{-6}$, 4.0×10^{-6} , $4.8\times10^{-6}, 5.6\times10^{-6}$, $6.4,\times10^{-6}$, 8.8×10^{-6}, $1.3\times10^{-5})$ M concentration.

4.4. Fluorescence Quenching of LVF and NRF

In order to explain the effect of other molecules on the photo-chemical behaviour of drugs, the experiment based on fluorescence quenching as a function of quencher concentration were

interesting method (Amjadi & Farzampour, 2014). Fluorescence quenching is a process of decreasing the fluorescence intensity due to energy transfer, ground state complex formation, excited state reactions and collisional quenching between the molecules (Lakowicz, 2006). In this study, the fluorescence quenching of LVF and NRF drugs with caffeine (CF) were investigated. The fluorescence spectra of LVF and NRF in the absence and presence of caffeine were described in Fig. 19a and b respectively.

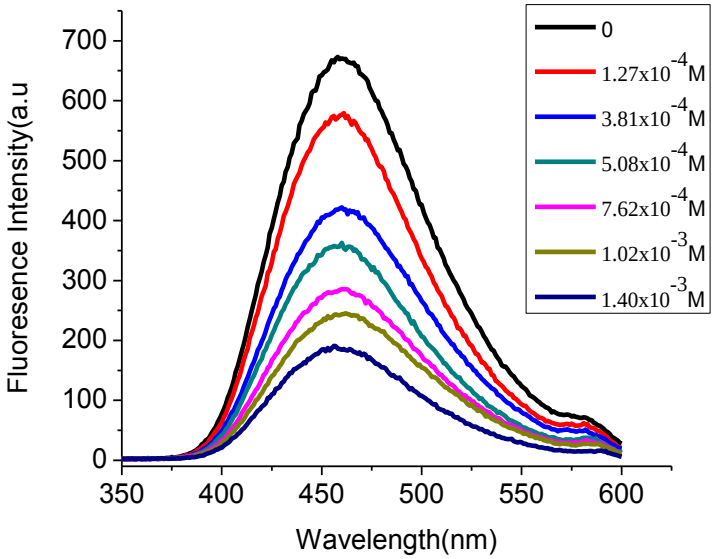

a)

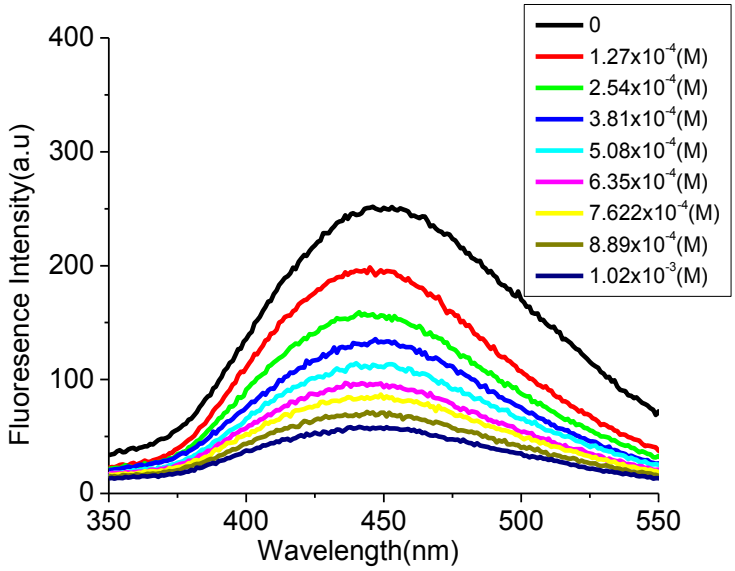

b)

Figure 19. Emission spectra of a) LVF and b) NRF in the presence of Caffeine

The result shows high intrinsic fluorescence quenching of drugs as concentration of caffeine is increasing. The decrease in fluorescence intensity of drugs indicate strong interaction of the drugs with caffeine in the system. However, there was no unusual change in the fluorescence

spectra of LVF and NRF drugs other than the reduction of fluorescence intensity and also no spectral shift was observed in presence of caffeine indicating that electronic transition of the fluorophore is not perturbed by the quencher (Panda et al., 2020).

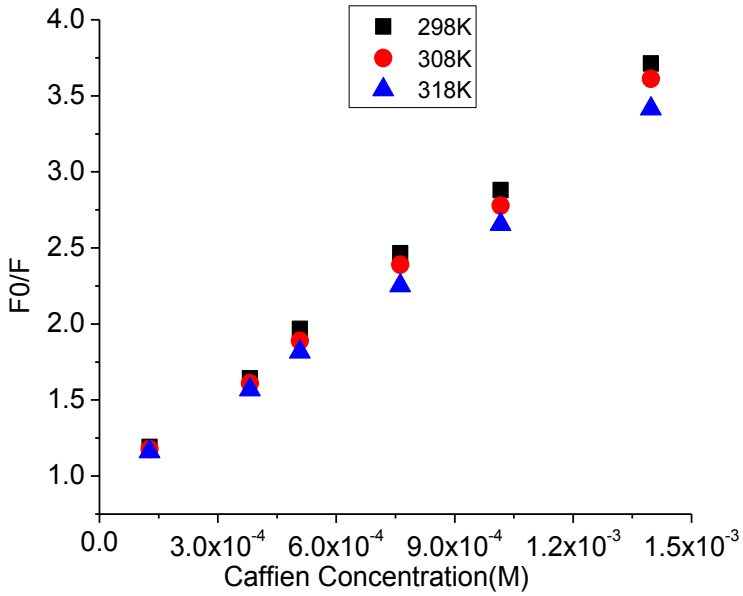

a)

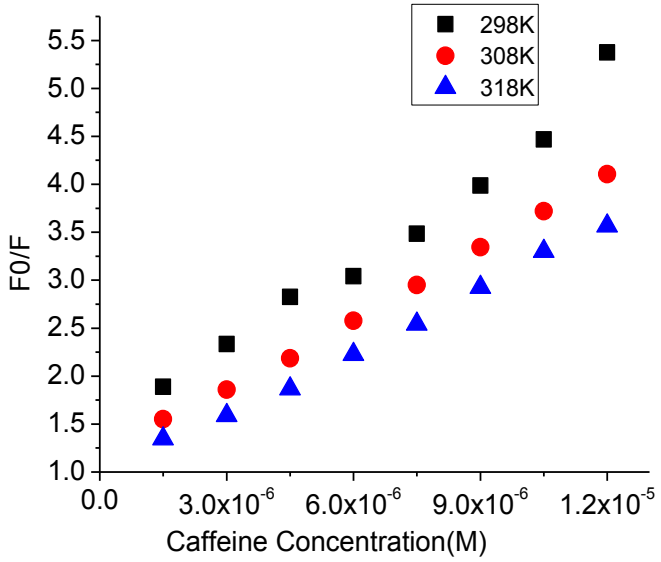

b)

Figure 20. Stern-volmer Plot quenching of (a) LVF $(8.8\times10^{-6}M)$ and (b) NRF $(1.2\times10^{-5}\text{M})$ by caffeine with different concentration at temperature of 298K, 308K, and 318K

The fluorescence quenching of LVF and NRF at different temperature are analysed by Stern-Volmer constant (K_{SV}) using Eq. (2.108) and the plot are displayed in Fig. 20a and b. Linear fittings (Fig. 20) of the experimental data afford K_{SV} and k_q (Table 8). The graphs show high

linearity (0.95, 0.98) with large slope (K_{SV}) of 1968.7 M^{-1} and 309514.1 M^{-1} respectively at 298K. The higher K_{SV} is an indication of strong interaction between the drugs and caffeine. The linearity suggesting the mechanism of quenching to be either static or dynamic (Rout et al., 2020). To know the nature of the interaction, the temperature dependent fluorescence spectrum was recorded at three distinct temperatures (298 K, 308 K, and 318 K). Result shown in Table 8 indicates, the Stern-Volmer constant decreased as the temperature is increasing which confirms that the quenching mechanism of both drugs are static quenching rather than dynamic quenching.

The value of bimolecular quenching rate constant (k_q) also determined in three varying temperature and the results are depicted in Table 8. The result found are in the range of $6.98 \pm 0.04 \times 10^{11}$ -$1.593 \pm 0.03 \times 10^{12}$ $M^{-1}s^{-1}$ and $1.55 \pm 0.21 \times 10^{14}$ - $2.104 \pm 0.50 \times 10^{15}$ $M^{-1}s^{-1}$ for LVF and NRF respectively. The value confirms that, k_q exceed by far diffusion controlled rate constant (2.0×10^{10} $M^{-1}s^{-1}$) in an aqueous solution (Belay, 2011, Kim, et al., 2016; Zhou et al., 1983). This point out the quenching mechanism does not involve a dynamic diffusion process, but rather occurs due to the formation of complexes of drugs-Caffeine.

Table 8. Stern-Volmer constant, and bimolecular quenching rate constant of LVF and NRF at different Temperature

Drugs	φ	$\tau_f(ns)$	$T(K)$	$K_{SV}(M^{-1})$	$k_q \times (M^{-1}s^{-1})10^{12}$	R
LVF	0.279±0.021	1.265±0.03	298	2015.6 ± 33	1.593 ± 0.03	0.95
			308	1868.5 ± 21	1.477 ± 0.02	0.98
			318	1777.3 ± 15	0.698 ± 0.04	0.94
NRF	0.0742±0.004	7.22±0.12	298	289676 ± 14	2104.3 ± 0.50	0.98
			308	244474 ± 12	1675.8 ± 0.14	0.94
			318	218983 ± 35	155.20 ± 0.21	0.97

4.4.1. Determination of Binding Site and Binding Constant

The fluorescence results can also be used to obtain the binding constant (k_a) and the number of binding sites (n) of interacting molecules. The values of k_a and n of the interaction between drug and caffeine is very important for understanding the distribution of the drug in plasma

which may have an impact on pharmacodynamics and pharmacokinetics of drugs (Mrkalić et al., 2021; Weiser & Weigmann, 2019). As mentioned under section 3.4, the quenching mechanism of LVF and NRF by caffeine were static through formation of non-fluorescent complex. If a non-fluorescence complex forms, the intrinsic binding constant and number of binding sites are calculated using the graph of $\log(F_0 - F)/F$ vs $Log([Q]-[D](F_0 - F)/F_0))$ stated in Eq. (2.109). The graph were shown in Fig. 21a and b and the results are given in Table 9. The value of binding site for both LVF and NRF is about 1, predicting that one molecule of caffeine is bound to one molecule of the drugs or suggesting 1:1 association for complex formed between the drugs and caffeine.

The value of binding constant of LVF and NRF with caffeine also studied in the vivo situation of drug temperature and the result indicates strong interaction of the LVF and NRF dugs with a caffeine. Strong drug-caffeine interaction might prolong the storage time of drug in plasma and consequently could reduce the efficacy of the drug (Stojanović et al., 2020). This is based on the free drug hypothesis which states the cellular uptake is proportional to the unbound concentration of drugs in circulating plasma (Lazo et al., 2021). The drug-ligand interaction also affects the pharmacokinetic properties of the drug. For example recent investigation on caffeine-clozapine interaction provide toxicity (Yartsev & Peisah, 2021). Moreover, the binding constant and binding site of both drugs decreases as the temperature is increasing, which confirms unstable compound formation that can be partly decomposed at highest temperature.

Table 9. Nature of binding parameters such as binding constant (k_a), number of binding sites of Levofloxacin and Norfloxacin at different Temperature (T)

Drug Molecules	$T(K)$	$Log(k_a)$	$k_a(M^{-1})\times 10^4$	n
Levofloxacin	298	3.544 ± 0.21	0.351± 0.05	1.10 ± 0.05
	308	3.538 ± 0.32	0.345 ± 0.02	1.09 ± 0.02
	318	3.527 ± 0.53	0.336 ± 0.04	1.01 ± 0.01
Norfloxacin	298	3.265 ± 0.02	0.191 ± 0.08	0.96 ± 0.06
	308	2.914 ± 0.07	0.082 ± 0.42	0.95 ± 0.01
	318	2.674 ± 0.21	0.047 ± 0.39	0.87 ± 0.04

Therefore, decreasing of binding constant suggested that the affinity of the LVF and NRF with caffeine were reduced which might improve the free concentrations of unbound drug and

enhanced its pharmacology effects (Lazo et al., 2021). On the other hand, the magnitude of k_a values of NRF is much larger than LVF, indicating Caffeine exhibit strong affinity to NRF than LVF.

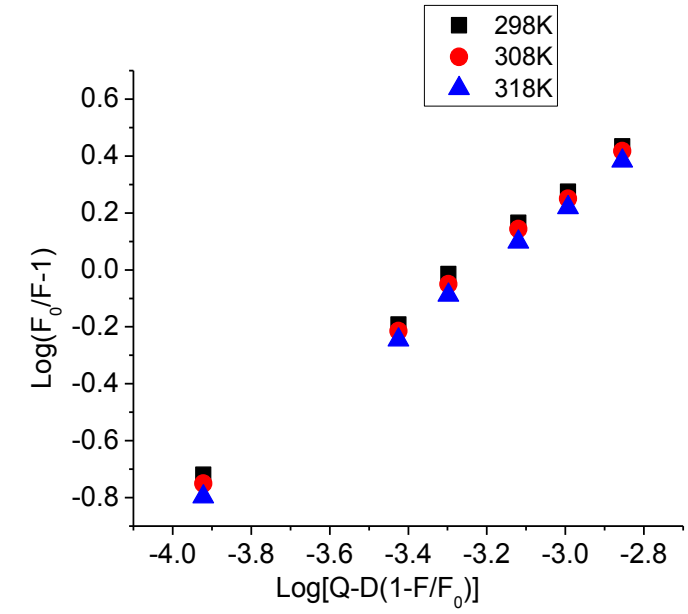

a)

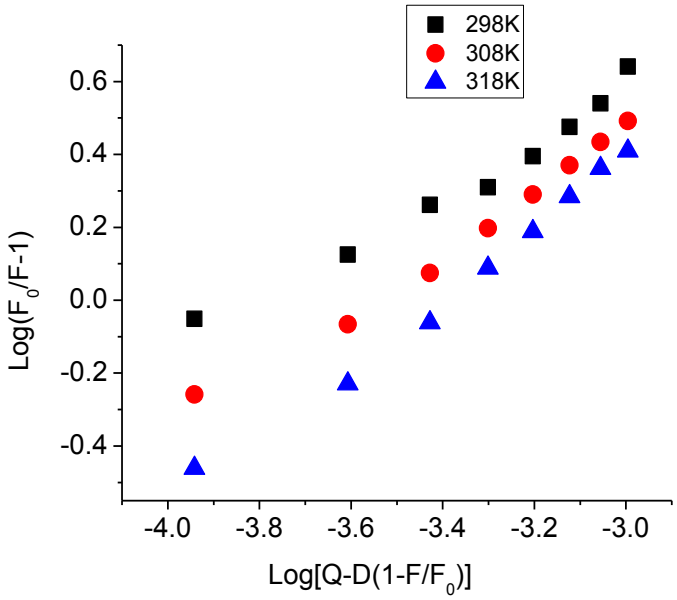

b)

Figure 21. Graph of $\log(F_0 - F)/F$ vs $Log([Q]-[D](F_0 - F)/F_0))$ when caffeine $(1.27\times10^{-4}M - 1.4\times10^{-3}M)$ binding to (a) LVF $(8.8\mu M)$ and (b) NRF $(12\mu M)$.

4.4.2. Thermodynamic Parameters and Nature of Binding Force between Drugs and Caffeine

Fluorescence spectroscopy can also employed to deduce thermodynamic parameters involved in drug-ligand interaction(Xiong et al., 2017). The evaluation of the thermodynamic and association parameters of drugs-caffeine interaction can provide crucial diagnostic information toward a molecular level understanding of the interaction process (Paul et al., 2017). To get further understanding about the interaction of LVF-CF and NRF-CF association, the thermodynamic parameters such as enthalpy (ΔH), entropy (ΔS) and Gibbs free energy change (ΔG) at three temperatures were determined using Vant-Hoff Eq. (2.110) (Meena & Kishore, 2021). The parameters were determined based on the data derived from fluorescence quenching of the LVF and NRF drugs with added caffeine and presented in Table 10. Result shows, the free energy change value is negative indicating binding between the drugs and caffeine occur spontaneously. The negative enthalpy suggested that the binding reaction was an exothermic process, thereby providing a reasonable explanation for the decreasing k_a as temperature is increasing.

The binding forces mostly include hydrogen bonding interaction, van der Waals forces, electrostatic interaction and hydrophobic interaction, which can be confirmed based on the signs and magnitudes of the thermodynamic parameters (Wang et al., 2016; Wang et al., 2020). The sign and value of ΔH and ΔS obtained for both drugs (Table 10) shows the responsible force for the interaction of LVF with caffeine is electrostatic interaction and for NRF are Van der Waals and hydrogen bond.

Table 10. Thermodynamic parameters such as enthalpy change (ΔH), Free Energy change (ΔG) and entropy change (ΔS) in different temperature (T)

Drug Molecules	$T(K)$	lnk_a	$\Delta H(molL^{-1})$	$\Delta S(JmolL^{-1}K^{-1})$	$\Delta G(kJ/mol)$
	298	8.16 ± 0.20	-1.58 ± 0.1 $\times 10^3$	- 62.8 ± 1	-21.5 ± 0.25
	308	8.14 ± 0.01			-20.8 ± 0.41
Levofloxacin	318	8.12 ± 0.31			-20.2 ± 0.12
	298	9.88 ± 0.04	-5.53 ± 08$\times 10^4$	123.9 ± 2	-12.4 ± 0.17
	308	8.96 ± 0.05			-11.6 ± 0.21
Norfloxacin	318	8.02 ± 0.41			-10.1 ± 0.65

Previous work suggests, if the thermodynamic parameters $\Delta H \leq 0$, and $\Delta S > 0$ the interaction force is electrostatic force (Kumar & Asuncion, 1993). Similarly, report were observed previously when the value of ΔH and ΔS are both negative, hydrogen bond and van der Waals forces are the main contributing interactions force in the binding process (Keswani et al., 2021).

4.4.3. UV/vis Absorption Spectroscopy Study

The electronic UV/Vis absorption measurement is very simple and applicable method that widely used to investigate the quenching mechanism and structural change of drug molecules interaction with other compound molecules (Mrkalić et al., 2021). If the fluorescence quenching mechanism of LVF and NRF induced by small molecule refers to dynamic quenching, the molecules only affects the excitation state of drugs instead of its absorption spectrum (Wang et al., 2016). Otherwise, if the fluorescence quenching mechanism is the static quenching or the ground state complex formation will resulting in the change of the absorption spectrum of LVF and NRF drugs. The UV/vis absorption spectra of the LVF and NRF were measured by varying the concentration of caffeine added to the drug solution and shown in Fig. 22a and b respectively. Up on addition of Caffeine to LVF and NRF solution, the absorption spectra of LVF around 340nm and NRF nearby 332nm were blue shifted. In addition, isosbestic point were appeared at 294nm on LVF-CF and at 289nm on NRF-CF complex spectra. Meanwhile, the formation of blue shift of absorption bands and isobestic point clearly indicates that, ground state complex formation of LVF and NRF with caffeine.

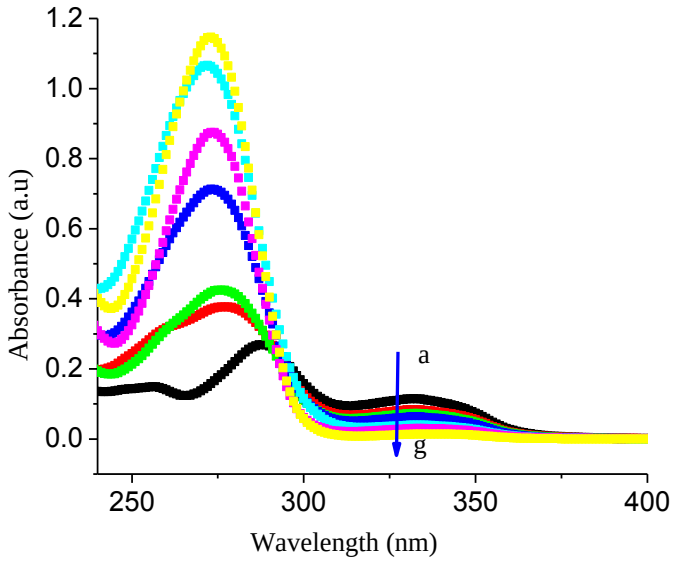

a)

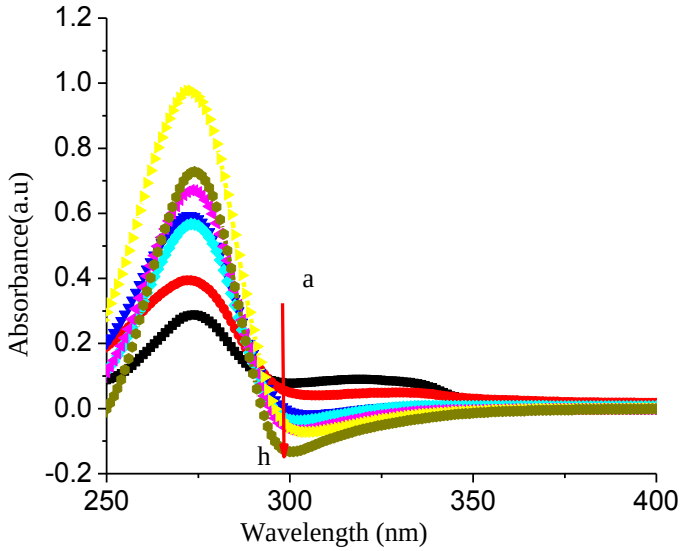

b)

Figure 22. UV/Vis Absorption spectra of (a) LVF-CF and (b) NRF-CF Complex

These confirms the results of fluorescence quenching mechanism of the molecules caused mainly by static quenching mechanism. The result obtained are in agreement with the reported studies on binding interaction of caffeine with caffeic acid and chlorogenic acid (Belay, 2011, Kim, et al., 2016).

4.4.4. Fourier Transform Infrared Spectroscopy

Fourier transform infrared spectroscopy (FTIR) is another essential technique that provides information related to functional groups present in the molecule. The data obtained from the experiment is in the form of a spectrum that acts as the molecular fingerprint of the compound (Mohd et al., 2010).To explore the conformation of the interaction of LVF-CF and NRF-CF, the FTIR spectra of the molecules are measured. The molecules of LVF and NRF are characterized due to carbonyl, carboxylic group and aromatic ring exist in the compounds. As observed in Fig.23a and b, typical characteristics of LVF and NRF FTIR absorption spectral peak 3200-3447 cm^{-1} corresponds to carboxylic group OH stretching and intermolecular hydrogen bonding, 1682 cm^{-1} is due to carbonyl $C=O$ stretching, and 2854 cm^{-1} attributed to aromatic $C-H$ group stretching (Sahoo et al., 2012).

In the case of caffeine spectra (Figs 20a and b) the symmetrical and asymmetrical stretching located at 2953 cm^{-1} and 3105 cm^{-1} are due to $C-H$, and spectra from 1550-1700 cm^{-1} corresponds to $C=O$ vibration band (Coates, 2006; Gunasekaran et al., 2005). The FTIR main absorption spectra of LVF observed on 2854 cm^{-1} due to aromatic $C-H$, 3247 cm^{-1}

from carboxylic OH and NRF observed on 2849.85 cm^{-1} from aromatic $C-H$, and 3447 cm^{-1} due to carboxylic OH are disappeared in LVF-CF and NRF-CF reaction.

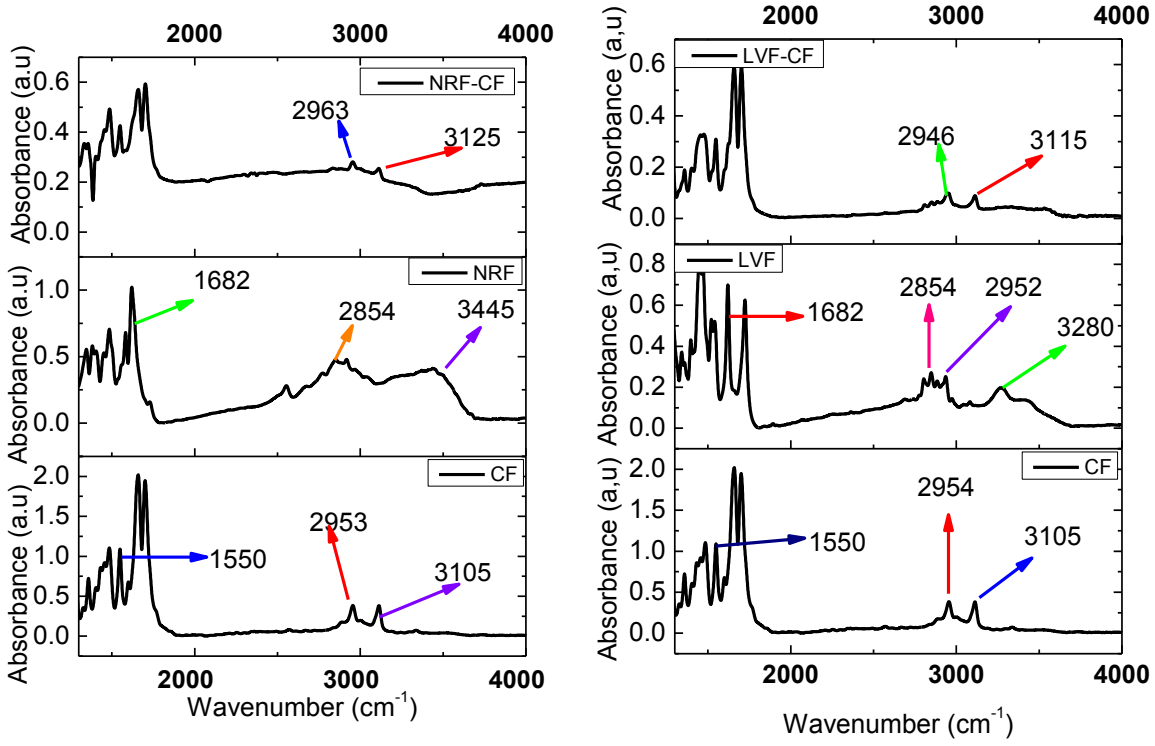

a) b)

Figure 23. FTIR absorption spectra of CF, NRF, LVF, NRF-CF, and LVF-CF

According to literature report, change in absorption spectra post interaction can be formed due to conformational change as result of reaction between the molecules (Alsaif et al., 2020). In general, the disappearance of existing spectra observed in the reaction of LVF-CF and NRF-CF are an indication of the binding between molecules.

5. CONCLUSIONS

In these research, the effects of solvent polarity on LVF and NRF absorption and emission spectra, the photophysical properties of varying sample concentration and solvent polarity effect, and the interaction of LVF and NRF drugs with caffeine were investigated. The results indicate that the emission spectra of both compounds are more strongly affected than the electronic absorption spectra. The effect of solvent polarity on the absorption and emission spectra of LVF and NRF were used to estimate the ground and excited state dipole moments. The dipole moments of LVF and NRF were estimated by Lippert-Mataga, Bakhshiev's, Kawski-Chamma-Viallet, and Reichardt methods. The excited state dipole moments calculated from experimental results are bigger than the ground state dipole moments showing that the probe compounds are significantly more polar in the excited state than the ground state. The dipole moment values, spectral properties and understanding the different resonance structures of drug molecules give important information about solute solvent interactions that can be useful in studying of these molecules operations in biological systems.

On another hand, Computational analysis was performed by Gaussian 09 using DFT methods at B3LYP-3-21G, B3LYP-6-31G level of theory and semi-empirical MP6 method. The calculated HOMO-LUMO energy band gap obtained by all methods are small and these indicate that both compounds are highly reactive. Larger dipole moments were obtained from computational work than from the experimental results, due to the absence of solvent effects. The result also assured that photophysical properties are influenced due to drugs concentration and solvent polarity. Quantum yield decreasing as the sample concentration is increasing, whereas fluorescence life time increasing with concentration.

In addition, the binding of fluoroquinolone antibiotic drugs LVF and NRF with caffeine is investigated and the fluorescence intensity of both drugs quenched by caffeine. As it is confirmed from steady state fluorescence measurement and UV-vis absorption, the quenching mechanism is static. Thermodynamic parameters value obtained from spectral analysis indicates, the reaction between the drugs and Caffeine occur spontaneously and it is due to electrostatic force in LVF and hydrogen bond and van der Waals force in NRF. Also the FTIR absorption spectra of LVF-CF and NRF-CF confirms the conformational change of the drugs and result obtained verify the structural change due to caffeine molecule bind to drug molecule.

6. FUTURE RESEARCH AND RECOMMENDATIONS

From an overall outlook, due to financial constraints and lack of characterizing instruments, a full characterization of drugs-caffeine interaction were not addressed in this research. Hence in the future, changes of the drug particles size happen during its binding interaction with caffeine which is important to determine the efficacy of the drug cytotoxicity is one of the area of investigation. In addition, cell imaging studies to check the capability to cross the cell membrane during drug caffeine interaction and in vivo application will be the other focusing areas. The investigation clearly identified that the drugs structural change as a result of their interaction with different solvents. Since the drugs geomtrical structure change affects the pharmacokinetic properties and provide drug toxicity, we suggested the pharmacologist to consider the issue in drug design. Also the study of LVF-Caffeine and NRF-Caffeine identified the presence of reaction or complex formation between the caffene and drugs. Complex formation between the drug and Caffeine affects the pharmacokinetic properties of the drugs. In the future, we will also further investigate other bioactive compounds found in the food we are consuming such as carotenoid, polyphenols, coenzymes and organosulfur intercation with these drugs and also to more study this area using advanced instrument such as nuclear magnetic resonance (NMR) spectroscopy.

7. LIST OF PUBLICATIONS

1. K. Woldegiorges, A. Belay, A. Kebede, T. Abebe, Estimating the Ground and Excited State Dipole Moments of Levofloxacin and Norfloxacin Drugs Using Solvatochromic Effects and Computational Work. *Journal of Spectroscopy*, 2021 (2021), 1-13. https://doi.org/10.1155/2021/7214182
2. K. Woldegiorges, A. Belay, A. Kebede, Woldegiorges, K., Belay, A., & Kebede, A. (2022). Photophysical properties of levofloxacin and norfloxacin drugs and their fluorescence quenching mechanism with caffeine. *Spectroscopy Letters*, *0*(0), 1–14. https://doi.org/10.1080/00387010.2022.2110596
3. U. Sherefedin, A. Belay, K. Gudishe, A. Kebede, S. Asemare, K. Woldegiorges, Determination of the ground and excited state dipole moments of Ferulic and Sinapic acids: Spectroscopic and Computational approaches. *Journal of Theoretical and Computational Chemistry* (in progress).

REFERENCES

Abraha, A., et al. (2016). Study Self-association , Optical Transition Properties and Thermodynamic Properties of Neomycin Sulfate Using UV-Visible Spectroscopy. *International Journal of Biophysics*, *6*(2): pp.16–20.

Akshaya, K. B., et al. (2016). Synthesis and photophysical properties of a novel phthalimide derivative using solvatochromic shift method for the estimation of ground and singlet excited state dipole moments. *Journal of Molecular Liquids*, *224(4)*: pp. 247–254.

Al-Tememee, N. A. A., et al. (2013). Effect of Solvents on the Dipole Moments and Fluorescence Quantum Yield of Rhodamine Dyes. *ISESCO Journal of Science and Technology*, *9*(16): pp.34–42.

Aldred, K. J., et al. (2013). Topoisomerase IV-quinolone interactions are mediated through a water-metal ion bridge: Mechanistic basis of quinolone resistance. *Nucleic Acids Research*, *41*(8): pp.4628–4639.

Alizadeh, K., et al. (2012). Spectrofluorimetric study of the interaction of ciprofloxacin with amino acids in aqueous solution following solvatochromic studies. *Spectrochimica Acta - Part A: Molecular and Biomolecular Spectroscopy*, *94*(1): pp. 72–77.

Allouche, A. (2011). Gabedit--a graphical user interface for computational chemistry softwares. *Journal of Computational Chemistry*, *32*(1): pp.174–182.

Alsaif, N. A., et al. (2020). Multi-spectroscopic investigation, molecular docking and molecular dynamic simulation of competitive interactions between flavonoids (quercetin and rutin) and sorafenib for binding to human serum albumin. *International Journal of Biological Macromolecules*, 12(4): pp. 2451-55.

Amjadi, M., & Farzampour, L. (2014). Fluorescence quenching of fluoroquinolones by gold nanoparticles with different sizes and its analytical application. *Journal of Luminescence*, *14594)*: pp. 263–268.

Antina, L. A., et al. (2021). Effect of polar protic solvents on the photophysical properties of bis(BODIPY) dyes. *Journal of Molecular Liquids*, *337(1)*: pp.116-122.

Ataklti, A., et al. (2016). Investigation of self-association, optical transition probability and hetero-association with chlorogenic acid of nicotinamide using UV-Vis spectroscopy.

International Journal of Physical Sciences, *11*(21): pp.269–278.

Bakhshiev, N. G., et al. (1969). Experimental Determination of the Dipole Moments of Organic Molecules in Excited Electronic States. *Russian Chemical Reviews*, *38*(9): pp. 740–754.

Banwell, C. N. (1983). *Colin N. Banwell - Fundamentals of Molecular Spectroscopy-McGraw-Hill (1983)*: pp. 106–116.

Barcelos, R. P., et al. (2020). Caffeine effects on systemic metabolism, oxidative-inflammatory pathways, and exercise performance. *Nutrition Research*, *80 p.*

Basavaraja, J., et al. (2016). Estimation of ground and excited state dipole moment of laser dyes C504T and C521T using solvatochromic shifts of absorption and fluorescence spectra. *Spectrochimica Acta - Part A: Molecular and Biomolecular Spectroscopy*, *154(3)*: pp. 177–184.

Bayliss, N. S. (1950). The effect of the electrostatic polarization of the solvent on electronic absorption spectra in solution. *The Journal of Chemical Physics*, *18*(3): pp. 292–296.

Bayliss, N. S., & Mcrae, E. G. (1954). Solvent effects in organic spectra: Dipole forces and the Franck-Condon principle. *Journal of Physical Chemistry*, *58*(11): pp. 1002–1006.

Belay, A. (2010). Measurement of integrated absorption cross-section, oscillator strength and number density of caffeine in coffee beans by integrated absorption coefficient technique. *Food Chemistry*, *121*(2): pp.585–590.

Belay, A. (2011). *Spectrophotometric Investigation of Major Bioactive Compounds of Coffee Beans*," Ph.D. Thesis Submitted to Addis Ababa University, 80 p.

Belay, A., & Gholap, a. V. (2009a). Characterization and determination of chlorogenic acids (CGA) in coffee beans by UV-Vis spectroscopy. *African Journal of Pure and Applied Chemistry*, *3*(11): pp. 234–240.

Belay, A., & Gholap, A. V. (2009b). Determination of integrated absorption cross-section, oscillator strength and number density of caffeine in coffee beans by the integrated absorption coefficient technique. *Inter. Journal of Physical Sciences*, *4*(11): pp.722–28.

Belay, A., et al. (2016). Binding of caffeine with caffeic acid and chlorogenic acid using

fluorescence quenching, UV/vis and FTIR spectroscopic techniques. *Luminescence*, *31*(2): pp. 565–572.

Belay, A., et al. (2016). Effects of solvent polarity on the absorption and fluorescence spectra of chlorogenic acid and caffeic acid compounds: Determination of the dipole moments. *Luminescence*, *31*(1): pp.118–126.

Belayneh, A., & Molla, F. (2020). *The Effect of Coffee on Pharmacokinetic Properties of Drugs*. Journal of BioMed Research International, *2020(8)*: pp.*1-11*.

Benazzouz, A., et al. (2016). Study of novel fluorescent coumarin-3,4-dihydropyrimidin-2(1H)-ones dyads. Estimation of ground- and excited-state dipole moments from a solvatochromic shift. *Journal of Molecular Liquids*, *219*(12): pp. 173–179.

Benvenga, S., et al. (2008). Altered intestinal absorption of L-thyroxine caused by coffee. *Thyroid*, *18*(3): pp. 293–301.

Bilot, L., & Kawski, A. (1962). Zur Theorie des Einflusses von Lösungsmitteln auf die Elektronenspektren der Moleküle. *Zeitschrift Fur Naturforschung - Section A Journal of Physical Sciences*, *17*(7) : pp. 621–627.

Biral Silva, C., et al. (2021). Concentration and solvent effects, photochemical and photophysical properties of methyl and tert-butyl zinc(II) and aluminum(III) phthalocyanines. *Journal of Molecular Structure*, *1246(5)* : pp. 131103.

Boraste, D. R., et al. (2018). Supramolecular host-guest interaction of antibiotic drug ciprofloxacin with cucurbit[7]uril macrocycle: Modulations in photophysical properties and enhanced photostability. *Journal of Photochemistry and Photobiology A: Chemistry*, *358*(4): pp. 26–37.

Bozkurt, E., et al. (2017). Investigation of solvent effect on photophysical properties of some sulfonamides derivatives. *Turkish Journal of Chemistry*, *41*(2): pp. 282–293.

Bratkowska, M., et al. (2020). *Experimental and theoretical insight into spectroscopic properties and bioactivity of 4-(4-formylbenzylidene)-2-phenyloxazol-5(4H)-one dye for future applications in biochemistry*. *Journal ofMolecular Liquids*, 314 (2020): pp. 113632.

Brooks, R. L. (2013). *The Fundamentals of Atomic and Molecular Physics* 5th edition.

Springer New York, pp 468.

Camarasa, J., et al. (2006). Association of caffeine to MDMA does not increase antinociception but potentiates adverse effects of this recreational drug. *Brain Research*, *1111*(1): pp. 72–82.

Capaz, R. B. (2014). Carsten A. Ullrich—Time-Dependent Density-Functional Theory: Concepts and Applications. *Brazilian Journal of Physics*, *44*(2–3): pp. 286–288.

Carrillo, J. A., & Benitez, J. (2000). Clinically significant pharmacokinetic interactions between dietary caffeine and medications. *Clinical Pharmacokinetics*, *39*(2): pp.127–153.

Chirasani, V. R., et al. (2021). Structural and functional interactions between the Ca2+-, ATP-, and caffeine-binding sites of skeletal muscle ryanodine receptor (RyR1). *Journal of Biological Chemistry*, *297*(3): pp. 101040.

Christina Pires Gonçalves, L. (2021). Photophysical properties and therapeutic use of natural photosensitizers. *Journal of Photochemistry and Photobiology*, *7*(6): pp. 100052.

Chuang, C., Chou, S. H., Wang, F. Der, Huang, Y. H., Tsai, T. H., & Lin, Y. T. (2020). Fluoroquinolones as an alternative treatment for Klebsiella pneumoniae liver abscess and impact on hospital length of stay. *International Journal of Antimicrobial Agents*, *56 (2020)*: pp. *106120*.

Coates, J. (2006). Interpretation of Infrared Spectra, A Practical Approach. *Encyclopedia of Analytical Chemistry*, pp. 10815–10837.

Congrave, D. G. (2018). Synthesis and Photophysical Properties of New Di- and Mononuclear Phosphorescent Iridium (III) Complexes. *Durham E-Theses Synthesis 4(1)*: pp. *20-32*.

Constantinos D. and Zenalipour-Yazdi, (2022). A DFT study of the interaction of aspirin, paracetamol and caffeine with one water molecule. Journal of molecular modeling, 2(28): pp. 285-290

Cuquerella, M. C., et al. (2006). Role of excited state intramolecular charge transfer in the photophysical properties of norfloxacin and its derivatives. *The Journal of Physical Chemistry. A*, *110*(8): pp. 2607–2612.

Das, S., et al. (2019). *Coffee Modify Pharmacokinetics of Acetaminophen*. *Journal of Pharmacology and Toxicology, 7(1)*: pp. 1091-1098.

De Guidi, G., et al. (2011). Photosensitization Reactions of Fluoroquinolones and Their Biological Consequences. *Photochemistry and Photobiology*, *87*(6): pp.1214–1229.

Demtröder, W. (1996). *Laser Spectroscopy*. Springer Berlin Heidelberg, 78(1): pp. 148-487.

Demtröder, W. (2003). *Laser Spectroscopy*. Springer Berlin Heidelberg, 86(3): pp.784-896.

Demtröder, W. (2010). *Atoms, Molecules and Photons*. Springer Berlin Heidelberg, 102(2): pp. 456-965.

Desai, V. R., et al. (2016). Steady state absorption and fluorescence study: Estimation of ground and excited state dipole moments of newly synthesized pyridazin-3(2H)-one derivatives. *Journal of Molecular Liquids*, *223*(9): pp. 141–149.

Dorohoi, D. O., et al. (2020). Computational and spectral means for characterizing the intermolecular interactions in solutions and for estimating excited state dipole moment of solute. *Symmetry*, *12*(8): pp. 1-23.

Downey, C., et al. (2014). An in vitro approach to assessing a potential drug interaction between MDMA (ecstasy) and caffeine. *Toxicology in Vitro, 28*(2): pp. 231–239.

El-Mossalamy, E. H., et al. (2011). Photophysical parameters and fluorescence quenching of 7- diethylaminocoumarin (DEAC) laser dye. *Optics and Laser Technology*, *43*(7): pp. 1078–1083.

Fàbrega, A., et al. (2009). Mechanism of action of and resistance to quinolones. *Microbial Biotechnology*, *2*(1): pp. 40–61.

Fahmy, H. M., et al. (2018). Spectroscopic Study of Solvent Polarity on the Optical and Photo-Physical Properties of Novel 9,10-bis(coumarinyl)anthracene. *Journal of Fluorescence, 28*(6): pp. 1421–1430.

Fatma, N., et al. (2021). Experimental and theoretical interpretations of spectral behavior of 6-methoxyflavone. *Journal of Photochemistry and Photobiology A: Chemistry, 404*(1) : pp.112945-4.

Ferrie, R. P., et al. (2017). A Fluorescence Quenching Analysis of the Binding of

Fluoroquinolones to Humic Acid. *Applied Spectroscopy*, *71*(11): pp. 2512–2518.

Fish, D. N. (2001). Fluoroquinolone adverse effects and drug interactions. *Pharmacotherapy*, *21*(10): pp.1–4.

Fowles, G. R. (1975). *Introduction to modern optics*. Courier Corporation. *American Journal of Physics*, 48(2): pp. 245- 381.

Fowles, G. R., & Lynch, D. W. (1968). Introduction to Modern Optics. *American Journal of Physics*, 36(8): pp.187-274.

Franklin, A. (2003). Nutrition and Diagnosis-Related Care. *Topics in Clinical Nutrition*, *18*(2): pp.146–147.

Frisch, M. J., et al. (2009). Gaussian 09, Revision B.01. *Royal society of chemistry*, 20 p.

Fukasawa, T., et al. (2006). Effects of caffeine on the kinetics of fluvoxamine and its major metabolite in plasma after a single oral dose of the drug. *Therapeutic Drug Monitoring*, *28*(3): pp.308–311.

Gao, F., et al. (2019). Quinolone hybrids and their anti-cancer activities: An overview. *European Journal of Medicinal Chemistry*, *165*(4): pp. 59–79.

García, C., et al. (2005). Substitution and solvent effects on the photophysical properties of several series of 10-alkylated phenothiazine derivatives. *Journal of Physical Chemistry A*, *109*(15): pp. 3360–3371.

Garcıa-Casal, M. N., et al. (1998). Nutrient Requirements and Interactions: Vitamin A and B-Carotene Can Improve Nonheme Iron Absorption from Rice, Wheat and Corn by Humans. *The Journal of Nutrition*, *128*(6): pp. 646–650.

Georgakopoulou, S., et al. (2004). Circular dichroism of carotenoids in bacterial light-harvesting complexes: Experiments and modeling. *Biophysical Journal*, *87*(5): pp. 3010–3022.

Goodman, L. S. (1996). *Goodman and Gilman's the pharmacological basis of therapeutics*. New York: McGraw-Hill, 1549(1): pp.1361-1373.

Glusko, C. A., et al. (2011). Dyes and Pigments An experimental and theoretical study on the photophysical properties of methylene green Cl -. *Dyes and Pigments*, *90*(1): pp. 28–35.

Granados-Soto, V., et al. (2011). Characterization of the Analgesic Effects of Paracetamol and Caffeine Combinations in the Pain-induced Functional Impairment Model in the Rat. *Journal of Pharmacy and Pharmacology*, *45*(7): pp. 627–631.

Gunasekaran, S., et al. (2005). Vibrational spectral investigation on xanthine and its derivatives - Theophylline, caffeine and theobromine. *Spectrochimica Acta - Part A: Molecular and Biomolecular Spectroscopy*, *61*(2): pp. 117–127.

Gutiérrez, D., et al. (2019). Development of a Steady-State Fluorescence Spectroscopy System and a Time-Resolved Fluorescence Spectroscopy System. *Journal of Physics: Conference Series*, *1247*(1): pp. 1-5.

Han, X., et al. (2003). Binding of perfluorooctanoic acid to rat and human plasma proteins. *Chemical Research in Toxicology*, *16*(6): pp. 775–781.

Hooper, D. C. (2001). Emerging mechanisms of fluoroquinolone resistance. *Emerging Infectious Diseases*, *7*(2): pp.337–341.

Hooper, D. C., & Jacoby, G. A. (2015). Mechanisms of drug resistance: Quinolone resistance. *Annals of the New York Academy of Sciences*, *1354*(1): pp. 12–31.

Horn, A. H. C. (2003). Essentials of Computational Chemistry Theories and Models. *Journal of Chemical Information and Computer Sciences*, 43, (5): pp. 420-456.

Itagaki, H. (2000). Fluorescence Spectroscopy. In *Experimental Methods in Polymer Science*. *Sprnger, 1000(1)*: pp. 155–260.

Ivan, L. M., et al. (2020). Excited state dipole moment of two pyridazinium-p-nitro-phenacylids estimated from solvatochromic study. *Spectroscopy Letters*, *53*(1): pp.1–11.

Jabłoński, A. (1935). Über den Mechanismus der Photolumineszenz von Farbstoffphosphoren. *Zeitschrift Für Physik*, *94*(1–2): pp.38–46.

Jeffrey, D. (2014). Mechanism of Quinolone Action and Resistance. *Biochemistry*, *53*(10): pp.1565-1574.

Karampela, I., & Dalamaga, M. (2020). Could Respiratory Fluoroquinolones, Levofloxacin and Moxifloxacin, Prove to be Beneficial as an Adjunct Treatment in COVID-19? *Archives of Medical Research*, *51*(7): pp.741–742.

Kawano, K., & Kitoh, T. (2004). *Introduction to Optical Waveguide Analysis: Solving Maxwell's Equation and the Schrödinger Equation*. J*ohn Wiley & Sons, 1*(7): pp.210-275.

Kawski, A. (2002). On the estimation of excited-state dipole moments from solvatochromic shifts of absorption and fluorescence spectra. *Zeitschrift Für Naturforschung A, 57*(5): pp.255-262.

Kawski, A., et al. (2002). Excitation Wavelength Dependence of Acrylodan Fluorescence Spectra in Some Polar Solvents. *Zeitschrift Für Naturforschung A, 57*(1–2): pp. 94–97.

Kesimli, B., et al., (2003). An interaction of caffeine and sulfamethoxazole: Studied by IR spectroscopy and PM3. Journal of molecular sructure 645(3): pp.199-204

Keswani, N., et al. (2021). Binding behaviour of aminoglycoside drug kanamycin with calf thymus DNA: Thermodynamic, spectroscopic and molecular modelling studies. *Thermochimica Acta, 697*(08), 178856 p.

Keyeta, T. A., & Gholap, A. V. (2011). Determination of oscillator strength of caffeine and caffeine in tea leaves by the integrated absorption coefficient technique at two different temperatures. *Journal of Engineering and Technology Research*, *3*(5): pp. 155–160.

Khadem Sadigh, M., et al. (2016). Environment and solute-solvent interaction effects on photo-physical behaviors of Folic acid and Folinic acid drugs. *Journal of Molecular Structure*, *1125*(4): pp. 177–185.

Khadem Sadigh, M., et al. (2017). Environment effect on spectral and charge distribution characteristics of some drugs of folate derivatives. *Spectrochimica Acta Part A: Molecular and Biomolecular Spectroscopy*, *171(7)*: pp. 10–17.

Khalil RM (1996). Interaction of Ibupofine and Indomethacinwith caffeine. Pharmazie, 51(12): pp. 970-973

Khashkhashi-Moghadam, S., et al. (2022). Novel perspective into the interaction behavior study of the cyanidin with human serum albumin-holo transferrin complex: Spectroscopic, calorimetric and molecular modeling approaches. *Journal of Molecular Liquids, 356(7)*: pp.11941-42.

Khazaee, M., et al. (2021). Perfluoroalkyl acid binding with peroxisome proliferator-

activated receptors α, γ, and δ, and fatty acid binding proteins by equilibrium dialysis with a comparison of methods. *Toxics*, *9*(3): pp. 1–16.

Kian, R., et al. (2015). Photo-physical properties of different types of vitamin A in solvent media. *Journal of Molecular Structure, 1080(8)*: pp. 8–13.

Kian, R., et al. (2020). Investigation of the spectroscopic features along with the media polarity effect in some symmetrical disc-shaped liquid crystals. *Journal of Molecular Liquids*, *309(5)*: pp. 11322-6.

Kian, R., et al. (2019). Study of the variation of intra/intermolecular interactions and configuration of a group of Enone anticancer drugs as a result of solvation. *Journal of Molecular Liquids, 274*(3): pp. 1–14.

Kian, R., et al. (2017). The interactional behaviors and photo-physical properties of two triarylmethane drugs in solvent media. *Journal of Molecular Liquids*, *225*(1): pp. 653–661.

Kian, R., et al. (2017a). Media and solute–solvent interaction effects on the photo–physical behavior of some drugs of 4H–Pyran derivatives. *Journal of Molecular Liquids*, *238(2)*: pp. 508–517.

Kokiashvili, N., et al. (2012). Revealing of pharmacokinetic peculiarities of surface active drug promethazine in its interaction with caffeine in rabbits. *Colloids and Surfaces A: Physicochemical and Engineering Aspects*, *413*(2): pp.169–173.

Krawczyk, P. (2015). Time-dependent density functional theory calculations of the solvatochromism of some azo sulfonamide fluorochromes. *Journal of Molecular Modeling*, *21*(5): pp. 118-122.

Krishna, N., et al. (2013). In Vitro In Vivo Pharmacokinetic Interaction Study of Escitalopram Oxalate when Co Administered with Caffeine / caffeinated Beverages. *Journal Open Conference Proceedings*, *4*(1): pp. 66–71.

Kumar, S., et al. (2001). An experimental and theoretical study of excited-state dipole moments of some flavones using an efficient solvatochromic method based on the solvent polarity parameter, ETN. *Spectrochimica Acta - Part A Molecular and Biomolecular Spectroscopy*, *57*(2): pp. 291–298.

Kumar Satpati, A., et al. (2005). Photophysical investigations of the solvent polarity effect on the properties of coumarin-6 dye. *Chemical Physics Letters*, *407*(3): pp. 114–118.

Kumar, C. V., & Asuncion, E. H. (1993). DNA Binding Studies and Site Selective Fluorescence Sensitization of an Anthryl Probe. *Journal of the American Chemical Society*, *115*(19): pp. 8547–8553.

Kumari, R., et al. (2017). Effect of solvent polarity on the photophysical properties of chalcone derivatives. *RSC Advances*, *7*(39): pp. 24204–24214.

Lakowicz, J. R. (2006). Principles of Fluorescence Spectroscopy. *Springer,* Third Edition *212 p*.

Lasswell, W. L., et al. (1984). In vitro interaction of selected drugs with coffee, tea, and gallotannic acid. *Drug-Nutrient Interactions*, *2*(4): pp. 235–241.

Lazo, J., et al. (2021). *Goodman & Gilman's The pharmacological basis of therapeutics*. Royal Society of Medicine, 8(1): pp.17-68

Li, H., et al. (2012). Photophysical properties of gatifloxacin in aqueous solution by laser flash photolysis and pulse radiolysis. *Radiation Physics and Chemistry*, *81*(1): pp.40–45.

Li, J., & Thumm, U. (2020). Semiclassical approach for solving the time-dependent Schrödinger equation in spatially inhomogeneous electromagnetic pulses. *Physical Review A*, *101*(1): pp. 013411-12.

Li, Y., et al. (2005). Binding of the bioactive component Jatrorrhizine to human serum albumin. *Biochimica et Biophysica Acta - General Subjects*, *1722*(1): pp. 15–21.

Liguori, A., et al. (1997). Absorption and subjective effects of caffeine from coffee, cola and capsules. *Pharmacology Biochemistry and Behavior*, *58*(3): pp. 721–726.

Lippert, E. (1955). Dipolmoment und Elektronenstruktur von angeregten Molekülen. *Zeitschrift Fur Naturforschung - Section A Journal of Physical Sciences*, *10*(7): pp. 41–45.

Liszt, K. I., et al. (2017). Caffeine induces gastric acid secretion via bitter taste signaling in gastric parietal cells. *Proceedings of the National Academy of Sciences of the United States of America*, *114*(30): pp. 6260–6269.

Lorenzo, F., et al. (2008). Primary photophysical properties of moxifloxacin - A fluoroquinolone antibiotic. *Photochemistry and Photobiology*, *84*(5): pp. 1118–1125.

Lorenzo, F., et al. (2009). Primary photoprocesses in a fluoroquinolone antibiotic sarafloxacin. *Photochemistry and Photobiology*, *85*(4): pp.886–894.

Ma, L. (2018). The Investigation of Fluorescence Spectra and Fluorescence Quantum Yield of Enrofloxacin. *Journal of Chemical, Environmental and Biological Engineering*, *2*(1): pp. 1–11.

MacManus-Spencer, L. A., et al. (2010). Binding of perfluorocarboxylates to serum albumin: A comparison of analytical methods. *Analytical Chemistry*, *82*(3): pp. 974–981.

Malik, N. A. (2015). Surfactant–Amino Acid and Surfactant–Surfactant Interactions in Aqueous Medium: a Review. *Applied Biochemistry and Biotechnology*, *176*(8): pp. 2077–2106.

Mallick, S., et al. (2016). Investigation of the effect of cucurbit[7]uril complexation on the photophysical and acid–base properties of the antimalarial drug quinine. *Physical Chemistry Chemical Physics*, *18*(44): pp.30520–30529.

Manohara, S. R., et al. (2013). Estimation of ground and excited-state dipole moments of 1 , 2-diazines by solvatochromic method and quantum-chemical calculation. *Journal of Molecular Liquids*, *189(1)*: pp.97–104.

Maridevarmath, C. V., et al. (2019). Synthesis, photophysical, DFT and solvent effect studies on biologically active benzofuran derivative: (5-methyl-benzofuran-3-yl)-acetic acid hydrazide. *Chemical Data Collections*, *21 (2019)*: pp.*100221-27*.

Marques, M. A. L., & Gross, E. K. U. (2004). Time-dependent density functional theory. *Annual Review of Physical Chemistry*, *55*(2): pp. 427–455.

Márquez-Lázaro, J., et al. (2021). Fluoroquinolone antibiotics and organophosphate pesticides induce carbonylation on Eisenia fetida muscle proteins. *Science of the Total Environment*, *758*(135): pp.143954-58.

Mataga, N., et al. (1956). Solvent Effects upon Fluorescence Spectra and the Dipolemoments Excited Molecules. *Bull. Chem. Soc. Jpn.*, *29*(4): pp. 465–470.

Matchette, et al. (2007). Fluoroquinolone antibiotics having the potential to interfere with fluorescence-based diagnosis. *Photochemistry and Photobiology*, *83*(6): pp. 1386–1393.

Meena, P., & Kishore, N. (2021). Thermodynamic and mechanistic analytical effect of albumin coated gold nanosystems for antibiotic drugs binding and interaction with deoxyribonucleic acid. *Journal of Molecular Liquids, 339 (2021)*: pp.*116718-12*.

Melavanki, R., et al. (2021). Solvation , rotational dynamics , photophysical properties study of aromatic asymmetric di-ketones : An experimental and theoretical approach. *Journal of Molecular Liquids, 337 (3)*: pp. 116456-9.

Messina, P., et al. (2005). Ultraviolet-circular dichroism spectroscopy and potentiometric study of the interaction between human serum albumin and sodium perfluorooctanoate. *Biopolymers*, *79*(6) : pp.300–309.

Milonni, P. W., & Eberly, J. H. (2010). Laser Physics. *John Wiley & Sons, 432 p*

Miotke, M. M., & Józefowicz, M. (2017). Solvatochromism of antiinflammatory drug – naproxen sodium. *Journal of Molecular Liquids*, *230*(7): pp. 129–136.

Mohd, A., et al. (2010). Interaction and fluorescence quenching study of levofloxacin with divalent toxic metal ions. *Eurasian J. Anal. Chem*, *5*(2): pp.177–186.

Montero, M. T., et al. (1990). *lumin- iscence. 18*(120): pp. 99–101.

Mora, A. (2019). *Light-Matter Interaction of Molecules with Intense Ultrashort Laser Pulses, 2(231*: pp.*542-550.*

Morosanu, A. C., et al. (2019). Excited state dipole moment of the fluorescein molecule estimated from electronic absorption spectra. *Journal of Molecular Structure*, *1180*(2): pp. 723–732.

Mrkalić, E., et al. (2021). Interaction between olanzapine and human serum albumin and effect of metal ions, caffeine and flavonoids on the binding: A spectroscopic study. *Spectrochimica Acta - Part A: Molecular and Biomolecular Spectroscopy*, *249 (2021)*: pp. *119295-8*.

Muchmore, S. W. (2004). Computational Chemistry Using the PC. *John Wiley & Sons*, *47*(1) : pp.78-89.

Muddapur, G. V., et al. (2014). “Estimation of Ground and Excited State Dipole Moments of aryl Boronic acid Derivative by Solvatochromic Shift Method.” *Journal of Fluorescence*, *24*(6): pp. 1651–1659.

Nad, S., & Pal, H. (2001). Unusual Photophysical Properties of Coumarin-151. *American Chemical Society*, *105*(7): pp. 1-14.

Nawrot, P., et al. (2003). Effects of caffeine on human health. *Food Additives and Contaminants*, *20*(1): pp. 1–30.

Nehlig, A. (2022). Effects of Coffee on the Gastro-Intestinal Tract: A Narrative Review and Literature Update. *Nutrients*, *14*(2): pp. 1–31.

Osswald, H., et al. (1997). Adenosine and tubuloglomerular feedback. *Blood Purification*, *15*(4–6): pp. 243–252.

Pal, H., Nad, S., & Kumbhakar, M. (2003). Photophysical properties of coumarin-120 Unusual behavior in nonpolar solvents. *Journal of Chemical Physics*, *119*(1) : pp. 443–452.

Panda, M., et al. (2020). Fluorescence quenching of chloroquine by Cu2+ in micelles. *Journal of Molecular Liquids*, *306*(5): pp. 112763.

Panigrahi, S. K., & Mishra, A. K. (2019). Inner filter effect in fluorescence spectroscopy : As a problem and as a solution. *Journal of Photochemistry and Photobiology C: Photochemistry Reviews, 41 (2019)*: pp.*100318*.

Panja, S. K. (2021). Dipolar state assisted aggregation induced optical behavior of push-pull Salen-type Schiff base in solution. *Journal of Molecular Structure*, *1234*(1) : pp. 130140-9.

Parisi, G., & Auletta, G. (2000). The foundations of quantum mechanics. *Oxiford*, 153 p.

Park, H. R., et al. (2002). Physicochemical properties of quinolone antibiotics in various environments. *European Journal of Medicinal Chemistry*, *37*(6): pp. 443–460.

Patel. (2019). *Modern introduction to classical and quantum optics*. *Oxiford*, 25 p.

Patil, M. K., et al. (2019). A combined solvatochromic shift and TDDFT study probing solute-solvent interactions of blue fluorescent Alexa Fluor 350 dye: Evaluation of

ground and excited state dipole moments. *Spectrochimica Acta - Part A: Molecular and Biomolecular Spectroscopy*, *215*(4) : pp. 142–152.

Patil, S. A., et al. (2021). Photo-physical study of coumarins in aqueous organic solvents: An experimental and theoretical approach. *Materials Today Communications*, *29*(6) : pp. 1033.

Paul, B. K., et al. (2017). Binding of ciprofloxacin to bovine serum albumin: Photophysical and thermodynamic aspects. *Journal of Photochemistry and Photobiology B: Biology*, *172*(4): pp. 11–19.

Persky, A. M. (2005). *Foundations in Pharmacokinetics*. *Springer*, 124 p.

Petrov, N. Kh, et al. (2002). Study of Preferential Solvation in Binary Mixtures by Means of Frequency-Domain Fluorescence Spectroscopy. *Journal of Fluorescence*, *12*(1): pp. 19–24.

Petrov, N., & Staerk, H. (2001). A simple kinetic model of preferential solvation in binary mixtures. *Chemical Physics Letters*, *349*(5–6): pp. 517–520.

Polishchuk, A. V., et al. (2012). Spectroscopic and photophysical properties of protonated forms of some fluoroquinolones in solutions. *Journal of Fluorescence*, *22*(1): pp.373–379.

Raikar, U. S., et al. (2006). Solvent effects on the absorption and fluorescence spectra of coumarins 6 and 7 molecules: Determination of ground and excited state dipole moment. *Spectrochimica Acta Part A: Mol. and Biomolecular Spectroscopy*, *65*(3–4): pp. 673–677.

Ravi, M., et al. (1995). Excited-state dipole moments of some Coumarin dyes from a solvatochromic method using the solvent polarity parameter, E. *Journal of the Chemical Society, Faraday Transactions*, *91*(17): pp. 2739–2742.

Razum, N. J. (1989). Laser physics. *Facial Plastic Surgery : FPS*, *6*(3): pp. 137–143.

Redgrave, L. S., et al. (2014). Fluoroquinolone resistance: Mechanisms, impact on bacteria, and role in evolutionary success. *Trends in Microbiology*, *22*(8): pp. 438–445.

Reichardt, C. (1994). Solvatochromic dyes as solvent polarity indicators. *Chemical Reviews*,

94(8): pp. 2319–2358.

Robeson, J. L., & Tilton, R. D. (1995). Effect of concentration quenching on fluorescence recovery after photobleaching measurements. *Biophysical Journal*, *68*(5): pp. 2145–2155.

Rodríguez, H. B., & San Román, E. (2013). Effect of concentration on the photophysics of dyes in light-scattering materials. *Photochemistry & Photobiology*, *89*(6):pp. 1273–78.

Rotkiewicz, K., et al. (2004). Specific solute-solvent interactions and dual fluorescence of electron donor substituted bis-pyrazoquinoline in binary mixed solvents. *Chemical Physics, 307*(1): pp. 45–52.

Rout, J., et al. (2020). Spectroscopic insight into the interaction of dopamine with spherical gold nanoparticles. *Journal of Photochemistry and Photobiology B: Biology*, *203*(12) : pp.111770.

Royer, C. A. (1995). Fluorescence spectroscopy. *Methods in Molecular Biology*, 89 p.

Rubinstein, E. (2001). History of quinolones and their side effects. *Chemotherapy, 7*8 p.

Sabahi, A. A., et al. (2020). *Photophysical and theoretical studies on the solvatochromic effects and dipole moments evaluation of substituted 1-phenyl-3-naphthyl-5- (4-ethyl benzoate) -2-pyrazoline*. *Journal ofMolecular Liquids*, *307*(2020): pp. 1129673-7.

Sahoo, S., et al. (2012). FTIR and Raman spectroscopic investigations of a norfloxacin/ carbopol934 polymeric suspension. *Journal of Young Pharmacists, 4*(3): pp. 138–145.

Sárközy, G. (2001). Quinolones: A class of antimicrobial agents. *Veterinarni Medicina, 46*(10): pp.257–274.

Sauter, N. K., et al. (1989). Hemagglutinins from Two Influenza Virus Variants Bind to Sialic Acid Derivatives with Millimolar Dissociation Constants: A 500-MHz Proton Nuclear Magnetic Resonance Study. *Biochemistry*, *28*(21): pp. 8388–8396.

Schmidt, R., & Fanchamps, A. (1974). Effect of caffeine on intestinal absorption of ergotamine in man. *European Journal of Clinical Pharmacology, 7*(3): pp. 213–216.

Sciscenko, I., et al. (2021). Fluorescence Spectroscopy and Chemometrics: A Simple and Easy Way for the Monitoring of Fluoroquinolone Mixture Degradation. *ACS Omega*,

6(7): pp.183–198.

Sekgota, K. C., et al. (2017). Application of the Morita-Baylis-Hillman reaction in the synthesis of 3-[(N-cycloalkylbenzamido)methyl]-2-quinolones as potential HIV-1 integrase inhibitors. *Bioorganic Chemistry*, *75*(1) : pp.310–316.

Sharma, M., (2021). Effect of solvent on the photophysical properties of isoxazole derivative of curcumin: A combined spectroscopic and theoretical study. *Journal of Photochemistry and Photobiology A: Chemistry*, *410*(10): pp.113164-66.

Sharma, P. C., et al. (2020). Insights on fluoroquinolones in cancer therapy: chemistry and recent developments. *Materials Today Chemistry*, *17(2)*: pp. 100296-98.

Sharma, P.M., et al. (2009). Fluoroquinolone antibacterials: A review on chemistry, microbiology and therapeutic prospects. *Acta Poloniae Pharmaceutica - Drug Research*, *66*(6): pp. 587–604.

Sharma, S. K., et al. (2018). Handbook of Materials Characterization. *Springer*, *20(7)*: pp. 1–613.

Siddlingeshwar, B., et al. (2011). Photophysical characteristics of three novel benzanthrone derivatives: Experimental and theoretical estimation of dipole moments. *Journal of Quantitative Spectroscopy and Radiative Transfer*, *112*(3): pp. 448–456.

Sidir, I., & Gülseven Sidir, Y. (2015). Estimation of ground and excited state dipole moments of Oil Red O by solvatochromic shift methods. *Spectrochimica Acta - Part A: Molecular and Biomolecular Spectroscopy*, *135*(6): pp. 560–567.

Sidir, I., et al. (2016). Specific and non-specific interaction effect on the solvatochromism of some symmetric (2-hydroxybenzilydeamino)phenoxy Schiff base derivatives. *Journal of Molecular Liquids*, *215(3)*: pp. 691–703.

Sissi, C., et al. (2001). Ciprofloxacin affects conformational equilibria of DNA gyrase A in the presence of magnesium ions. *Journal of Molecular Biology*, *311*(1): pp. 195–203.

Sıdır, İ., & Sıdır, Y. G. (2011). Ground state and excited state dipole moments of 6,8-diphenylimidazo[1,2-α]pyrazine determined from solvatochromic shifts of absorption and fluorescence spectra. *Spectrochimica Acta Part A: Molecular and Biomolecular Spectroscopy, 79*(5): pp.1220–1225.

Skoromnik, O. D., et al. (2017). Analytic model of a multi-electron atom. *Journal of Physics B: Atomic, Molecular and Optical Physics, 50 (2017)*: pp. *245007-10*

Soltani, A., et al. (2020). A comparative theoretical study on the interaction of pure and carbon atom substituted boron nitride fullerenes with ifosfamide drug. *Journal of Molecular Liquids, 297(11)*: pp. 111894-98.

Sonnessa, A. J., & Wilson, M. K. (1967). Introduction to Molecular Spectroscopy. In *The Physics Teacher,* 5(4): pp.188–189.

Stojanović, S. D., et al. (2020). Spectroscopic studies on the drug–drug interaction: the influence of fluoroquinolones on the affinity of tigecycline to human serum albumin and identification of the binding site. *Monatshefte Fur Chemie, 151*(6): pp. 999–1007.

Strickler, S. J., & Berg, R. A. (1962). Relationship between absorption intensity and fluorescence lifetime of molecules. *The Journal of Chemical Physics, 37*(4): pp. 814–822.

Suppan, P. (1983). Excited-state dipole moments from absorption/fluorescence solvatochromic ratios. *Chemical Physics Letters, 94*(3): pp. 272–275.

Tanaka, N. (1983). Mechanism of action of and resistance to aminoglycoside antibiotics. *Archives of Pharmacal Research, 6*(1): pp. 93–102.

Tardioli, S., et al. (2010). Interaction of bovine serum albumin with gemini surfactants. *Journal of Colloid and Interface Science, 347*(1): pp. 96–101.

Thakur, R., et al. (2012). Photophysical and photodynamical study of fluoroquinolone drug molecule in bile salt aggregates. *Photochemistry and Photobiology, 88*(5): pp. 1248–1255.

Thiaré, D. D., et al. (2015). Determination of ground and excited state dipole moments of amino-benzimidazole by solvatochromic shift methods and theoretical calculations. *Journal of Molecular Liquids, 211*(2): pp. 640–646.

Tran, A., & Yijun Zhang, C. (2015). The Role of Coffee in the Therapy of Parkinson Disease. *Journal of Alzheimer's Disease & Parkinsonism, 05*(03): pp.12-17.

Urry, E., et al. (2016). Assessment of CYP1A2 enzyme activity in relation to type-2 diabetes

and habitual caffeine intake. *Nutrition and Metabolism*, *13*(1): pp. 1–9.

Uv, T., et al. (2017). *Experimental and theoretical investigation of the molecular , electronic structure and solvatochromism of phenyl salicylate : External electric fi eld effect on the electronic structure* 216 p.

Valeur, B. (2001). Related Titles from WILEY-VCH Analytical Atomic Spectrometry with Flames and Plasmas Handbook of Analytical Techniques Single-Molecule Detection in Solution . *Methods and Applications*, *8(7)* : pp. 72-123.

Van De Weert, M., & Stella, L. (2011). Fluorescence quenching and ligand binding: A critical discussion of a popular methodology. *Journal of Molecular Structure*, *998*(3): pp.144–150.

Vanattou-Saïfoudine, N., et al. (2012). Caffeine provokes adverse interactions with 3,4-methylenedioxymethamphetamine (MDMA, 'ecstasy') and related psychostimulants: Mechanisms and mediators. *British Journal of Pharmacology*, *167*(5): pp. 946–959.

Vinet, L., & Zhedanov, A. (2010). A "missing" family of classical orthogonal polynomials. *Journal of Physics A: Mathematical and Theoretical*, *44*(8): pp. 0852-08.

Viola, G., et al. (2004). Photophysical and phototoxic properties of the antibacterial fluoroquinolones levofloxacin and moxifloxacin. *Chemistry and Biodiversity*, *1*(5): pp. 782–801.

Viola, G., et al. (2007). Photophysical properties and photobiological behavior of amodiaquine, primaquine and chloroquine. *Photochemistry and Photobiology*, *83*(6): pp. 1415–1427.

Walki, S., et al. (2021). Synthesis, spectroscopic properties, and DFT correlative studies of 3,3′- carbonyl biscoumarin derivatives. *Journal of Molecular Structure*, *1243)* : pp. 13078-81.

Wang, Q., et al. (2016). Binding interaction of atorvastatin with bovine serum albumin: Spectroscopic methods and molecular docking. *Spectrochimica Acta - Part A: Molecular and Biomolecular Spectroscopy*, *156(5)*: pp. 155–163.

Wang, Y., et al. (2020). Evaluation of the binding interactions of p-acetylaminophenol, aspirin, ibuprofen and aminopyrine with norfloxacin from the view of antipyretic and

anti-inflammatory. *Journal of Molecular Liquids*, *312*(1): pp. 113397.

Weiser, T., & Weigmann, H. (2019). Effect of Caffeine on the Bioavailability and Pharmacokinetics of an Acetylsalicylic Acid-Paracetamol Combination: Results of a Phase I Study. *Advances in Therapy*, *36*(3): pp.597–607.

Wendl, B., et al. (1994). Effect of decaffeination of coffee or tea on gastro-oesophageal reflux. *Alimentary Pharmacology & Therapeutics*, *8*(3): pp. 283–287.

Willson, C. (2018). The clinical toxicology of caffeine: A review and case study. *Toxicology Reports*, *p* 1152.

Woldegiorges, K., et al. (2021). *Estimating the Ground and Excited State Dipole Moments of Levofloxacin and Norfloxacin Drugs Using Solvatochromic Effects and Computational Work. Journal of spectroscopy, 2021(12)*: pp. *1-13*.

Xiong, X., et al. (2017). Investigation on the interaction of antibacterial drug moxifloxacin hydrochloride with human serum albumin using multi-spectroscopic approaches, molecular docking and dynamical simulation. *RSC Advances*, *7*(77): pp. 48942–48951.

Xu, Z., et al. (2012). Fluorescence spectroscopy measures yeast PAH1-encoded phosphatidate phosphatase interaction with liposome membranes. *Journal of Lipid Research*, *53*(3): pp. 522–528.

Yartsev, A., & Peisah, C. (2021). Caffeine-clozapine interaction associated with severe toxicity and multiorgan system failure: a case report. *BMC Psychiatry*, *21*(1): pp. 1–5.

Zakerhamidi, M. S., et al. (2017). Photo-physical and interactional behavior of two members of group B vitamins in different solvent media. *Journal of Molecular Structure*, *1144*(1): pp.265–272.

Ženata, O., et al. (2019). The Effect of Caffeine on Calcitriol-Inducible Vitamin D Receptor-Controlled Gene Expression in Intestinal and Osteoblastic Cells. *Calcified Tissue International*, *105*(6): pp. 651–659.

Zhang, H., et al. (2019). Photophysical and photochemical insights of the photodegradation of norfloxacin: The rate-limiting step and the influence of Ca2+ ion. *Chemosphere*, *219*(2019): pp. 236–242.

Zhang, X., et al. (2020). Solvent effect on the photophysical properties of thermally activated delayed fluorescence molecules. *Spectrochimica Acta - Part A: Molecular and Biomolecular Spectroscopy*, *225*(2): pp.117473-80.

Zhang, Y. F., et al. (2017). Investigation of the binding interaction between estazolam and bovine serum albumin: Multi-spectroscopic methods and molecular docking technique. *Journal of Biomolecular Structure and Dynamics*, *35*(16): pp. 3605–3614.

Zhao, C. C., et al. (2021). Solvation effect on photophysical and photochemical properties of mono-biotinylated curcumin. *Chemical Physics Letters*, *774*(4), 138616-20.

Zhao, J., et al. (2019). Photophysical Properties Controlled by Substituents with Lone-Pair Electrons at the Ortho- or Para-Positions of Fluoroquinolone Antibiotics [Research-article]. *Journal of Physical Chemistry B*, *123*(15): pp. 3156–3162.

Zhou, G., et al. (1983). Diffusion-controlled reactions of enzymes. An approximate analytic solution of Chou's model. *Biophysical Chemistry*, *18*(2): pp. 125–132.